ASSESSMENT OF COPPER REMOVAL FROM HIGHWAY STORMWATER RUNOFF USING APATITE II™ AND COMPOST: LABORATORY AND FIELD TESTING

Final Report

SPR 730

ASSESSMENT OF COPPER REMOVAL FROM HIGHWAY STORMWATER RUNOFF USING APATITE II™ AND COMPOST: LABORATORY AND FIELD TESTING

Final Report

SPR 730

by
Jason R. Silvertooth
Hsiao-Wen Huang
Justin J. Provolt
Jeffrey A. Nason, Ph.D
Dept. of Chemical, Biological, and Environmental Engineering
Oregon State University

for

March 2015

1. Report No. FHWA-OR-RD-15-13	2. Government Accession No.	3. Recipient's Catalog No.
4. Title and Subtitle Assessment of Copper Removal From Highway Stormwater Runoff Using Apatite II™ and Compost: Laboratory and Field Testing		5. Report Date -March 2015-
		6. Performing Organization Code
7. Author(s) Jason R. Silvertooth, Hsiao-Wen Huang, Justin J. Provolt, Jeffrey A. Nason, Ph.D		8. Performing Organization Report No.
9. Performing Organization Name and Address Dept. of Chemical, Biological and Environmental Engineering Oregon State University 102 Gleeson Hall Corvallis, Oregon 97331		10. Work Unit No. (TRAIS)
		11. Contract or Grant No. SPR 730
12. Sponsoring Agency Name and Address Oregon Dept. of Transportation Research Section and Federal Highway Admin. 555 13th Street NE, Suite 1 400 Seventh Street, SW Salem, OR 97301 Washington, DC 20590-0003		13. Type of Report and Period Covered Final Report
		14. Sponsoring Agency Code

15. Supplementary Notes

16. Abstract-Stormwater runoff introduces heavy metals to surface waters that are harmful to aquatic organisms, including endangered salmon. This work evaluates Apatite II™, a biogenic fish bone based adsorbent, for removing metal from stormwater. The metals removal by Apatite II™ is compared to that of compost. Compost is commonly used in stormwater BMPs.

At equilibrium and in column tests, both compost and Apatite II™ removed copper and zinc to trace levels.. The introduction of natural organic material (NOM) rendered both adsorbents less effective in all tests. There was indication that dissolved copper in the effluent was fully complexed with NOM, effectively removing the bioavailable, free copper (Cu^{+2}). In field testing Apatite II™ removed, copper for three of seven storms with efficiencies ranging from 16.1% to 59.8%. Compost removed copper in three of five storms sampled, with efficiencies ranging from 24.7% to 45.4%. Ion leaching was observed for both media types. At the field level, steady state phosphate release of approximately 1.5 mg/L was observed for Apatite II. For compost, field levels of leaching trend of nitrate and phosphate had not yet stabilized after approximately 7,300 gallons of flow through the filter.

Due to the superior performance of compost, the steady state leaching of phosphate from Apatite II™, and the potential for Apatite II™ to release copper back into solution, compost is viewed as the more promising adsorbent for stormwater applications.

17. Key Words stormwater, copper, Apatite II, compost, filter, leaching, aquatic, fish bone	18. Distribution Statement Copies available from NTIS, and online at http://www.oregon.gov/ODOT/TD/TP_RES/		
19. Security Classification (of this report) Unclassified	20. Security Classification (of this page) Unclassified	21. No. of Pages 139	22. Price

Technical Report Form DOT F 1700.7 (8-72)   Reproduction of completed page authorized   ♻ Printed on recycled paper

SI* (MODERN METRIC) CONVERSION FACTORS

APPROXIMATE CONVERSIONS TO SI UNITS					APPROXIMATE CONVERSIONS FROM SI UNITS				
Symbol	When You Know	Multiply By	To Find	Symbol	Symbol	When You Know	Multiply By	To Find	Symbol
LENGTH					**LENGTH**				
in	inches	25.4	millimeters	mm	mm	millimeters	0.039	inches	in
ft	feet	0.305	meters	m	m	meters	3.28	feet	ft
yd	yards	0.914	meters	m	m	meters	1.09	yards	yd
mi	miles	1.61	kilometers	km	km	kilometers	0.621	miles	mi
AREA					**AREA**				
in^2	square inches	645.2	millimeters squared	mm^2	mm^2	millimeters squared	0.0016	square inches	in^2
ft^2	square feet	0.093	meters squared	m^2	m^2	meters squared	10.764	square feet	ft^2
yd^2	square yards	0.836	meters squared	m^2	m^2	meters squared	1.196	square yards	yd^2
ac	acres	0.405	hectares	ha	ha	hectares	2.47	acres	ac
mi^2	square miles	2.59	kilometers squared	km^2	km^2	kilometers squared	0.386	square miles	mi^2
VOLUME					**VOLUME**				
fl oz	fluid ounces	29.57	milliliters	ml	ml	milliliters	0.034	fluid ounces	fl oz
gal	gallons	3.785	liters	L	L	liters	0.264	gallons	gal
ft^3	cubic feet	0.028	meters cubed	m^3	m^3	meters cubed	35.315	cubic feet	ft^3
yd^3	cubic yards	0.765	meters cubed	m^3	m^3	meters cubed	1.308	cubic yards	yd^3
NOTE: Volumes greater than 1000 L shall be shown in m^3.									
MASS					**MASS**				
oz	ounces	28.35	grams	g	g	grams	0.035	ounces	oz
lb	pounds	0.454	kilograms	kg	kg	kilograms	2.205	pounds	lb
T	short tons (2000 lb)	0.907	megagrams	Mg	Mg	megagrams	1.102	short tons (2000 lb)	T
TEMPERATURE (exact)					**TEMPERATURE (exact)**				
°F	Fahrenheit	(F-32)/1.8	Celsius	°C	°C	Celsius	1.8C+32	Fahrenheit	°F

*SI is the symbol for the International System of Measurement

ACKNOWLEDGEMENTS

DISCLAIMER

TABLE OF CONTENTS

LIST OF TABLES

LIST OF FIGURES

1.0   INTRODUCTION

Stormwater runoff has been shown to be a significant source of heavy metals to surface waters *(USEPA 1982; Chen et al. 1996; Kayhanian et al. 2007).* Due to the toxicity of some metals, concern has risen over the ecological impacts stormwater has on aquatic systems. Of particular interest is copper, which is deposited onto roadways primarily from brake pad wear and building siding *(Davis et al. 2001).* Dissolved copper has been shown to have negative impacts on many aquatic organisms, including coho salmon *(Sandahl et al. 2007),* chinook salmon *(Hansen et al. 1999),* rainbow trout *(Julliard et al. 1996),* brown trout *(Moran et al. 1992),* fathead minnow *(Carreau and Pyle 2005),* Colorado pikeminnow *(Beyers and Farmer 2001),* and tilapia *(Bettini et al. 2006).* Recent research has shown that temporary exposure to dissolved copper concentrations as low as 2 µg/L causes impairment of the olfactory sense of juvenile coho salmon *(Sandahl et al. 2007; McIntyre et al. 2008).* This is of particular concern because four major populations of coho salmon are listed as either *threatened* or *endangered* under the Endangered Species Act, and 2 µg/L is a concentration that is often exceeded in stormwater runoff *(USEPA 1982; Kayhanian et al. 2007; Nason et al. 2012a).* Impairment of the olfactory system is especially harmful to salmonid species due to the role olfaction plays in predatory avoidance, locating food, navigation, and social behavior *(Baldwin et al. 2003).*

Current best management practices (BMPs) only reduce dissolved copper concentrations to 5 µg/L in best case scenarios *(Wright Water Engineers and Geosyntec Consultants 2011),* so amendments to current methods or novel treatment approaches need to be developed to avoid harmful impacts on aquatic systems. Due to the nature of existing roadway infrastructure, it is often impossible to treat stormwater runoff at a central location. This makes active treatment methods such as chemical precipitation or membrane filtration unreasonable in most instances, because they require skilled operators and consistent maintenance. Economically feasible, passive treatment technologies need to be developed that can be installed and left to operate with minimal maintenance for long periods of time.

The work here focuses on the evaluation of Apatite II™, a biogenic fish bone based adsorbent, for use in metal removal from stormwater runoff. The efficacy of metals removal by Apatite II™ is compared to that of compost to show the range and scope of metals removal that is achievable. Compost represents a current best available technology due to its ability to bind dissolved metals, and is commonly used in stormwater BMPs.

1.1   OBJECTIVES

The overarching goal of this project is to identify an efficient and cost effective means of remediating copper in highway stormwater runoff. Specific objectives include:

1. Evaluate the current "state of science" with respect to removing metals (copper in particular) from stormwater runoff.

2. Identify the mechanisms responsible for copper removal with Apatite II™ and compost.

3. Assess the capacity of Apatite II™ and compost to remove copper from stormwater, and offer a comparison to other media types from the available literature.

4. Test promising adsorbents at the field scale to assess performance in actual stormwater runoff.

1.2   APPROACH

To achieve the first objective, a comprehensive literature review was performed that provided detailed information relative to stormwater runoff, metals removal processes, and the media involved in this project. The second objective was accomplished using batch experiments at the lab scale. The third objective was completed through the use of batch and column experiments that gauged the capacity of the media types to remove metals in equilibrium and continuous flow scenarios with varying metal and organic matter concentrations. The fourth objective was achieved by taking flow-weighted influent and effluent samples at a field site where highway stormwater runoff was diverted into a packed media filter. These samples were analyzed for copper concentration as well as a host of common water quality parameters to evaluate the overall effect the filter media had on downstream water quality. Finally, the information gained in the first four objectives was synthesized into a comprehensive assessment of the media types, and this information was used to achieve the final objective.

The remainder of this report is divided into six additional chapters. Chapter 2 includes a literature review that evaluates the current scientific knowledge with respect to metals removal from stormwater and provides the foundation for experiments that were performed. Specific topics within the literature review include characterization of copper in stormwater runoff, BMPs for metals removal, available technologies for removing metals from aqueous solutions, adsorption theory, media types chosen for this study, the impact of natural organic matter on removal processes, and stormwater sampling methodology. Chapter 3 details the materials and methods utilized in this project, and is subdivided into sections based on lab experiments, field work, and sample analysis. Chapter 4 describes the results obtained from laboratory experiments, including analysis of copper removal mechanisms, equilibrium and dynamic copper and zinc removal, and the effect of natural organic matter (NOM) on copper removal. Chapter 5 includes results from testing of compost and Apatite II™ at the field level. Chapter 6 summarizes the conclusions that can be drawn from this work and suggests future directions that could be explored in future work. Chapter 7 is the bibliography. Supplemental materials, including kinetics tests, hydraulic conductivity experiments, and full data reports from field sampling can be found in the Appendix.

2.0   LITERATURE REVIEW

2.1   COPPER IN STORMWATER RUNOFF

Heavy metals such as Cu, Zn, Pb, Ni, and Cd are commonly present in stormwater runoff. Consequently, stormwater runoff represents a significant source of metals to surface waters *(USEPA 1982; Davis et al. 2001; Kayhanian et al. 2007; Nason et al. 2012a).* Many of these metals are harmful to aquatic life, leading to concern over their concentrations and pervasiveness in stormwater. Of particular concern is copper, which has been shown in recent studies to inhibit olfactory function of juvenile coho salmon when exposed to concentrations as low as 2 µg/L for 3 hours *(Sandahl et al. 2007).* Follow-up studies determined that alkalinity and water hardness do not alter the toxic effects of copper, but dissolved organic carbon (DOC) can have a protective effect. However, this effect is strongly dependent on DOC concentration, and most rivers in the western states that provide salmon habitat have DOC concentrations that offer little protection from copper toxicity *(McIntyre et al. 2008).* Additionally, based on similar loss in olfactory function of steelhead salmon after 3 hour exposure to 5 µg/L of copper, it has been proposed that copper toxicity could potentially be extrapolated to other less studied fish species *(Baldwin et al. 2011).*

Copper in stormwater is derived from a variety of sources, including building siding, roofing, brake pad wear, and atmospheric deposition *(Davis et al. 2001; Joshi and Balasubramanian 2010).* Of these sources, brake pad wear is considered the largest contributor of copper to stormwater runoff *(Legret and Pagotto 1999; Davis et al. 2001).* Because brake pads fabricated with copper are ubiquitous, copper deposition occurs on all roadways and must be treated as a non-point source pollutant. Median dissolved copper concentrations across four sampling sites in Oregon ranged from 9.08-40.9 µg/L *(Nason et al. 2012a),* and similar work utilizing data from 34 stormwater sampling locations throughout California found the median dissolved copper concentration to be 10.2 µg/L *(Kayhanian et al. 2007).* In both cases, median values are well above the 2 µg/L concentration threshold for negatively affecting coho salmon. Dissolved copper has been shown to be positively correlated with both DOC and alkalinity and negatively correlated with pH, and total copper is positively correlated with total suspended solids (TSS) and DOC *(Nason et al. 2012a).*

Several studies have demonstrated that pollutant concentrations are considerably higher in the early stages of a rainfall event, a phenomenon known as the first flush *(Sansalone and Buchberger 1997; Kayhanian and Stenstrom 2005).* This demonstrates that even in situations where the mean concentration for the entire runoff event is at an environmentally benign level, there could still be pulses with copper concentrations high enough to negatively affect aquatic organisms. It is important to note that dissolved copper, which is operationally defined as the copper that passes through a 0.45 µm filter, is only a fraction of the total copper in stormwater. Copper can also exist as a precipitate or in the adsorbed phase, and depending on the chemistry of the receiving waters could potentially partition back into the aqueous phase as dissolved

copper. Accordingly, a complete analysis of copper and other trace metals in stormwater must include characterization of dissolved and total metal concentrations.

2.2   BEST MANAGEMENT PRACTICES FOR METALS REMOVAL

A variety of Best Management Practices (BMPs) are commonly applied for the remediation of stormwater runoff. These BMPs are utilized both for hydraulic control and to treat a number of stormwater constituents, including sediment, nutrients, metals, and other pollutants. To appropriately select a BMP, consideration of treatment goals, construction cost, and overall effectiveness must be taken into account. Generally, BMPs can be categorized by several removal processes, including sedimentation, filtration, biological uptake, and infiltration. Some BMPs rely on a single removal mechanism, while others may involve a combination of several processes. What follows is an introduction to the primary categories of BMPs, with particular emphasis on metals removal.

2.2.1 Sedimentation BMPs

Detention ponds (including wet ponds, dry ponds and dual-purpose ponds), wetlands, and vegetated swales are all considered sedimentation designs. For these BMPs, the effectiveness is dependent on residence time, the particle size distribution, and particle densities. Long retention times, laminar flows, and larger particles sizes allow for more efficient settling of particles and associated pollutants. Biological remediation of contaminants may also be carried out with longer settling times. The addition of coagulants or longer retention times is often required for the goal of removing small particles *(Wright Water Engineers and Geosyntec Consultants 2011)*.

An approximately 2-year study of a detention pond in Washington state revealed that the removal efficiencies for total suspended solids (TSS) varied from 68.1%-99.4% when the influent concentrations were between 9.6-1850 mg/L *(Hossain et al. 2005)*. The efficacy of detention ponds for metals removal, which depends on metal species as well as the loading concentrations, has been evaluated by several groups *(Farm 2002; Barrett 2005; Hossain et al. 2005)*. In one study, dissolved copper was reduced from initial concentrations of 18 μg/L to approximately 9 μg/L, while zinc initially at 122 μg/L was reduced to 30 μg/L *(Barrett 2005)*. In another study, removal efficiencies for total copper ranged between 20.8%-99.3% at influent concentrations of 7-209 μg/L *(Hossain et al. 2005)*. In general, the average removal efficiencies for total metals are higher than for dissolved species, likely due to the settling out of particulate and adsorbed phase metals. This is an important consideration in the design of stormwater BMPs; significantly reducing total metals concentration will reduce the amount of metals available to dissolve if a change in aquatic chemistry occurs.

2.2.2 Swale BMPs

Swales consist of a channeled area that is typically vegetated with grass or other plants. Bioswales or vegetated swales (e.g., grassed swales) used for metals abatement from stormwater operate by several mechanisms, including biological uptake, sedimentation and infiltration. Metals removal in vegetated swales is typically greater than sedimentation based BMPs due to the additional mechanisms for removal. However, the performance of swales depends on

whether scouring of previously deposited sediment occurs. That is, metals concentrations can increase if previously deposited sediment containing metals are re-suspended *(Backstrom 2003; Wright Water Engineers and Geosyntec Consultants 2011)* It has been shown that at low influent metal concentrations swales can act as metal sources, causing higher concentrations in the effluent water *(Backstrom 2003)*. For instance, in one study total zinc concentrations varied from 50 to 135 µg/L at the inlet to a swale, while concentrations after treatment ranged between 67-94 µg/L. The same report also noted instances in which swales acted as a dissolved copper source, resulting in effluent concentrations two to four times higher than the influent concentrations *(Backstrom 2003)*.

2.2.3 Filtration BMPs

In filtration BMPs, such as filter strips and media filters, beds of single or mixed media are employed for treatment. Each media type will have its own metals removal capacity, which will vary based on the type of metal treated as well as the influent metal concentration. In addition to metals removal, there will be ancillary advantages and disadvantages associated with each media type. For example, in one study it was shown that a peat-sand mix showed the greatest potential for clogging among tested filter materials (peat-sand mix, compost, and zeolites), whereas color, which is likely a result of organic carbon leaching, was added to the effluent by compost *(Johnson et al. 2003)*. It has also been shown that when adsorptive media was used in filtration BMPs, clogging typically occurred before the media reached breakthrough with respect to metal adsorption *(Johnson et al. 2003)*. Filter devices can last longer with an up-flow design based on a reduction of clogging as compared to a down-flow filter. Similar to sedimentation BPMs, longer residence times are generally preferred for metal remediation by filtration BMPs *(Davis et al. 2003; Johnson et al. 2003)*.

Several studies have demonstrated high removal efficiencies of dissolved metals when utilizing media filtration. In a study examining the use of zeolites for the removal of heavy metals, synthetic stormwater solutions were created with initial concentrations of 25 µg/L Cd, 50 µg/L Pb, 250 µg/L Cu, and 500 µg/L Zn, and then combined with synthetic zeolite in batch reactors. The resulting metal removal efficiencies were 100% for Pb, 98.4% for Cu, 96.8 % for Zn, and 100% for Cd. Parallel experiments were conducted using stormwater runoff spiked to the same initial concentrations as the synthetic stormwater, and yielded removal efficiencies of 100% for Pb, 91.6% for Cu, 96.5% for Zn, and 100% for Cd *(Pitcher et al. 2004)*. Another study utilized synthetic stormwater solutions with initial concentrations of approximately 80 µg/L Cu, 80 µg/L Pb, and 600 µg/L Zn, and applied this solution to several different bioretention basins at a loading rate of 4.1 cm/h. In these experiments, effluent samples were taken at the bottom of the soil media, resulting in copper removal efficiencies ranging from 43-98%. The author attributed the removal to adsorpfion of the heavy metals to the biofiltration media, which was comprised of mulch, compost, and soil *(Davis et al. 2003)*. However, both of these studies were performed with metal concentrations at values considerably higher than typical stormwater concentrations, and removal efficiencies have been shown to drop significantly when influent concentrations are lower *(Johnson et al. 2003)*.

Barrett *(Barrett 2005)* compared the performance of several BMPs, including sand filters, detention basins, multi-chambered treatment trains (MCTT), biofiltration strips, and vegetated

swales. The results indicated that removal of TSS in sand filters was independent of influent concentrations, whereas TSS remediation by swales and detention basins were correlated with inlet concentrations. All of the examined BMPs achieved more than 80 percent reduction of TSS at influent concentration of 114 mg/L, with the exception of swales and detention basins. Metals removal was also evaluated, showing that removal efficiencies for zinc (initial concentration of 122 ppb) were generally better than for copper (initial concentration of 18 ppb) among all examined BMPs. At the reported influent concentrations, strips resulted in the greatest removal of dissolved copper (70-80%).

A report of international stormwater BMP databases summarizes the performance of a variety of BMPs for metal abatement *(Wright Water Engineers and Geosyntec Consultants 2011)*. For total zinc, all of the tested BMPs showed significant reductions in concentration. In the studies that were surveyed, effluent values typically fell between 15 and 30 μg/L when inlet concentrations were in the range of 50-99 μg/L. Similarly, most types of BMPs resulted in statistically significant reductions of total copper, with the lone exception being wetland channels. Bioretention ponds, bioswales, filter strips, media filters, porous pavement, retention ponds, and wetland basins all worked for removing dissolved zinc, resulting in effluent concentration of 8-25 μg/L. However, fewer of the BMPs were effective for the removal of dissolved copper. Only detention basins, filter strips, and retention ponds showed significant decreases of dissolved copper, where the corresponding effluent (influent) concentrations were 4.8 (5.3), 5.3 (11.1), and 5.0 (7.5) μg/L, respectively. However, none of the BMPs reduced dissolved copper to below about 5 μg/L. Accordingly, cost-effective alternatives to current BMPs need to be developed that are pragmatic and relatively easy to maintain.

2.3   TECHNOLOGIES FOR REMOVING COPPER FROM SOLUTION

Heavy metal contamination is a major problem facing the management of stormwater, mine drainage, industrial wastewater, municipal wastewater, surface water, and groundwater. To mitigate this problem, a number of treatment technologies have been developed and utilized. The most well-known and prevalent technologies include membrane filtration, adsorption, chemical precipitation, bioremediation, and ion exchange. What follows are descriptions of the different treatment technologies along with an analysis of their abilities to remediate copper, as well as a discussion of their advantages and disadvantages with respect to stormwater treatment.

2.3.1 Membrane Filtration

Membrane filtration processes are typically categorized by the membrane pore size and the driving force that enables flow across the membrane. A review by Fu and Wang *(Fu and Wang 2011)* summarized a variety of membrane filtration processes, including ultrafiltration (UF), nanofiltration (NF), reverse osmosis (RO), and electrodialysis (ED). UF, NF, and RO are pressure driven processes where the membrane pore size decreases in the order of UF > NF > RO. Typical cutoff molecular weights for separation by UF, NF and RO range between 1000 ~ 500000 Daltons, 100 ~ 1000 Daltons, and less than 100 Daltons, respectively. Because copper ions are smaller than the pore sizes of UF membranes, large molecular weight surfactants or polymers are complexed with metal ions prior to UF. The removal efficiency by UF varies considerably, and depends on the addition of surfactants, the type of metal and metal

concentrations. However, efficiencies for removal of copper by UF can be as high as 94% ~ 99.5% for initial concentrations from 10 to 160 ppm when conditions are optimized. A semi-permeable membrane is used in RO that prevents metal cations from passing through the pores. Similarly, NF can potentially contain pores small enough for metal ion exclusion, but this is dependent on the specific membrane. The efficiencies for remediation of copper are approximately 70-99.5% for RO and 47-98% for NF. Electrodialysis (ED) is a charge driven membrane processes where the separation of ions by an electric field is achieved by charged membranes. Although membrane filtration processes can usually remove metals or other contaminants to very low levels, the high costs of membrane filtration (materials and power requirements, along with the need for continual attention from skilled operators) makes it inappropriate for distributed stormwater treatment.

2.3.2 Chemical Precipitation

Chemical precipitation is known for its low cost and simplicity. Chemical reagents are added to solutions containing metals, resulting in the formation one or more metal precipitates when solubility products are exceeded. Insoluble metal hydroxides, for example, can be formed at elevated pH (usually > pH 6). The use of lime and limestone in metal removal from acid mine drainage has been successfully carried out, indicating that both materials are useful for waste neutralization and metals abatement *(Singh and Rawat 1985; Wu et al. 2003)*. Both research groups demonstrated that most of the studied metals (Cu, Ni, Cd, Zn, Pb, Mn, Al, Hg, and Fe) can be efficiently removed. For instance, 23.18 mg/L of copper in copper mine drainage was reduced to 0.02 mg/L when pumping the solution through a limestone fluidized bed system *(Wu et al. 2003)*. The high removal efficiency was attributed to the increase of pH (from pH 6.3 to pH 8.7) and resulting formation of metal hydroxides. A drawback of chemical precipitation is that it typically requires the addition of chemical reagents. Furthermore, adequate reaction time and facilities for particle removal are required, typically necessitating a large basin and control over the process flow rate. Chemical addition to an intermittent and variable flow is challenging, making it difficult to perform with stormwater runoff. Ultimately, this process is dependent on the solubility of the precipitated substance, which is often not suitable for removing metals to trace quantities. Based on these limitations, chemical precipitation processes are not a desirable method for trace metals removal in stormwater treatment.

2.3.3 Biological Remediation

A variety of microorganisms, including yeasts, bacterial strains, and algae have been studied for bioremediation and have demonstrated promise with respect to water quality improvement *(Chatterjee et al. 2011; Imani et al. 2011; Joshi et al. 2011; Ramirez-Paredes et al. 2011)*. Depending on the organisms used, biosorption, ion exchange, complexation, microprecipitation, and redox reactions can be involved in metal ion removal. For instance, biosorption onto cell walls and precipitation by components generated from cellular metabolites can occur in microbial bioremediation *(Imani et al. 2011)*. The results from this study also revealed two stages (rapid and slow) for metal removal by Dunaliella alga. In the first (rapid) stage, sorption onto the surface of microorganisms occurred, resulting in > 65% removal of Cd, Pb, and Hg. In the second (slow) stage, metal ions were transported through the cell membranes, resulting in a final removal of over 80%. Several fungi have also demonstrated promise as metal adsorbents. The adsorption capacities for aqueous lead by Aspergillus terreus and aqueous cadmium by

Trichoderma viride were 59.67 and 16.25 mg/g, respectively, at initial metal concentration of 50 mg/L *(Joshi et al. 2011)*.

Although numerous studies have demonstrated that bioremediation has the potential for metals abatement, most tests were executed at high metal concentrations (ppm levels). Further studies are needed to determine the capabilities of bioremediation at low metals concentrations typical of stormwater runoff. Furthermore, metal removal by biological processes is highly pH and temperature dependent. For example, tests involving a chromium-reducing bacterial strain Cellulosimicrobium cellulans KUCr3 indicated the organism performed optimally in a pH range from 7 to 8 and a temperature range of 30 to 40°C *(Chatterjee et al. 2011)*. It would be difficult to control these variables in stormwater runoff, and thus it is challenging to predict removal efficiencies accurately.

2.3.4 Ion Exchange

Another technique that is widely used in water treatment is ion exchange. This process is related to adsorption (see section 2.4) and can be referred to as exchange adsorption. In ion exchange, the metal or metal complex to be removed is exchanged for a different ion on the surface of a resin until equilibrium is achieved. The exchangeable ions on the surface of ion exchangers are replaced for a stoichiometrically equivalent amount of ions that need to be removed. In general, counter-ions with high valence are preferred. A typical cation exchange process is shown in Equation 2.1.

$$2MX(\text{ion exchanger}) + Me^{+2}_{(aq)} \rightleftharpoons MeX_2 + 2M^+ \tag{2.1}$$

The resins are regenerable in most ion exchange processes. The regeneration processes consists of backwashing to remove any sediment, followed by a regeneration step where a solution with high concentration of M^+ (Equation 2.1) is used to displace the adsorbed metals. Finally, the resin is flushed to rinse out the chemicals used in regeneration. In the regeneration step, the removed ions are highly concentrated and disposal is a key issue *(Wachinski and Etzel 1997)*. If it is a strong-acid resin, acid must be used in regeneration processes so that H^+ can be exchanged with the removed cations.

One example of an ion exchange process is the utilization of zeolites to remove heavy metals, a process that has been studied by several groups and has demonstrated fairly high removal efficiencies *(Pitcher et al. 2004; Genc-Fuhrman et al. 2007; Wu and Zhou 2009; Fu and Wang 2011)*. Increases in the concentrations of sodium, calcium and other ions during batch studies were considered to be an indication of ion exchange process, where metal ions were replacing the released cations at the zeolite surface. However, Pitcher et al. *(Pitcher et al. 2004)* indicated that metal precipitation resulting from elevated pH might also contribute to the removal efficiencies. Dowex XFS-4195, a commercial exchange resin, has been reported to have high affinity for copper and nickel and suitable for use in solutions with low pH. However, when using this resin at low pH, strong acid is required for regeneration *(Czupyrna et al. 1989; Dabrowski et al. 2004)*. Other commercial ion exchange resins, such as Amberlite IRC-718 (Rohm and Haas Co.), and Duolite CS-346 (Diamond Shamrock), have also been demonstrated to have high selectivity for copper.

In general, commercial resins are characterized by different functional groups and have variable selectivity with respect to different metals. Ion exchange resins are typically regenerable, require little energy, and have relatively low operating costs. However, special regenerating treatment is required under specific circumstances. For instance, cheap and readily available acids like sulfuric acid cannot be used in regenerating resins containing a high proportion of calcium, due to the formation of calcium sulfate precipitates. The selectivity toward different metals needs to be considered to remove specific target metals efficiently. The effective operating time of resins should also be appropriately studied before using resins in stormwater treatment. While exchange resins have been shown to be effective at removing metals, the necessity of regeneration and the potentially prohibitive costs makes using commercial ion exchange resins challenging for stormwater treatment.

2.3.5 Adsorption

Adsorption has proven to be a highly effective and economical choice for the remediation of a number of contaminants, including heavy metals. A wide variety of adsorbents exist. The efficiency of these materials is a function of the solution chemistry as well as the specific metal involved. What follows is a review of available adsorbents for heavy metals and the efficiencies that were achieved for metals removal.

The adsorption capacities of clays *(Malandrino et al. 2006; Swami and Buddhi 2006; Jiang et al. 2010)* and red mud *(Swami and Buddhi 2006; Nadaroglu et al. 2010)* have been examined by many groups. For example, Jiang et al. *(Jiang et al. 2010)* demonstrated the efficient removal of lead from industrial wastewater using kaolinite clay (from 160 mg/L to 8 mg/L) and showed that adsorption equilibrium was reached within 30 minutes. Trivalent chromium was effectively removed (99.9%) by red mud *(Swami and Buddhi 2006)*, although the removal efficiency for copper was much lower (27-31%) *(Nadaroglu et al. 2010)*.

Several bio-adsorbents have also been explored. Seafood processing wastes such as sludge and crab shell were observed to have effective uptake of the studied heavy metals (Cu, Cd, Mn, Co, Pb, Zn, Ni) *(Lee and Davis 2001; Vijayaraghavan et al. 2010)*. In particular, more than 60% copper was adsorbed by the wastes when the initial pH was approximately 5. Adsorption processes can be pH dependent, and the adsorption capacity of the abundantly available and cost-effective bio-adsorbent brown seaweed-*Cystoseira indica* is maximized at pH 6. In one study, the adsorption capacities of brown seaweed were 125.42 mg/g for copper at an initial concentration of 195.7 mg/L, and 97.96 mg/g for nickel at an initial concentration of 146.9 mg/L *(Basha et al. 2009)*. Bioretention systems with compost-amended soil have also been investigated, demonstrating the potential for adsorption of as much as 88% of dissolved copper *(Davis et al. 2003; Sun and Davis 2007; Li and Davis 2009)*.

Animal bone, primarily consisting of hydroxyapatite, has also demonstrated promise as an adsorbent of heavy metals *(Ma et al. 1994; Al-Asheh et al. 1999; Wright and Conca 2002; Conca and Wright 2006; Bogya et al. 2009; Kim et al. 2009; Oliva et al. 2010)*. In one study, 86.7% of copper and 31.8% of nickel were remediated by animal bone at initial metal concentrations of 100 mg/L *(Al-Asheh et al. 1999)*. Apatite II™, a fish bone derived material, has also been shown to achieve high removal efficiencies. Several metals (Zn, Pb, Mn, Fe) initially

present at concentrations of 30-75 mg/L were reduced to below 0.1 mg/L by Apatite II™ in acid mine drainage *(Oliva et al. 2010)*.

Removal efficiencies of metals using different adsorbents are summarized in Table 2.1, along with the corresponding initial concentrations. These results indicate that there a number of promising adsorbents that have shown the ability to remove heavy metals from aqueous solutions.

Table 2.1: Metal Removal Efficiencies by Different Adsorbents

Adsorbents	Metals	Initial Concentration	Removal Efficiency (%)	References
Clay	Pb, Ni, Cd, Cu	30 (mg/L)	>60% for all metals	*(Jiang et al. 2010)*
	Cd, Cu, Mn, Ni, Pb, Zn	0.1 (mM)	>98% for all metals	*(Malandrino et al. 2006)*
Red Mud	Cr	1500 (mg/L)	99.9%	*(Swami and Buddhi 2006)*
	Cu	0.537 (mg/L)	31.3%	*(Nadaroglu et al. 2010)*
		0.506 (mg/L)	27.5%	
Seafood Processing Waste Sludge	Cu	0.01 (mM)	>60%	*(Lee and Davis 2001)*
	Cd	0.01 (mM)	>50% at pH >5	
Crab Shell	Mn	20.6 (mg/L)	86.9%	*(Vijayaraghavan et al. 2010)*
	Cu	5.14 (mg/L)	99.3%	
	Co	4.96 (mg/L)	85.8%	
	Cd	3.22 (mg/L)	98.7%	
	Ni	4.85 (mg/L)	99.8%	
	Zn	4.39 (mg/L)	99.8%	
	Pb	1.01 (mg/L)	≥95.0 %	
Apatite II™	Zn	50 (mg/L)	>99.5%	*(Oliva et al. 2010)*
	Pb	29 (mg/L)		
	Mn	75 (mg/L)		

Adsorbents	Metals	Initial Concentration	Removal Efficiency (%)	References
Apatite II™	Zn	44.7-147 (mg/L)	>99.8%	*(Conca and Wright 2006)*
	Pb	0.5-1.4 (mg/L)	>90%	
	Cd	0.3-0.8 (mg/L)	>93%	
Brown Seaweed	Cu	1305 (mg/L)	90-95% at pH 6	*(Basha et al. 2009)*
	Ni	1075 (mg/L)		
Compost (Bioretention)	Zn	1.44 (mg/L)	97%	*(Sun and Davis 2007)*
	Cu	0.17 (mg/L)	93%	
	Pb	0.16 (mg/L)	97%	
	Cd	0.048 (mg/L)	>98%	
	Cu	0.047 (mg/L)	97% at pH 6	*(Davis et al. 2003)*
	Pb	0.091 (mg/L)	≈100%	
	Zn	0.85 (mg/L)	≈100%	
Banana Peel	Cu, Pb	10 (mg/L)	>90% at pH 3, >98% at pH 4 & 5	*(Castro et al. 2011)*

In many instances, several of the processes described above occur simultaneously, and it is difficult to attribute metals removal to just one process. For example, it is common for chemical precipitation, adsorption, and ion exchange to be occurring simultaneously when many alternative adsorbents are used. Regardless of the adsorbent, metals removal by these processes can be affected by environmental conditions such as temperature *(Wu et al. 2003; Nadaroglu et al. 2010)*, pH *(Lee and Davis 2001; Pitcher et al. 2004; Basha et al. 2009; Jiang et al. 2010; Kannan and Veemaraj 2010; Nadaroglu et al. 2010; Liu and Zhang 2011; Moreno-Pirajan and Giraldo 2011)*, and ionic strength *(Malandrino et al. 2006; Jiang et al. 2010)*.

Metals removal has been shown to increase with increasing temperature due to the insolubility of metal precipitates at higher temperature *(Wu et al. 2003)*, and from increases in adsorption kinetics and capacities *(Nadaroglu et al. 2010).* Adsorption capacity is also a function of pH, with efficiency increasing at higher pH. This is due in part to the coupled precipitation reactions that occur at pH values greater than 6, as well as the deprotonation of surface oxide groups at high pH values, which results in more negatively charged surface sites that are capable of binding metals. Additionally, at low pH, protons outcompete metals for adsorption sites, resulting in lower adsorption capacities *(Nadaroglu et al. 2010; Moreno-Pirajan and Giraldo 2011)*. In other studies, increases in ionic strength (up to 0.1 M) resulted in decreased metal removal due to competition for available adsorption sites *(Malandrino et al. 2006; Jiang et al. 2010)*. Finally, it is also known that adsorption capacity increases with available surface area

(Malandrino et al. 2006; Swami and Buddhi 2006). As such, smaller adsorbent particles are typically more efficient due to their higher surface area to volume ratios.

Of the available technologies, adsorption shows the most promise for application in stormwater BMPs, a conclusion that was echoed by a recent report summarizing methods for measuring and removing dissolved metals from stormwater *(Barrett et al. 2014).* Adsorption processes have demonstrated high removal efficiencies and require less maintenance than the alternative mechanisms. Additionally, there is a variety of available adsorbents, including an array of cost-effective and natural alternatives. Based on this evaluation, selecting and evaluating promising adsorbents for remediating metals from stormwater runoff is an appropriate next step in implementing effective BMPs.

2.4 ADSORPTION THEORY

Adsorption is the adhesion and accumulation of dissolved molecules on the surface of a solid phase. One mechanism for this process is via direct chemical bonding to a surface site, and is often indistinguishable from ion exchange processes. Non site-specific mechanisms include electrostatic and van der Waals interactions between the solid phase (adsorbent) and the chemical of interest (adsorbate). Adsorption processes are limited both by equilibrium and the kinetics of mass transfer, and a proper evaluation of adsorption involves an assessment of each of these parameters *(Faust and Aly 1987).*

Adsorption processes typically involve flow of a liquid or gas through a porous solid phase, resulting in solid partitioning of the adsorbate. In environmental engineering, the most commercially available and readily studied adsorbent is activated carbon, which has been shown to remove a wide variety of chemicals. It is highly porous, resulting in a large surface area to volume ratio and providing an abundance of surface sites. However, activated carbon is expensive and its production is energy intensive, leading to studies aimed at utilizing more economical and equally effective adsorbents.

To evaluate the equilibrium adsorption capacity, relationships are developed plotting the equilibrium adsorption density (q_e) against the equilibrium aqueous phase concentrations (C_e). The resulting plot is referred to as the *adsorption isotherm.* In environmental applications, isotherms are typically modeled by fitting the curve to a *linear, Langmuir,* or *Freundlich* equation.

The linear isotherm characterizes systems where aqueous concentration is directly proportional to adsorption density. The slope of the linear relationship is termed the *partitioning coefficient*, and is typically given the symbol K_d. Linear isotherms are typical in situations where adsorbate concentration is low and adsorbent is readily present, resulting in an excess of available adsorption sites. The linear isotherm is shown in Equation 2.2.

$$q_e = K_d C_e \qquad\qquad (2.2)$$

The Langmuir isotherm is relevant in situations where adsorption is limited to a finite number of specific adsorption sites, where all sites are assumed to be identical. A maximum adsorption capacity is the result, where an increase in aqueous concentration no longer changes adsorption density. The Langmuir isotherm is shown in Equation 2.3, where q_{max} is the maximum adsorption capacity, and K_L is the Langmuir adsorption coefficient.

$$q_e = \frac{q_{max}K_L C_e}{1 + K_L C_e} \tag{2.3}$$

The Freundlich isotherm is used in situations where adsorption capacity is limited based on the available binding area on the solid surface, but cannot be accurately modeled by the finite surface site approach. A maximum is not reached, but the rate of increase of q_e decreases with increasing C_e. The Freundlich isotherm is modeled using Equation 2.4, where n and K_f are the Freundlich fitting parameters.

$$q_e = K_f C_e{}^n \tag{2.4}$$

In addition to the classic adsorption isotherms in Equations 2.2-2.4, apparent adsorption density can be modeled using the approach developed by Farley et al. *(Farley et al. 1985)* which combines surface adsorption and surface precipitation. In this model, surface precipitation (q_{sp}) is governed by Equation 2.5, where φ is the mass of adsorbent that contributes to precipitation divided by adsorbent surface area, and C_e' is the adsorbate concentration that would be in equilibrium with the pure precipitated solid. Apparent adsorption density ($q_{e,app}$) is the sum of surface adsorption and surface precipitation, and is shown in Equation 2.6. Typically, adsorption dominates at lower concentrations, surface precipitation dominates at higher concentrations, and the resulting isotherm is concave up based on the unbounded potential for precipitation at values above C_e'.

$$q_{sp} = \frac{\varphi(C_e/C_e')}{1 - (C_e/C_e')} \tag{2.5}$$

$$q_{e,app} = q_e + q_{sp} \tag{2.6}$$

Example isotherms for each of these models are shown in Figure 2.1. These curves are meant to represent the general shape of each isotherm, and do not reflect exact magnitudes.
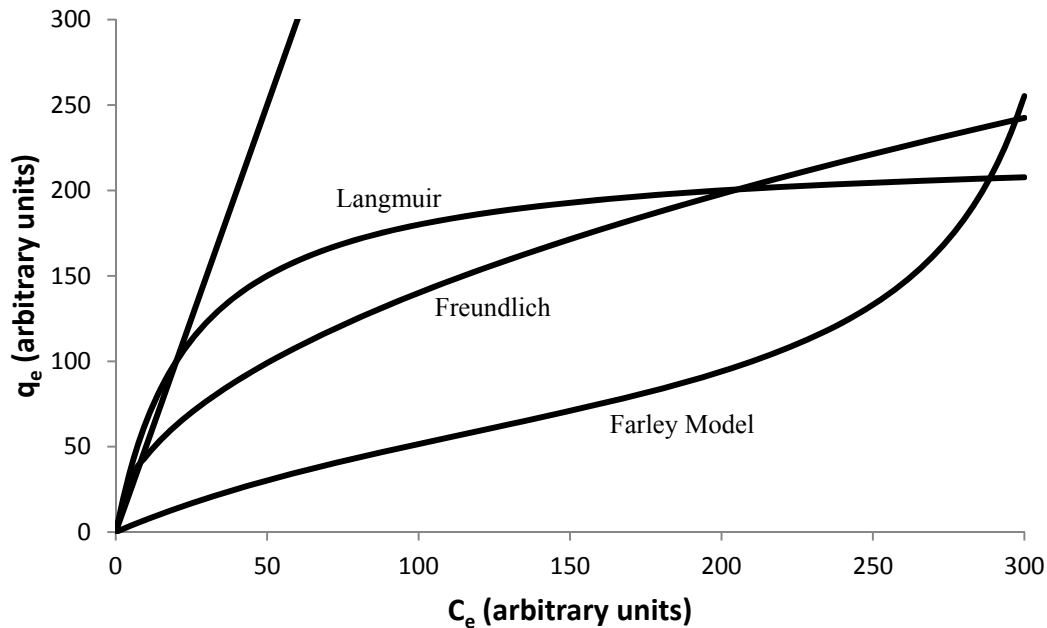
Figure 2.1: Example linear, Langmuir, Freundlich, and Farley model isotherms

2.5   MEDIA TYPES FOR STORMWATER FILTRATION

Based on the analysis of stormwater BMPs, as well as the review of available technologies for removing metals, it was concluded that filtration based BMPs using efficient adsorbents are the most promising method for removing dissolved metals from stormwater runoff. However, field experiments using actual stormwater have not achieved effluent concentrations lower than 4.8 µg/L. This indicates a need to evaluate promising media types that could result in effluent concentrations below the desired 2 µg/L threshold. The following is a detailed evaluation of the available literature concerning the two media types that were chosen for evaluation.

One media type chosen for this project was Apatite II™ (US Patent #6,217,775), a biogenically derived hydroxyapatite. Hydroxyapatite, $[Ca_{10}(PO_4)_6(OH)_2]$, is the major component of animal bone, and known for its high removal capacity for heavy metals. Apatite II™ has high affinity toward strontium, europium, trivalent actinides, and uranium. Because of this, it could potentially be a cost-effective adsorbent for nuclear waste treatment *(Wright and Conca 2002; Krejzler and Narbutt 2003)*. Aside from radionuclide remediation, recent studies have also indicated that Apatite II™ can effectively remove divalent heavy metals *(Conca and Wright 2006; Oliva et al. 2010)*. Due to the composition of Apatite II™, $[Ca_{10-x}Na_x(PO_4)_{6-x}(CO_3)_x(OH)_2]$ (where $x < 1$), the release of PO_4^{3-} upon dissolution promotes metal precipitation as metal-phosphate solids. Additionally, metals can be adsorbed onto the surface of Apatite II™ through the uncompensated hydroxyl and phosphate groups. These metals can also be precipitated as metal salts stimulated by biological processes. It is thought that CH_2O contained in the Apatite II™ structure supplies electrons and serves as the carbon sources for SO_4^{-2} reducing bacteria to generate sulfide, leading to the precipitation of metal sulfides *(Conca and Wright 2006)*. Furthermore, dissolution of Apatite II™ makes it a strong pH buffer

14

(releasing phosphate, carbonate, and hydroxide), typically resulting in a final pH of 6.5-7.5, where many metal hydroxide species are insoluble.

In experiments utilizing rapid small-scale column tests (RSSCTs) to evaluate heavy metals removal in passive treatments, Apatite II™ was shown to be effective at removing Cd, Cu, Ni, Co, Hg, Zn, Pb, Mn, and Fe *(Oliva et al. 2010, 2011)*. The proposed removal mechanism was precipitation of metal phosphates, with a hypothesized copper precipitate of $Cu_2(PO_4)OH(s)$ *(Oliva et al. 2011)*. Apatite II™ has also been used as a permeable reactive barrier to treat acid mine drainage in shallow alluvial groundwater. While this work principally evaluated removal of Zn, Pb, and Cd, it was reported that copper levels were reduced from 230 µg/L to less than 2 µg/L *(Conca and Wright 2006)*. However, the available literature concerning copper removal using Apatite II™ is from experiments analyzing acid mine drainage in groundwater. These situations have much higher metal concentrations, lower flow rates, and different aqueous chemistry than stormwater runoff. As a result, additional testing in laboratory and field settings is warranted to evaluate the use of Apatite II™ in stormwater applications.

Compost amended BMPs such as vegetated swales, detention ponds, and media filter drains are currently utilized in Oregon. They serve as a benchmark for metals removal. As such, alternative media such as Apatite II™ should not be used to replace compost in BMPs until a direct comparison of the two media is performed. In batch reactions with compost in synthetic stormwater containing Cu, Pb, and Zn, compost was found to be a highly effective adsorbent, exhibiting removal efficiencies of 93% for Cu, 97% for Pb, and 88% for Zn when reacting 200 mL solutions containing 100 mg/L initial metal concentrations with 5 g of compost *(Seelsaen et al. 2007)*. This study also found that smaller particle sizes have greater adsorption capacities due to larger surface area to volume ratios, which has important implications on design and estimation of a treatment system's service life. Another study evaluated the removal of the same three metals with compost and found adsorption to follow a Langmuir isotherm with maximum adsorption capacities of 1 mmol/g for Pb, 0.5 mmol/g for Cu, and 0.3 mmol/g for Zn *(Paradelo and Barral 2012)*. A key conclusion from that study was that sorption affinity for the three metals was in the following order: Pb>Cu>Zn. A similar study evaluating metals removal from compost arrived at the same binding order for Pb, Cu, and Zn *(Grimes et al. 1999)*. This demonstrates that copper will adsorb preferentially over zinc despite being at significantly lower concentrations in stormwater runoff. Additionally, Grimes *et al. (Grimes et al. 1999)* found that once adsorbed, heavy metals were not found to leach back into solution. As a result, compost can be used in filters for an extended period of time without the possibility of contaminants re-entering the effluent stormwater. It is important to note that these studies were all performed at concentrations much higher than typically found in stormwater, so further lab investigations are warranted to see if compost remains a viable adsorbent at metal concentrations relevant to stormwater runoff.

In addition to lab experiments, compost has been evaluated in a variety of field or pilot scale applications. In pilot-scale work evaluating a bioretention system with compost amended soils in synthetic runoff, 88% of dissolved copper was removed as a result of water percolating through the system at a loading rate of 4.1 cm/hr *(Sun and Davis 2007)*. Of this removal, >90% was attributed to adsorption to the compost amended soils. In similar pilot scale work using filters with layers of compost and sand, copper removal efficiency was variable depending on influent

concentrations, but effluent concentrations were consistently 5-10 µg/L *(Johnson et al. 2003)*. This indicates that compost would likely be an effective media for higher concentration copper loading associated with the first flush and in areas with high runoff concentrations, but may not be capable of removing copper to concentrations lower than 5 µg/L. However, compost will inherently vary from vendor to vendor, and extension of results from other studies should be exercised with an appropriate amount of caution.

While copper is the focal point of this project, It is important to note that copper is not the only constituent of concern in stormwater runoff. In particular, stormwater BMPs are typically designed to removed sediment and nutrients such as dissolved carbon, nitrogen, and phosphate. As mentioned previously, there are also several other heavy metals commonly present in stormwater runoff. Accordingly, any evaluation of a proposed treatment method should include a comprehensive analysis of the effect on downstream water quality, with particular focus on parameters that are commonly treated in stormwater runoff. This is especially important in light of the evidence seen in previous work that Apat*ite II™ leaches significant amounts of carbon and phosphate (Martin et al. 2008; Oliva et al. 2011)*, and compost has the potential to leach carbon and other nutrients *(McLaughlan and Al-Mashaqbeh 2009)*.

2.6   IMPACT OF NATURAL ORGANIC MATTER ON REMOVAL PROCESSES

A thorough understanding of metal speciation and complexation is critical to evaluating the effect metals will have on the environment. In particular, bioavailability and environmental fate and transport are strongly dependent on metal speciation *(Luoma 1983; Bhavsar et al. 2004)*. For copper, speciation in the environment is typically governed by the presence of organic ligands *(Buck and Bruland 2005)*. In stormwater runoff, recent work has demonstrated that across four sampling locations in Oregon >99.9% of total dissolved copper was complexed with organics *(Nason et al. 2012b)*. Organic matter in stormwater is derived from both natural sources such as decaying plant matter and anthropogenic sources such as petroleum products. It is widely present in stormwater runoff, with concentrations that vary due to temporal effects and land cover *(McElmurry et al. 2013)*. Recent stormwater sampling analysis found median DOC concentrations ranging from 2.5-7.0 mg/L across four sites in Oregon *(Nason et al. 2012a)*. Similar work in California found the median concentration across 34 sampling sites to be 13.1 mg/L *(Kayhanian et al. 2007)*. Because of the importance of organic matter on speciation, and its ubiquitous presence in stormwater runoff, it is vital to understand the effect NOM has on any proposed treatment process.

The effect NOM has on metal removal is variable and dependent upon the specific combination of solid phase, metal, and organic matter. However, these interactions can be grouped based on the mechanism by which NOM affects removal. In many cases, Cu-NOM complexes form and subsequently reduce partitioning into the solid phase. This effect has been observed with dissolved organic carbon impacting fate and transport of metals in rivers *(Lu and Allen 2001)*; the formation of copper and humic acid complexes (Cu-HA) subsequently reducing copper adsorption onto calcite *(Lee et al. 2005)*; metal-NOM complexes inhibiting adsorption of copper, cadmium, and nickel onto goethite in groundwater samples *(Buerge-Weirich et al. 2002)*; and Cu-NOM complexes reducing copper adsorption onto compost and montmorillonite *(Martínez-Villegas and Martínez 2008)*. Removal can also be inhibited by sorption of organics onto the

solid phase, thereby blocking surface adsorption sites or preventing the growth of precipitates. This effect was observed with NOM reducing adsorption of cis-1,2-dichloroethene and hexahydro-1,3,5-trinitro-1,3,5-triazocine (RDX) onto activated carbon *(Speth 1991; Morley et al. 2005)*, and NOM adsorption onto ferrihydrite preventing copper partitioning onto the solid phase *(Martínez-Villegas and Martínez 2008)*. Aside from inhibiting adsorption, NOM has also been shown to prevent precipitation and even solubilize copper precipitates *(Gao and Korshin 2013)*. However, in some instances NOM has been shown to improve metal adsorption rates. This occurs when NOM serves as a bridge between the adsorbent and metal, as was seen with humic acid increasing the uptake of copper by goethite *(Tipping et al. 1983)*. Furthermore, the effect of NOM can be a function of solution pH. This was demonstrated in experiments with copper and colloidal hematite particles in solution with fulvic acid, where sorption of copper onto hematite increased in the presence of fulvic acid at pH values below 6 and decreased at pH values above 6 *(Christl and Kretzschmar 2001)*. It is important to note that NOM partitioning onto the solid phase is not uniform among different types of organic molecules. Molecular weight, aromatic fraction, and abundance of phenolic and carboxylic functional groups dictate adsorption and complexation reactions *(Gao and Korshin 2013)*, and these properties will vary based on the organic molecule. This should be kept in mind as many studies utilize humic or fulvic acids to model NOM, which in reality may not correspond to the properties of NOM in stormwater.

In general, there are far more examples of NOM inhibiting metal removal as opposed to promoting removal, and this should be taken into account when evaluating a removal process. However, from the discussion above it is evident that the impact of NOM is not uniform among different treatment processes. It is therefore imperative to incorporate experiments with NOM into the evaluation of treatment options. Furthermore, in cases where NOM does inhibit metal removal, it may be unclear if NOM inhibition is occurring due to metal-NOM complexes or NOM adsorption onto the solid surface, which could have impacts on how a treatment process is designed.

Both media types evaluated in this study have been shown to leach organic matter. Thus, even if the influent water was free of organics, the impact of NOM cannot be entirely ignored because organics will be introduced into the solution by the media itself. For compost, leaching occurs in two phases, with an initial period characterized by rapid release of organics, followed by much lower leaching rate controlled by intra-particle diffusion *(McLaughlan and Al-Mashaqbeh 2009)*. Organic leaching from Apatite II™ is dependent upon pretreatment methods, and has been directly shown to impact the sorption of lead *(Martin et al. 2008)*.

2.7   STORMWATER SAMPLING

There has been a considerable amount of work evaluating potential media types for stormwater treatment in laboratory settings, typically in batch systems that yield an isotherm or report the removal efficiency *(Jang et al. 2005; Seelsaen et al. 2007; Paradelo and Barral 2012)*. However, this work was all performed with synthetic stormwater that may not accurately model actual stormwater runoff. Additionally, there has been little work that directly compares laboratory and field results. This makes it difficult to assess how well laboratory results reproduce actual performance in field settings. In one study that did attempt to validate laboratory data with pilot scale experiments, copper removal efficiencies were much lower in the

pilot scale experiment *(Johnson et al. 2003)*. Accordingly, it is imperative that evaluation of media for stormwater BMPs includes field-based studies to confirm laboratory results.

To monitor stormwater characteristics in the field accurately, a properly chosen field-sampling plan must be employed. In a project evaluating different stormwater sampling designs, over 1700 stormwater samples were collected over an entire wet season and Monte Carlo simulations were performed to assess the optimal sampling strategy for within storms and among different storms *(Leecaster et al. 2002)*. It was found that for in-storm sampling, the best strategy is to take flow-weighted composite samples, with a recommended 12 samples forming the composite. For sampling among storms, the best approach is to randomly choose medium to large sized storms. For evaluating annual mean concentrations, sampling seven randomly chosen storms is the most efficient method for attaining a small confidence interval on the mean.

The Washington State Department of Ecology has published comprehensive guidelines for the evaluation of a prospective stormwater treatment technology *(Washington State Dept. of Ecology 2008)*. Some of the most important points with respect to stormwater sampling within the scope of this project are outlined below:

- Automated samplers with Tygon or Teflon tubing should be used.

- Flow-weighted composite samples are the most appropriate for short detention time flow-through devices. As a general rule, 10 samples should be targeted for a given event.

- Depth measurement devices are the most suitable for assessing flow in low velocity scenarios. Flow should be logged continuously on <15 minute intervals.

- Inlet and outlet samples should be taken to measure system performance accurately, with samples taken at representative locations.

- Store and transport all samples on ice.

- Decontaminate sample bottles and tubing between each sampling event, and perform sampling blanks at least once to demonstrate decontamination procedure is effective.

3.0   MATERIALS AND METHODS

3.1   APATITE II™

Apatite II™ (US Patent #6,217,775) is a biogenically derived hydroxy calcium phosphate mineral that was purchased from PIMS NW, Inc. Apatite II™ is comprised of a mineral phase with a general composition of $Ca_{10-x}Na_x(PO_4)_{6-x}(CO_3)_x(OH)_2$, with $x<1$, and an organic phase within the inorganic matrix that makes up 30-40% of the overall mass *(Conca and Wright 2006)*. In field experiments, the Apatite II™ was used as received (Figure 3.1), with the average particle size being approximately ½ inch. For laboratory experiments, Apatite II™ was ground in a blender and recovered from a 40x50 mesh sieve (Figure 3.2), then autoclaved and air-dried before use.

Figure 3.1: Whole Apatite II™

Figure 3.2:Sieve Apatite II™

3.2   COMPOST

Compost was acquired from Lane Forest Products Inc. in Eugene, OR, where it is produced at an industrial scale. It is sold as *Garden Compost*, and derived from selected yard debris that is composted using the company's established best management practices. The compost is frequently tested under the US Composting Council's Seal of Testing Assurance Program (STA), which mandates the compost be tested in certified independent labs for a suite of physical, chemical, and biological parameters. These data are summarized in reports that are made available upon request. The same compost was used in previous Oregon Department of Transportation (ODOT) media filter drain installations. The compost meets all required ODOT specifications. In field experiments, compost was used as received (Figure 3.3) and for laboratory experiments compost was dried, ground in a blender, and recovered in a 40x50 mesh sieve (Figure 3.4), then stored in an airtight bag until use.

Figure 3.3: Whole Compost

Figure 3.4: Sieved Compost

3.3   REAGENTS

All standards, solutions, and dilutions were prepared using 18.2 MΩ-cm distilled deionized (DDI) water from an ELGA Purelab Ultra System. Sample digestion and acidification prior to ICP analysis was done with ultrapure nitric acid (Aristar Ultra). Synthetic stormwater solutions were created with puratronic grade sodium chloride (Alfa Aesar) and ACS grade sodium

bicarbonate (EMD chemicals, Inc.). Suwanee River Natural Organic Matter (SRNOM) was used in experiments considering effects of organic matter. SRNOM isolate was obtained from the International Humic Substance Society (IHSS), and SRNOM solutions were prepared by dissolving the isolate in DDI water at pH 4.0 for 24 hours then filtering through a 0.22 μm membrane filter. Buffering of synthetic stormwater to the desired pH was done using ACS grade sodium hydroxide and ultrapure nitric acid (Aristar Ultra). Single element stock solutions (BDH Aristar, Sigma Aldrich TraceCERT, and Ricca) were diluted to create the desired standard concentrations for Inductively Coupled Plasma (ICP) spectroscopy and Ion Chromatography (IC).

3.4   APATITE II™ ANALYSIS

3.4.1 Crystal Structure

The crystal structure of the Apatite II™ media was characterized before and after column experiments. Samples were dried completely at 100°C in the oven for approximately 30 minutes, and then characterized using x-ray diffraction (Bruker AXS, D8 Discover 203259, XRD) with an Cu Kα x-ray source (λ=1.5406 Å). The measurement was conducted from 2θ = 20 – 55 degrees. Bruker Diffrac.EVA software was used for data processing and analysis.

3.4.2 Elemental Analysis

Surface morphology and chemical composition analyses of dried Apatite II™ were conducted using an FEI Quanta 600F Field Emission Scanning Electron Microscopy (SEM) operated at 30 kV. Chemical composition analyses were conducted using an EDAX Energy Dispersive Spectrometry (EDS) system. EDAX Genesis software was used to calculate the chemical composition using the ZAF method.

3.5   EQUILIBRIUM MODELING

Final metal concentrations in the batch tests with Apatite II™ were compared with those predicted by an equilibrium chemical thermodynamics model (visual MINTEQ). Parameters used in equilibrium modeling were determined based on the equilibrium conditions of batch tests, where pH was approximately 7.3, and phosphate and calcium concentration were chosen to be 20 and 6 mg/L, respectively. Other conditions such as ionic strength and other ions (i.e., Na^+, Cl^-, and $HCO3^-$) were all input at the initial concentrations of batch studies.

3.6   LABORATORY EXPERIMENTS

3.6.1 Equilibrium Batch Studies

Equilibrium batch studies were performed to assess metal removal capacity and determine the mechanisms driving metal ion removal by Apatite II™ and compost. Synthetic stormwater solutions were created with 0.185 mM $NaHCO_3$ and 1.0 mM NaCl based on background ionic strength and alkalinity found in highway stormwater runoff *(Nason et al. 2012a)*. In experiments considering the effects of organic matter, 0-10 mg/L Suwanee River Natural Organic Matter (SRNOM) was added to solutions. Synthetic stormwater solutions containing 0-20,000 μg/L Cu

were created, with each solution adjusted to an initial pH of 6. 100 mL aliquots of the synthetic solutions were added to acid-washed 125 mL high-density polyethylene (HDPE) bottles, with each initial metal concentration performed in triplicate. 200 mg of Apatite II™ or compost was added to each bottle, and bottles were subsequently placed in a tumbler for 48 hours based on time to achieve equilibrium (Figure 8.2). The solutions were then filtered through 0.45 μm Millipore filters and aliquots of filtered solution were taken for measurement of pH, phosphate, calcium, copper, and in some cases DOC. The pH was measured immediately, the aliquot for anion analysis was stored in polystyrene IC vials at 4°C until measurement using IC, the aliquot for DOC was stored in ashed TOC vials at 4°C until measurement, and the aliquot for metal analysis was acidified to pH 2 using ultrapure nitric acid and stored in polystyrene culture tubes at 4°C until measurement using ICP-OES. A flow chart of this process is shown in Figure 3.5.

Batch experiments without Apatite II™ were carried out to gain insight into metals removal by precipitation alone. Solutions containing copper or zinc at various concentrations (100-6400 μg/L), 1 mM of NaCl, 0.185 mM of $NaHCO_3$, 20 mg/L phosphate and pH adjusted to 7.3 were selected to predict possible precipitation (metal phosphates or metal hydroxides) during batch studies containing Apatite II™. 100mL of solution was placed in high-density polyethylene bottles and then placed in a tumbler for 2 days. Samples were then filtered and acidified for metals analysis. To further probe the role of phosphate in the precipitation process, solutions containing NaCl, $NaHCO_3$ and copper or zinc were adjusted to pH 7.3 without the addition of phosphate.
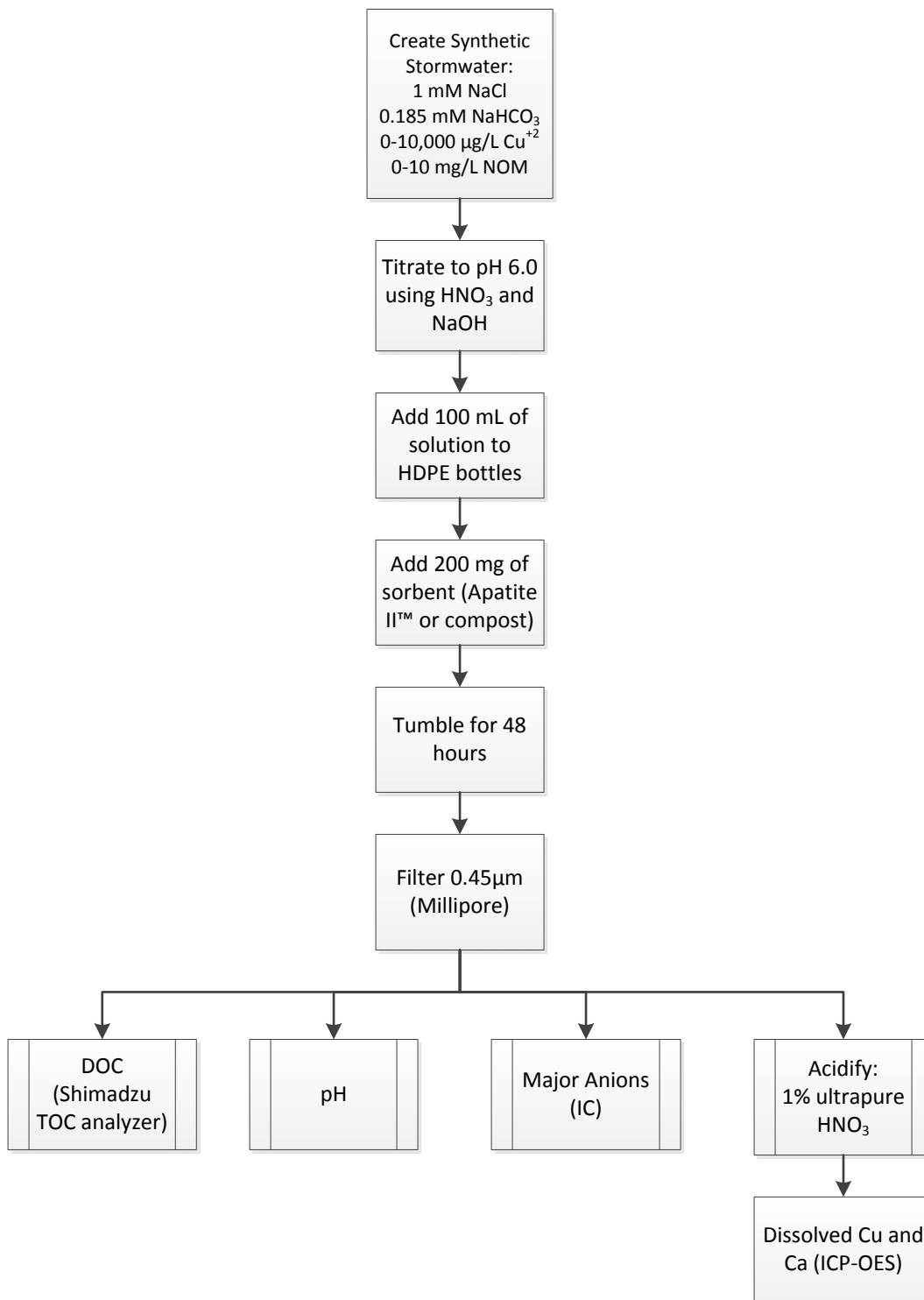
Figure 3.5: Process diagram for batch equilibrium experiments

3.6.2 Kinetic Studies

Kinetic studies evaluating copper sorption onto compost and Apatite II™ were performed to determine the time to reach sorption equilibrium. Synthetic stormwater samples were prepared with 0.185 mM NaHCO$_3$, 1.0 mM NaCl, and copper (95 µg/L for compost and 3 mg/L for Apatite II™), and then buffered to pH 6. Aliquots of synthetic stormwater and sieved media were added to polyethylene bottles with a liquid volume to media mass ratio of 1 mL to 2 mg, and then placed on a tumbler. Samples were removed from the tumbler after 1, 2, 3, 4, 5, 7.5, 24, 48, and 120 hours and immediately filtered through 0.45 µm membrane filters into polystyrene culture tubes. These samples were subsequently acidified with ultrapure nitric acid and analyzed for copper using ICP-OES.

A supplementary kinetics study was performed to analyze differences in copper removal kinetics between sieved and whole compost. Synthetic stormwater solutions were prepared as in previous studies, with an initial copper concentration of 110 µg/L. 500 mL aliquots of synthetic stormwater were added to 2.00 g of sieved and whole compost and each solution was immediately placed on a tumbler. After 0.25, 0.5, 0.75, 1, 1.5, 2, 4, 8, and 24 hours a 5 mL aliquot of each solution was taken and immediately filtered through 0.45 µm membrane filter into a polystyrene culture tube, then acidified with ultrapure nitric acid and subsequently analyzed for copper using ICP-OES.

3.6.3 Compost Mechanism Batch Study

Stock synthetic stormwater solutions were created containing 0.185 mM NaHCO$_3$, 1 mM NaCl, and 100 µg/L Cu. 100 mL aliquots of stock solution were combined with 200 mg of sieved compost in high-density polyethylene bottles. These solutions were then buffered to pH values of approximately 2, 3, 4, 6, and 8, with each initial pH performed in triplicate. Samples were then placed in a tumbler for 48 hours based on time to achieve equilibrium (Figure 8.2). After 48 hours samples were filtered through 0.45 µm membrane filters, an aliquot was taken for immediate measurement of pH, and an aliquot for metal analysis was acidified using ultrapure nitric acid and stored in polystyrene culture tubes at 4°C until measurement using ICP-OES.

3.6.4 NOM Inhibition Batch Study

Stock solutions were prepared using synthetic stormwater that consisted of 0.185 mM NaHCO$_3$, 1 mM NaCl, 50 µg/L Cu, and NOM concentrations of 0, 1, 4, and 10 mg/L. These solutions were then buffered to pH 6 using HNO$_3$ and NaOH, and processed using the following four cases, which are diagrammed in Figure 3.6.

1. Control: Synthetic stormwater solution without NOM reacted with Apatite II™

2. Synthetic stormwater pre-reacted with NOM for 48 hours, then reacted with Apatite II™

3. Apatite II™ pretreated with synthetic stormwater containing NOM but no copper for 48 hours, then supernatant replaced with synthetic stormwater that had been pre-reacted with Apatite II™, and finally this solution was spiked with copper

4. Copper and synthetic stormwater with NOM added to Apatite II™ simultaneously

Apatite II™ was pretreated with NOM for 48 hours based on previous work on the kinetics of NOM adsorption onto calcite *(Lee et al. 2005)* and ferric oxide *(Genz et al. 2008)*. To maintain consistency, copper was pretreated with NOM for 48 hours as well, which satisfies kinetic limitations of Cu-NOM complexation *(Paradelo and Barral 2012)*. After pre-treatment, the 50 mL samples were added to 100 mg of Apatite II™ in high-density polyethylene bottles and placed on a tumbler for 48 hours. Samples were subsequently filtered through 0.45 μm Millipore filters, and aliquots were taken for measurements of pH, DOC, phosphate, copper, and calcium.
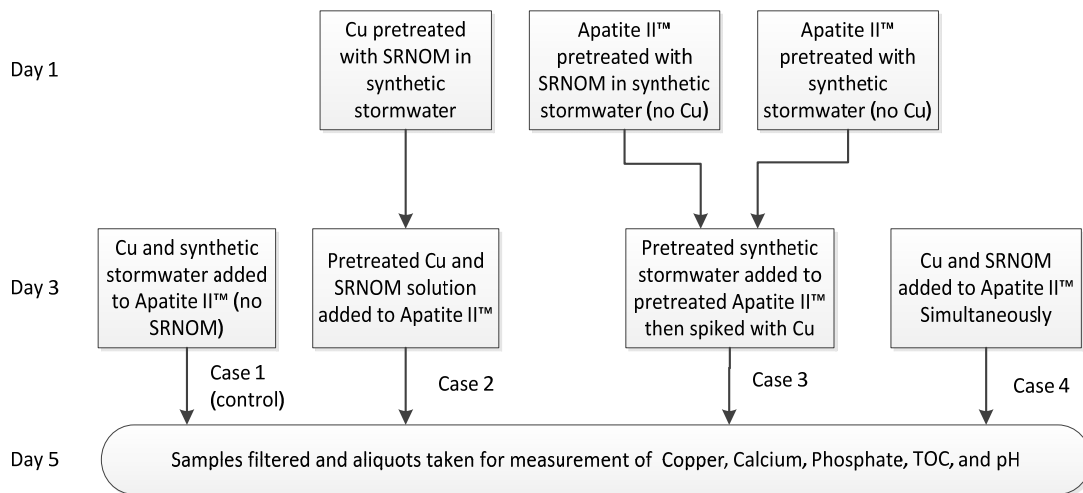
Figure 3.6: Process diagram for NOM inhibition batch studies

A similar experiment was performed using compost instead of Apatite II™. However, this experiment did not include Case 4, and in Case 3 synthetic stormwater that had not been pretreated was added to the pretreated compost on Day 3.

3.6.5 Column Tests

To assess the dynamic removal capacity of copper using compost and Apatite II™, Rapid Small Scale Column Tests (RSSCTs) were performed. A field-scale filter depth of 4 inches was chosen to represent a reasonable media depth in engineered stormwater systems. A loading rate of 1 gpm/ft2 was chosen as a practical stormwater flow rate, and was within the range of loading rates used in studies assessing other adsorbent media *(Hsieh et al. 2007; Champagne and Li 2009; Johir et al. 2009)*. The particle size of the media used in the small column (RSC = 0.18 mm) was selected to be in between the sizes used in previous work with other adsorbent media *(Genc-Fuhrman et al. 2007; Jiang et al. 2010; Vijayaraghavan et al. 2010)*. Using the chosen field depth and loading rate, column dimensions and loading rates were determined using RSSCT scaling relationships *(Crittenden et al. 1986)*. A glass column with a 1 cm inner diameter and adjustable Teflon plungers was used as the housing for the packed bed. This resulted in a

column to particle diameter ratio of 27.8, minimizing any potential wall effects *(Chu and Ng 1989)*. Prior to packing, the column and all tubing were purged with 10% HNO3 for 30 minutes followed by 45 minutes of DDI water at a flow rate of 20 mL/min. The column was then wet packed to a height of approximately 4.4 cm with ground media that had been recovered from a 40x50 mesh sieve. The flow rate through the column was 7.5 mL/min, and influent and effluent samples were taken on regular intervals to monitor column progress.

3.6.5.1 Synthetic Stormwater

To create a synthetic stormwater solution equivalent to those used in batch tests, stock solutions of Cu^{+2}, NaCl, $NaHCO_3$, and HNO_3 were pumped into a mixing chamber where they were diluted with DI water to achieve the desired concentrations and pH. The stock solutions were all pumped into the mixing chamber using syringe pumps, and DI water was pumped using a peristaltic pump. The resulting solution was pumped from the mixing chamber through the column using a peristaltic pump. Pressure leading into the column was monitored to ensure tubing stability. A schematic of this process is shown in Figure 3.7.
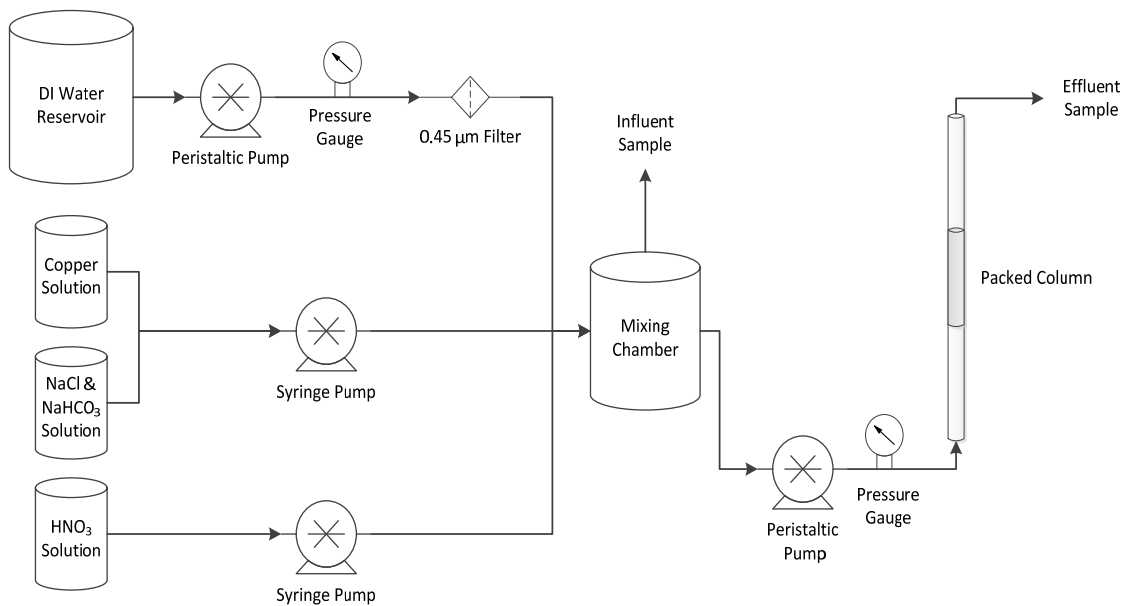
Figure 3.7: Flow diagram of RSSCT using synthetic stormwater

3.6.5.2 Natural Water

To provide for an adequate source of NOM and a closer approximation of actual conditions, natural water column tests were performed with both Apatite II™ and compost. Due to similarities in organic matter, pH, and conductivity, water from the Willamette River near Corvallis, OR was chosen as a reasonable stormwater surrogate for experimentation during the dry summer months. During the wet season a stormwater sample was taken from highway runoff in Salem, OR at the project field site. To prevent

clogging of the column with particulates, natural water samples were filtered with a 0.45 μm filter and stored at 4°C prior to being added to the influent tank. Aliquots of the filtered water were taken for pH, conductivity, copper, calcium, and DOC analysis. Natural water was pumped with a peristaltic pump at a flow rate of 8.5 mL/min into a mixing chamber, where it was mixed with a stock Cu^{+2} solution that was pumped from a syringe pump at 0.025 mL/min. This resulted in a 50 μg/L copper solution for the Apatite II™ in river water experiment, and a 95 μg/L copper solution for the compost in stormwater experiment. The resulting solutions were pumped though the column using a peristaltic pump. For the Apatite II™ column test, the syringe pump with the copper solution was turned off after 9 days, the mixing chamber was emptied and replaced, and the experiment was continued for two additional days with just river water flowing through the column. A schematic of the natural water column experiments is shown in Figure 3.8.
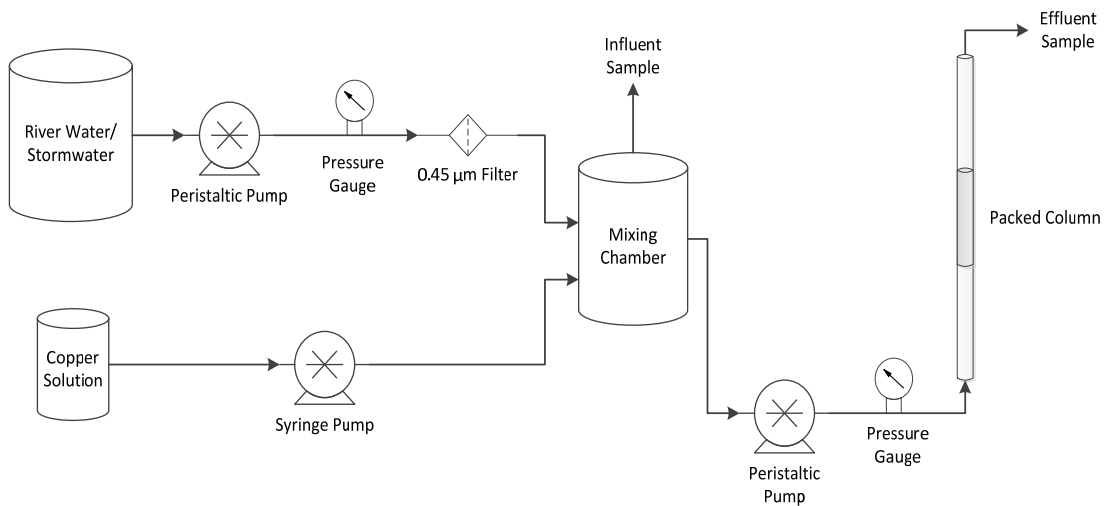
Figure 3.8: Flow diagram of TSSCT using natural water

3.7 FIELD EXPERIMENTS

3.7.1 Field Site Design

The field site design contained three components: an inlet box, a filter box, and an outlet box. The inlet box was built out of 3/8 inch polycarbonate sheeting and attached to the stormwater culvert using watertight silicone caulking. Two Johnson Ultima Bilge pumps (Model 32-47261), which are electronically activated when submerged, were fixed to the base of the inlet box using epoxy glue. A 1 foot wide contracted rectangular weir was positioned 3 inches above the base of the inlet box to stabilize the head above the bilge pumps, which delivered water to the filter box at a relatively stable rate when flow occurred over the weir. Pumps were used due to limitations in available head from the invert of the culvert to the water level in the ditch downstream of the culvert. Additionally, using pumps allowed for treatment of a fraction of total flow, allowing for

the construction of a reasonably sized filter while maintaining the desired loading rate of 1 gpm/ft^2 (based on scaling relationships discussed in section 3.6.5).

The filter box was built from 2 x 4 lumber and ½-inch plywood, was lined with polyethylene sheeting, and contained a PVC underdrain. The filter was 4x4 ft and divided vertically into three layers that were separated by cutouts of a highly permeable geotextile (ODOT drainage unwoven geotextile type 1, 85 gpm/ft^2 hydraulic capacity). The top layer was approximately an inch of pea gravel, the middle layer was 4 inches of Apatite II™ or compost, and the bottom layer was 3 inches of pea gravel, as shown in Figure 3.9. Pea gravel was used to keep the media in place, while preventing head loss in the filter. The underdrain flowed into a 1.5 inch inner diameter tube that connected the filter box to the outlet box, which exerted outlet control on the filter box. This resulted in water pooling just above the media, creating vertical flow through the filter and the desired residence times. Additionally, saturated flow conditions were created by this setup, which aligned with conditions in laboratory column experiments.

| Freeboard |
| Pea Gravel (1") |
| Geotextile |
| Apatite II™ (4") |
| Geotextile |
| Pea Gravel (3") |
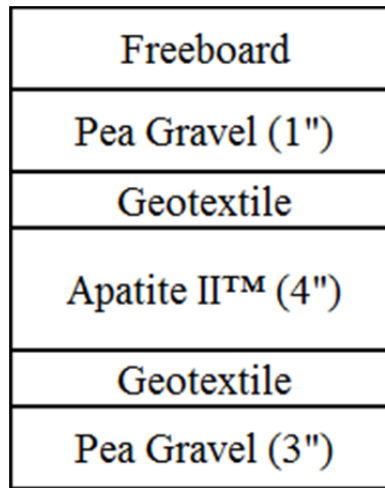
Figure 3.9: Vertical profile of the filter bed

The outlet box was also constructed out of 3/8 inch polycarbonate sheeting. A diffuser plate was located near the inlet to minimize turbulence, allowing for more representative sampling and accurate measurement of water depth. A 90-degree V-notch weir was installed to allow for flow measurements through the structure. A housing for the ISCO bubbler tube was installed to allow for depth measurements, and was located 1 foot from the V-notch weir to eliminate the effect of water drawdown on depth measurements.

Head loss calculations were performed to estimate the vertical distance between each of the three components, and the system was field tested to ensure proper function. An AutoCAD drawing of each component's dimensions is shown in Figure 3.10, and a photo of the site when set up with sampling equipment is shown in Figure 3.11.
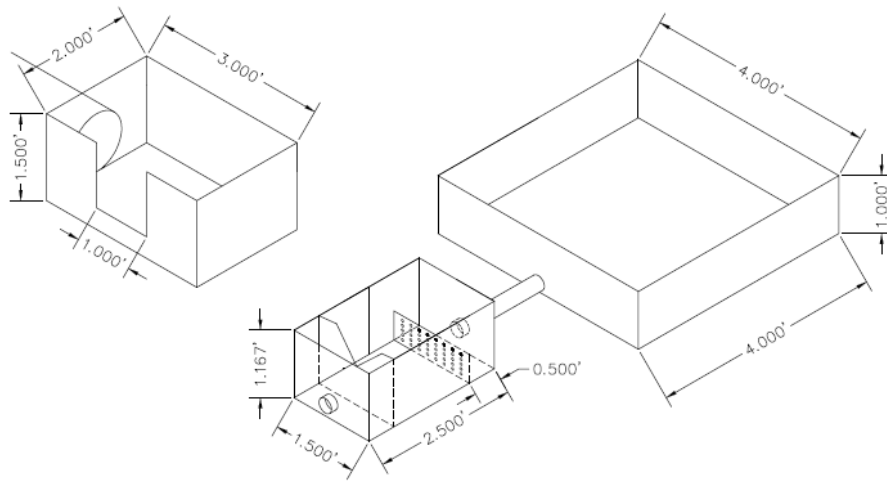
Figure 3.10: AutoCAD drawing of field site components
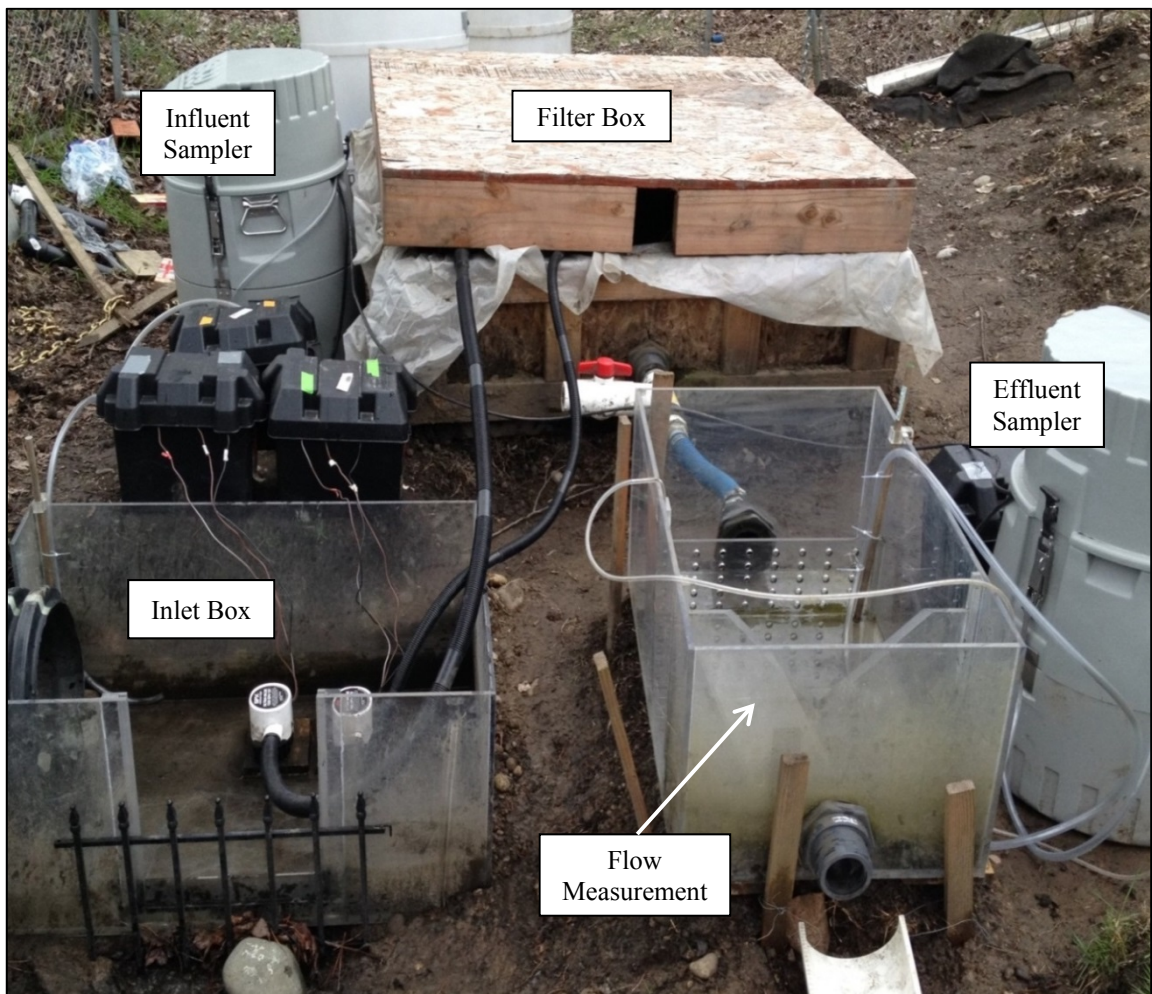
Figure 3.11: Photo of field site prior to sampling

3.7.2 Site Description

Field sampling was performed on the south side of highway 22/99E (Mission St.) near milepost 8 in Salem, OR. The annual average daily traffic (AADT) is approximately 46,600 *(ODOT 2012)*. A network of five curbside storm drains collected water from all eastbound traffic lanes and into a single 12 inch high density polyethylene (HDPE) culvert which flowed directly into the inlet box (as seen in Figure 3.11). The culvert drains 1.52 acres of exclusively highway stormwater runoff. The site is adjacent to McNary Field Airport, which contains a NOAA Quality Controlled Local Climatological Data (QCLCD) Weather station. The station (NOAA 24232/SLE) has quality controlled hourly rainfall data that is available for download at NOAA.gov. In Figure 3.12, the drainage area is outlined in red, and the filter box location is shown with a yellow star.
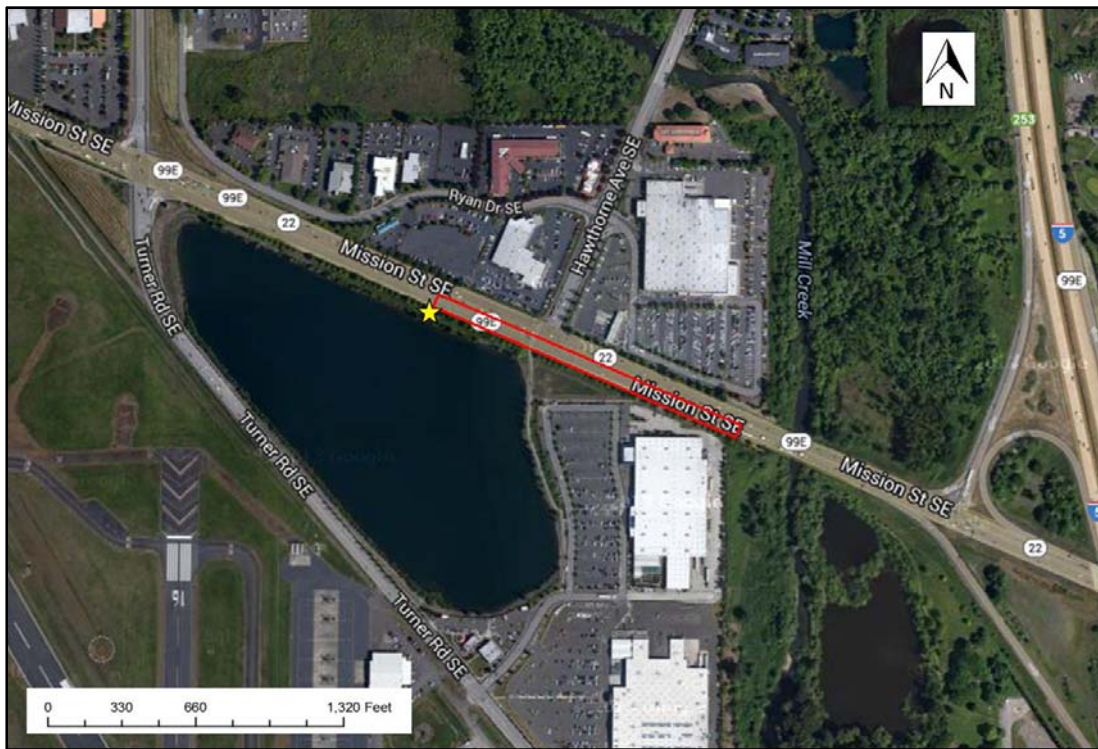
Figure 3.12: Aerial view of the field site

3.7.3 Sampling Equipment

Influent and effluent samples were taken using ISCO 6712 autosamplers. The effluent autosampler was connected to an ISCO 730 Bubble Flow Module, which measured the water depth in the outlet box to the nearest 0.001 ft at one-minute time intervals. Flow-weighted composite samples were taken in 10 L polyethylene bottles, using 10 ft long, 3/8 inch inner diameter Tygon intake tubing. Intake tubing in the inlet box was attached to a Teflon-coated strainer to prevent clogging with large debris. The autosamplers were each powered by a 12 V

30

marine battery, and connected to one another via an I/O cable. Data was uploaded from the samplers using ISCO Flowlink software (version 5.1).

3.7.4 Storm Selection and Flow Estimate

Targeted storms were those predicted to exceed 0.15 inches of rainfall over a 24-hour period. Storms with an antecedent dry period with less than 0.04 inches over 24 hours were preferred, but this condition was relaxed on several occasions due to an imminent need for data collection. An effort was made to sample a variety of storm lengths and rainfall intensities in an attempt to monitor the filter performance in a manner that represents natural rainfall variability throughout the rainy season. The minimum recommended number of aliquots in a composite sample is 10 *(Washington State Dept. of Ecology 2008)*, and the autosampler was programmed to take no more than 95 samples to avoid overflow in the sample bottles. Therefore, a sampling interval was chosen such that the estimated volume through the filter would produce 30 samples, allowing for a successful sample even when there was three-fold error in the volume estimate. The volume estimate was calculated by approximating the storm duration based on the NOAA.gov forecast, and multiplying that value with the average pumping rate into the filter, which was predicted based on laboratory experiments and previous field sampling events.

3.7.5 Equipment Programming and Preparation

The ISCO connected to the bubbler flow module installed in the outlet box was programmed to correlate the depth of water to flow rate using a 90-degree V-notch weir equation, which is shown in Figure 3.13. This flow rate was integrated over time and the cumulative volume was calculated. The autosampler was programmed to take a 100 mL sample every time the desired volume interval flowed through the outlet box, resulting in a single composite sample per storm. Every time a sample was taken, the effluent autosampler was programmed to send an 'Enable' signal through the I/O cable to the influent autosampler, which was programmed to take a 100 mL sample every time this signal was received. This allowed the two autosamplers to take simultaneous water samples, facilitating direct comparison between the influent and effluent samples. Prior to sampling events, sample volume was calibrated in the lab for each autosampler, and the depth measurement produced by the Bubble Flow Module was calibrated in the field. In between each sampling event, the intake tubes were rinsed with 10% HNO_3 continuously for 15 minutes, followed by rinsing with DDI water for 15 minutes. Composite sample bottles were rinsed with DI water after use, soaked overnight in 1% HNO_3, then rinsed and filled with DI water until field sampling. The 12 V marine batteries were charged in between each sampling event to prevent loss of power during a storm.
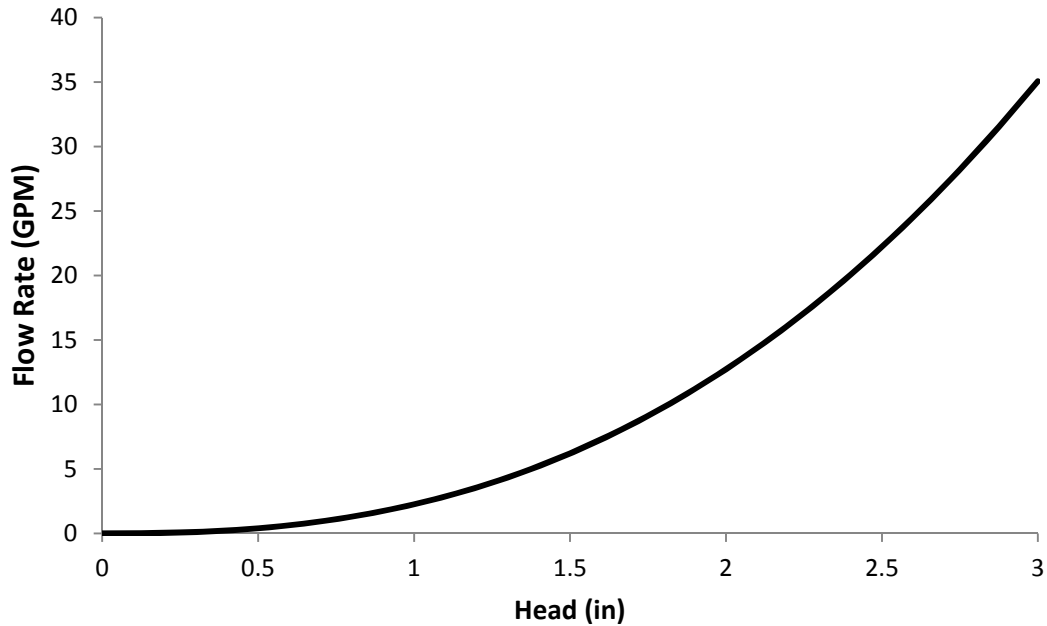
Figure 3.13: Head-Discharge relationship for the 90-degree V-Notch weir

3.7.6 Sampling Procedure

Prior to each rainfall event, the two ISCO autosamplers and bilge pumps were brought to the field site and connected to 12 V marine batteries. Standing water was pumped out of the inlet and outlet boxes, and any remaining sediment or biological films were removed with a hand trowel and paper towels. DI water that had been stored in the sampling bottles was then poured in the inlet and outlet boxes in an effort to clean any existing contamination, and again the water was pumped out and any lingering sediment was removed. Sample intake tubes were then fastened inside the inlet and outlet boxes, the empty sample bottles were put on ice inside the autosamplers, and the programs were enabled. For early season storms, filter hydraulics were observed to ensure proper function, until confidence was developed that everything was working properly. When the storm ended samples were capped and put on ice, and all equipment was returned to the lab. The filter box was drained of any standing water, and valves allowing flow into and out of the filter box were closed until the next sampling event. Precipitation data was downloaded from the Salem/McNary rain gauge (from NOAA.gov), and samples were processed in the lab.

3.8   LABORATORY ANALYSIS METHODS

3.8.1 Sample Processing

After retrieval from the field site, samples were stored on ice and brought directly back to the lab for processing. Within 24 hours of sample collection, samples were filtered through Millipore 0.45 μm filters using vacuum filtration and separated into aliquots for measurement. These

aliquots were measured for pH, conductivity, anions, trace metals, major cations, and DOC. The aliquots were extracted from 10 L round bottles by pipetting from the middle of the stirred solution using a pipette with a broad tip to avoid particle exclusion. For measurement of trace metals and major cations, samples were filtered directly into 14 mL polystyrene culture tubes to avoid any potential contamination, then acidified with ultrapure nitric to make a 1% (v/v) acid solution. All other aliquots were filtered into acid-washed glassware. Anion samples were prepared by pipetting 0.6 mL aliquots of filtered samples into IC vials. Dissolved organic carbon samples were prepared by pipetting a known volume of filtered samples into ashed TOC vials, then filling to a total volume of 40 mL with DDI water. Conductivity and pH samples were prepared by pipetting the filtered sample into small beakers. Concurrently, samples were digested for total cations in accordance with Standard Method 3030E.2 *(APHA et al. 2005)*. Additional aliquots of the original samples were then filtered through dried and pre-weighed glass microfiber filters for analysis of TSS and TDS. Samples were stored in the dark at 4°C until they could be analyzed. All samples were measured in triplicate unless specified otherwise. A flow chart of sample processing is shown in Figure 3.14.
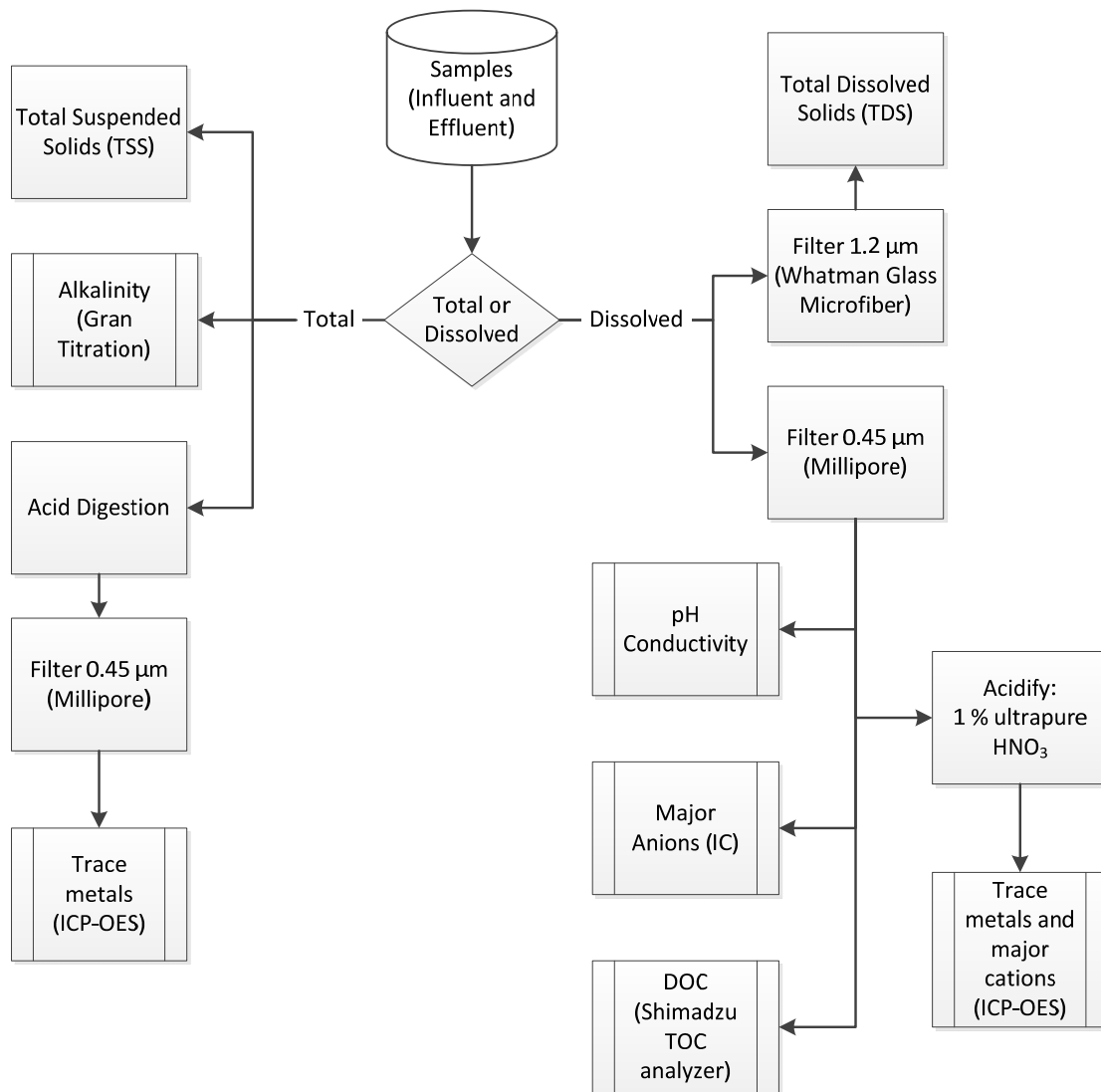
Figure 3.14: Flow chart of sample processing for analysis of field samples

3.8.2 Conductivity and pH

Conductivity was measured using an Accumet conductivity probe connected to an AR50 control panel. The conductivity probe was standardized using a 0.01 M KCl (1410 μS/cm) solution in accordance with EPA method 120.1. Sample pH was measured using a VWR sympHony probe and the same control panel. The pH probe was calibrated on a regular basis using standard buffers of pH 4, 7, and 10 (BDH General).

3.8.3 TSS and TDS

Total suspended solids (TSS) was measured by means of standard method 2540D *(APHA et al. 2005)*. The volume of water used in the filtration process depended on the concentration of solids in the sample, but was typically 100 mL. Total dissolved solids (TDS) were tested by taking aliquots of the samples filtered in the TSS process and placing them in pre-weighed beakers. These samples were allowed to dry for 24 hours at 105°C, cooled in a desiccator, and then reweighed. Aliquots of 50-100 mL were used for TDS.

3.8.4 Alkalinity

Titrations were performed on 50 mL samples using 0.02 N H_2SO_4. The volume of titrant and pH were recorded at regular intervals, and data was then graphed using a Gran Titration plot to determine the pH endpoint. Alkalinity measurements for both influent and effluent samples were typically done in duplicate.

3.8.5 Major Anions

Major stormwater anions (chloride, nitrate, phosphate, and sulfate) were tested using a Dionex DX500 Ion Chromatograph. Calibration curves were constructed with standards prepared using ACS grade stock solutions and DDI water. Influent samples were typically analyzed without dilution, and effluent samples were typically analyzed at dilution factors of 1:1 and 1:5.

3.8.6 Trace Metals

Total and dissolved trace metals were measured using a Leeman Labs Prodigy Inductively Coupled Plasma Optical Emission Spectrometer (ICP-OES). Metals analyzed include Cu, Zn, Pb, Ni, and Cd. Method blanks that had undergone the filtration process were included in analysis. Standard solutions ranging from 2 to 250 ppb were prepared using single element stock solutions (BDH Aristar, Sigma Aldrich TraceCERT). Blanks and check standards were typically measured every 15 samples.

3.8.7 Major Cations

Major cations were also measured using Inductively Coupled Plasma Optical Emission Spectroscopy (ICP-OES). Cations analyzed include Ca, Mg, Na, K, and Fe. Standard solutions ranging from 0.2 to 25 ppm were prepared using single element stock solutions (BDH Aristar, Sigma Aldrich TraceCERT). All samples were analyzed without dilution.

3.8.8 Dissolved Organic Carbon

Dissolved organic carbon (DOC) was measured by using a Shimadzu TOC-V$_{CSH}$ total organic carbon analyzer. Calibration curves were constructed using standards that had been prepared at Oregon State's Institute for Water and Watersheds Collaboratory. Standard concentrations were 0, 0.2, 0.5, 1.0, 2.0, and 5.0 mg C/L, using potassium hydrogen phthalate as the organic carbon source. Blanks and 1.0 mg/L quality control standards were measured every 10 samples. Samples were typically run at dilution factors of 1:20 and 1:2.

3.8.9 General Labware Cleaning Procedures

All labware used in analysis was cleaned with successive acid baths and DDI water. The cleaning procedure was as follows:

1. Rinse and scrub labware with DI water, removing any visible contamination.

2. Fully submerge labware in 10% (v/v) HCl for a minimum of 18 hours.

3. Remove labware from HCl bath, rinse with DI water, and fully submerge in 10 % (v/v) HNO$_3$ for a minimum of 18 hours.

4. Remove labware from HNO$_3$ bath, rinse with DI water, and fully submerge in DI water for at least 30 minutes.

5. Remove labware from DI bath and rinse three times with DDI water, then hang dry upside-down. Once dried, labware was covered with parafilm and stored until use.

Acid baths were made with DI water and ACS grade HCl and HNO$_3$, and all baths were changed out every 4-6 months.

3.8.10 TOC Vial Cleaning Procedures

After use, TOC vials were rinsed with DI water and submerged in the HCl bath for a minimum of 24 hours. After the HCl bath, they were rinsed with DI water and soaked in the DI bath for at least 30 minutes. They were subsequently rinsed with DDI water and hung to dry. Once dry, they were ashed at 550°C in a muffle furnace for two hours. The vials were then allowed to cool and stored in a clean Ziploc bag.

3.8.11 TOC Septum Caps Cleaning Procedures

Organic septum caps were rinsed with DI water after use, and then soaked in a DDI bath for at least 24 hours. They were subsequently removed from the bath and rinsed three times with DDI water. They were allowed to dry and then stored in a clean Ziploc bag.

3.9   STATISTICAL TECHNIQUES

To aid with data analysis, several statistical techniques were employed. To test whether the means of two samples were statistically different, a two-sided hypothesis test was performed. To

accomplish this, a value for $\bar{x}_{crit}$ was calculated using Equation 3.1, and if this value was less than the difference between the sample means, the samples were deemed statistically different. In Equation 3.1, s is the sample standard deviation, n is the number of data points for the sample, and $t_{\alpha/2}$ is the t-statistic obtained from statistical tables.

$$\bar{x}_{crit} = t_{\alpha/2} \sqrt{\frac{s_1^2}{n_1} + \frac{s_2^2}{n_2}}$$ (3.1)

In many cases, it was useful to analyze the difference between influent and effluent concentrations. To provide a standard deviation of that difference, propagation of errors analysis was used. For two normally distributed and independent samples, the variance (σ^2) of the difference in the two samples (x and y) is given by Equation 3.2.

$$\sigma_{(x-y)}^2 = \sigma_x^2 + \sigma_y^2$$ (3.2)

For analysis to determine whether two variables were correlated, a correlation coefficient for simple linear correlation (r_{xy}) was calculated using Equation 3.3. A correlation coefficient of 1 corresponds to perfect correlation, and a coefficient of 0 indicates no correlation.

$$r_{xy} = \frac{\sum_{i=1}^n \frac{(x_i - \bar{x})(y_i - \bar{y})}{n-1}}{s_x s_y}$$ (3.3)

To test for significance in the difference of two regression slopes, a confidence interval on the slope of the regression line was computed using Equation 3.4. The slope (β_1) was obtained from the linear best-fit line of a scatterplot in Microsoft Excel, which utilizes least squares analysis for calculations. Equations 3.5-3.8 define variables used for calculation. This analysis was also used to test whether there was a statistically significant trend over the course of an experiment. Specifically, if the confidence interval of the slope of the regression line had negative and positive values, it indicated there was not a statistically significant trend.

$$\beta_1 \pm t_{\alpha/2} \frac{S}{\sqrt{S_{xx}}} \qquad (3.4)$$

$$S = \sqrt{\frac{S_{yy} - \beta_1 S_{xy}}{n-2}} \qquad (3.5)$$

$$S_{xx} = \frac{n \sum x^2 - (\sum x)^2}{n} \qquad (3.6)$$

$$S_{yy} = \frac{n \sum y^2 - (\sum y)^2}{n} \qquad (3.7)$$

$$S_{xy} = \frac{n \sum xy - \sum x \sum y}{n} \qquad (3.8)$$

4.0   LABORATORY RESULTS AND DISCUSSION

4.1   CHARACTERIZATION OF APATITE II™ AND COMPOST

An SEM image of the virgin Apatite II™ is shown in Figure 4.1. The EDS spectrum of Apatite II™ shown in Figure 4.2 indicates that calcium, phosphorus, oxygen, and carbon are the major components present in Apatite II™. The strong peaks shown in the XRD pattern (Figure 4.3) largely correspond to the crystal structure of hydroxyapatite, $[Ca_5(PO_4)_3OH]$ (JCPDS-ICDD file number 09-0432). These results are similar to previous XRD analysis of pig and cow bone, where hydroxyapatite was also the primary component *(Kim et al. 2009)*. The amorphous nature of the Apatite II™ likely prevented the identification of crystalline structures containing carbon and sodium by XRD.

It has been reported that the apatite mineral in bone differs from abiotic hydroxyapatite. Apatite II™ has the general composition $Ca_{10-x}Na_x(PO_4)_{6-x}(CO_3)_x(OH)_2$ with x<1, and contains up to 30-40 weight percentage of organics within the pore structure *(Conca and Wright 2006)*. Based on the results shown in Figure 4.2, the molar ratio of Ca:P:Na:C:O in the Apatite II™ used in this study is 8.18:4.93:0.91:50.03:35.86. This result corresponds well with the ratio of Ca:P:Na:C:O $\approx$ 9-10:5-6: 0-1: 0-1:25-26, based on structure described above. The fact that carbon and oxygen were detected at much higher concentrations than the suggested molar percentage can be explained by the presence of organic matter in the internal pores of the inorganic structure.
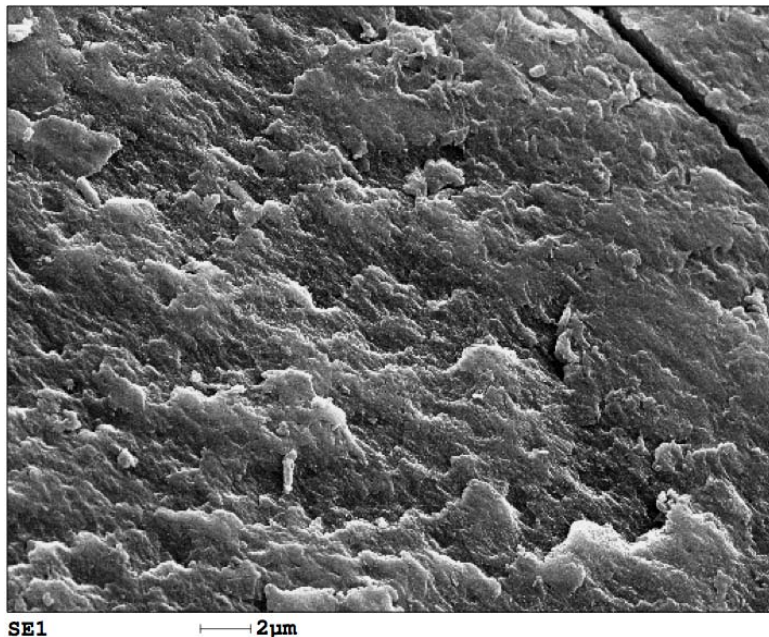
Figure 4.1: SEM image of virgin Apatite II™
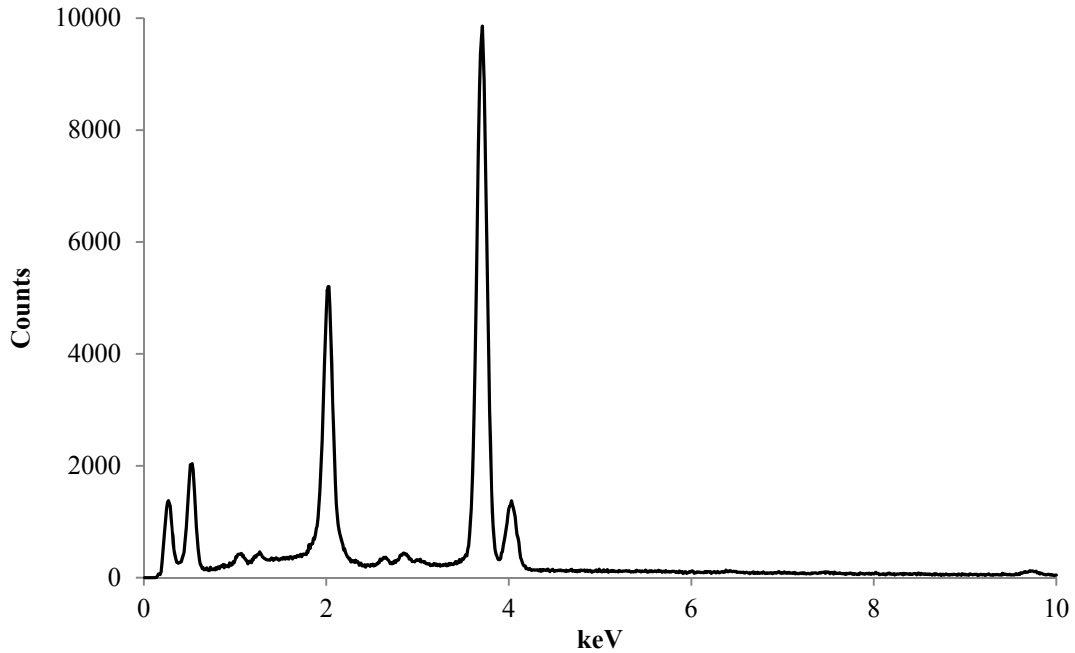
Figure 4.2: EDS spectrum of Apatite II™
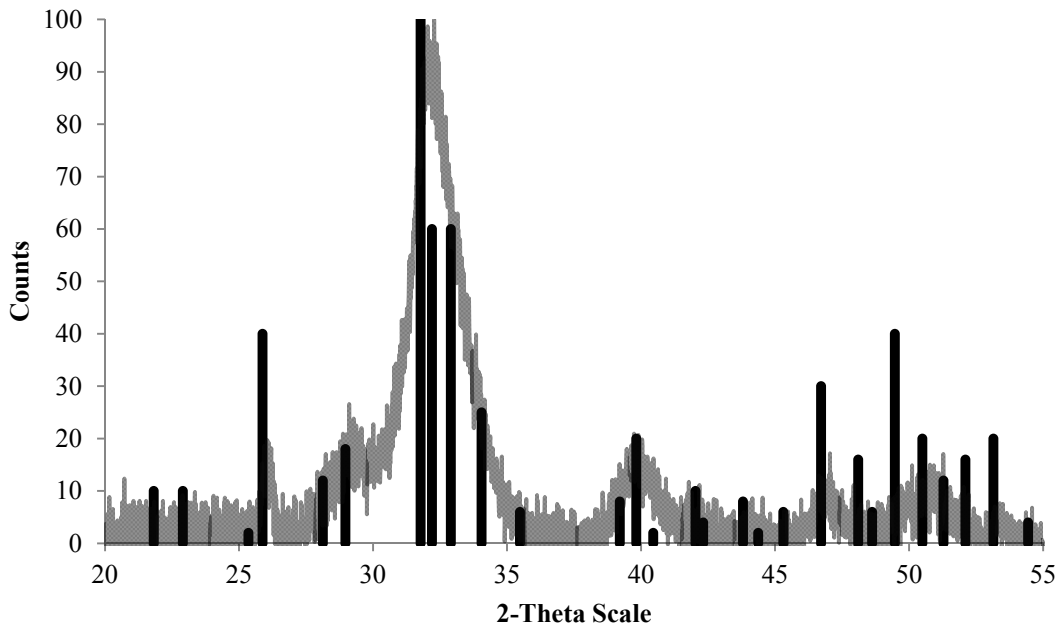
Figure 4.3: XRD pattern of Apatite II^{TM} with the diffraction pattern for abiotic hydroxyapatite (JCPDS-ICDD file number 09-0432) shown as column plot for comparison

The compost used in this project is produced at an industrial scale and tested regularly in accordance with the US Composting Council's Seal of Testing Assurance Program. Field experiments were performed with compost that was sampled by the producer on 2/4/14 and sent

to a certified independent lab for testing. The results of that testing is shown in Table 4.1 (data courtesy of Lane Forest Products, Inc.).

Table 4.1: Characterization of compost used in field-testing

Compost Parameter	Test	Unit		Value
Size Classification	TMECC 02.02-B	% dry weight passing through sieve	3"	100
			1"	100
			3/4"	100
			5/8"	100
			1/2"	no data
			1/4"	95
Manufactured Inerts	TMECC 03.08-A	% dry weight		<0.5
pH	TMECC 04.11-A	-		6.7
Organic Matter Content	TMECC 05.07-A	% dry weight		67.8
Soluble Salts	TMECC 04.10-A	dS/m		1.8
Carbon to Nitrogen Ratio	TMECC 04.02-D	-		22
Stability Indicator	TMECC 05.08-B	mg CO_2-C/g OM/day		2.5
Maturity Indicator	TMECC 05.05 A	% germination		100
Moisture Content	TMECC 03.09-A	% total weight		45.8

4.2 BATCH EQUILIBRIUM EXPERIMENTS

4.2.1 Apatite II™ Batch Experiments

Results from the single element batch experiments with copper and zinc are shown in Figure 4.4. As will be discussed in more detail in section 4.3.1, metals removal can be attributed to a combination of adsorption and precipitation processes. To facilitate comparison with other adsorbents and to gain insight into the RSSCT design, equilibrium liquid and solid phase concentrations are reported here as "isotherms" where q_e represents the total mass of adsorbed and precipitated metals normalized by the initial mass of Apatite II™. Copper removal was characterized by a linear isotherm (K_d=0.0131), whereas zinc removal was best modeled by a Langmuir isotherm (K_L=0.00145, q_{max}=21.73). At equilibrium, the removal of zinc (i.e. q_e) was greater than that of copper at all aqueous metal concentrations (C_e) that were tested.

$$q_{e,\,Zn} = \frac{(21.73)(0.00145)C_e}{1 + (0.00145)C_e}$$

$q_{e,Cu} = 0.0131C_e$
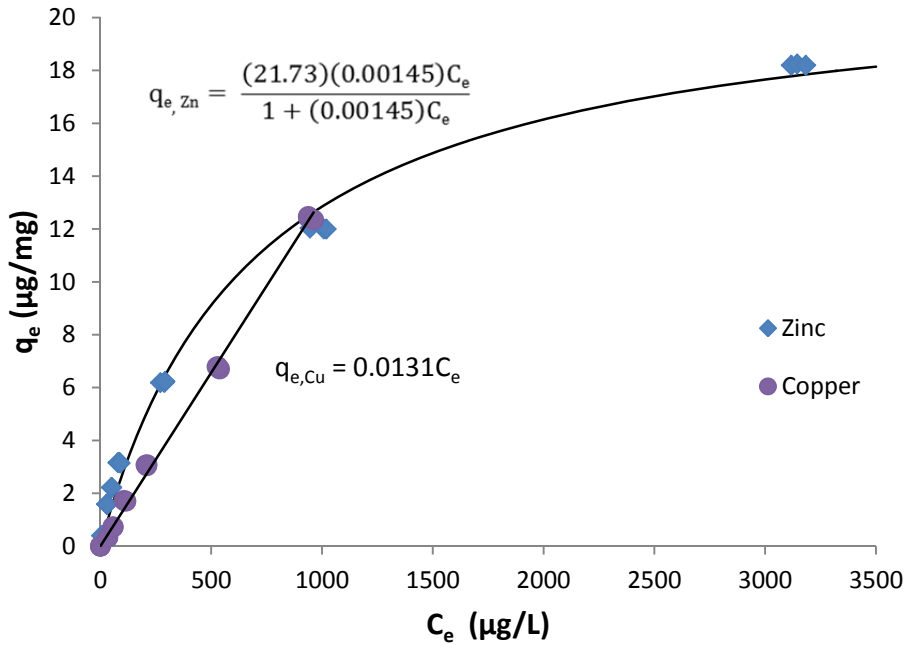
Figure 4.4: Equilibrium copper and zinc removal in single element batch experiments with Apatite II™

In actual stormwater, copper and zinc will both be present, necessitating an evaluation of the competitive effects of the two metals. Accordingly, binary element batch tests were performed at equilibrium copper concentrations relevant to stormwater runoff. Experiments were performed with 1:1, 1:4, and 1:8 copper to zinc ratios, and these results as well as single element copper isotherm results are shown in Figure 4.5. In each case, the data is best modeled with a linear isotherm, and there is no observable pattern with increasing amounts of zinc. This was confirmed by calculating a 95% confidence interval on the slope of each regression line, which revealed no statistically significant differences in slope among the four experiments. This indicates that the presence of zinc in solution does not alter the capacity of Apatite II™ to remove copper, even in cases when zinc is present at significantly higher concentrations than copper.
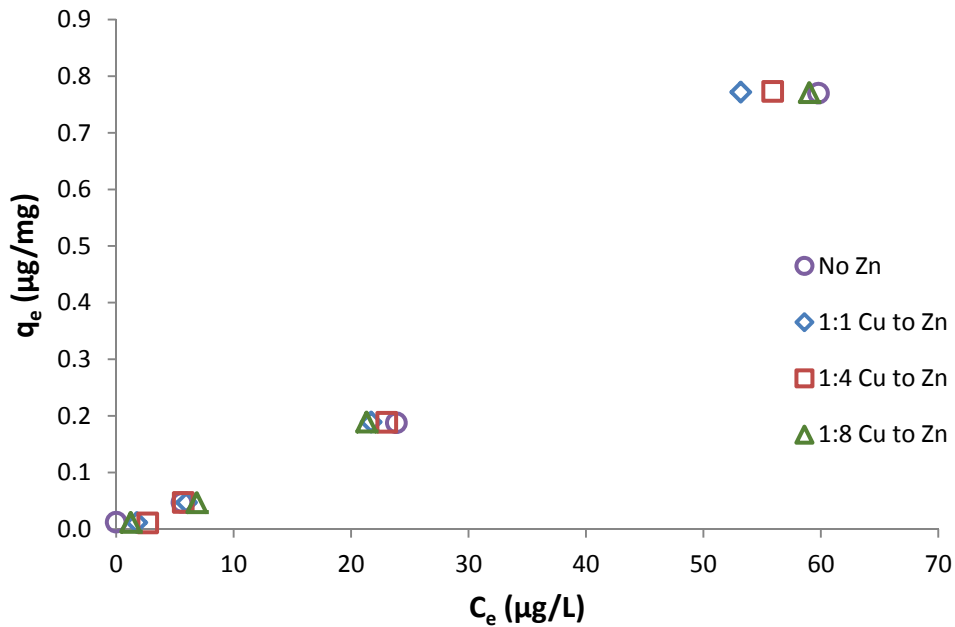
Figure 4.5: Equilibrium copper removal in the presence of zinc at varying copper to zinc ratios

Due to the impact NOM can have on metal removal processes and the ubiquity of NOM in stormwater runoff, it is important to examine the impact NOM has on removal processes. Figure 4.6 compares the results of equilibrium batch experiments using synthetic stormwater with and without NOM. It is evident that NOM concentrations as low as 0.8 mg/L inhibit copper removal, as demonstrated by the decreased slope for the linear isotherm with NOM. The difference between the two isotherms was confirmed with a 95% confidence interval on the slope of the regression lines. The mechanism for this inhibition is discussed in detail in section 4.4.
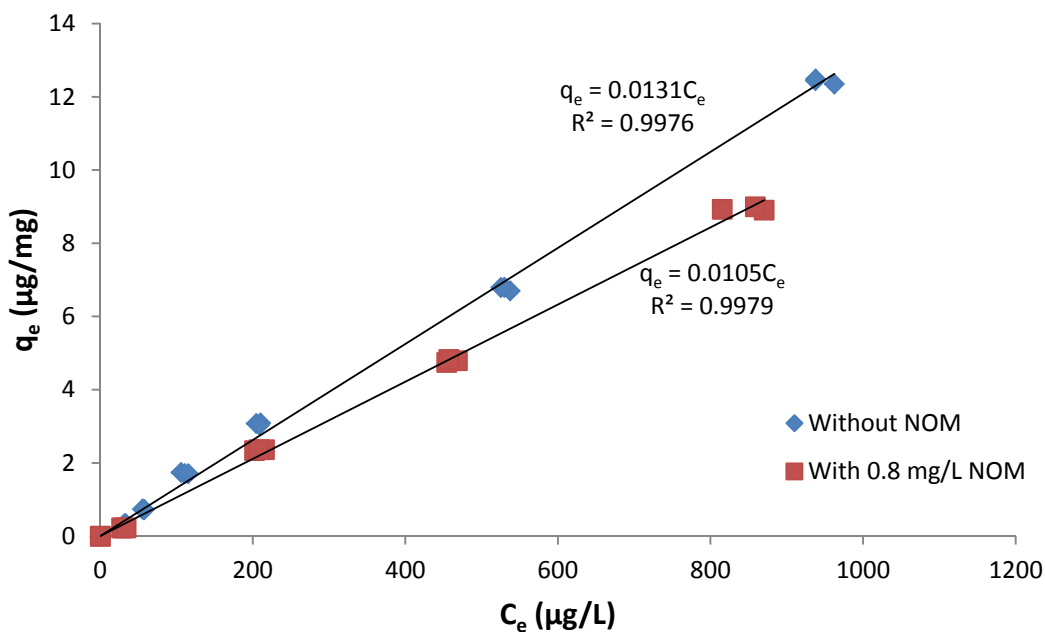
Figure 4.6: Equilibrium copper removal from synthetic stormwater with NOM using Apatite II™

In addition to monitoring final metal concentrations, equilibrium pH, phosphate, and calcium were measured in batch experiments. From Table 4.2, it is apparent that the dissolution of Apatite II™ resulted in high equilibrium concentrations of calcium and phosphate. This was expected based on the high molar fraction of P and Ca measured in characterization of Apatite II™ with SEM-EDS (Figure 4.2). Additionally, these data are in agreement with previous work with Apatite II™, which also documented large releases of calcium and phosphate *(Conca and Wright 2006)*. The pH measurements are also in line with previous work that highlighted the ability of Apatite II™ to buffer solutions to circumneutral pH *(Conca and Wright 2006; Oliva et al. 2011)*. The elevated levels of phosphate are of concern due to negative environmental impacts resulting from phosphate discharge to aquatic systems. The implications of the high release of phosphate by Apatite II™ are further discussed in later sections.

Table 4.2: Average calcium, phosphate, and pH at equilibrium in batch studies

	Cu Only	**Zn Only**	**Binary System**
Ca^{2+} (mg/L)	7.65±0.32[a]	6.57±0.64	5.79±0.26
PO_4^{3-} (mg/L)	25.0±0.8	25.0±2.3	18.1±0.7
pH	7.28±0.02	7.26±0.05	7.22±0.04

[a]95% confidence interval

4.2.2 Compost Batch Experiments

As with Apatite II™, isotherms were developed for compost that plotted equilibrium solid phase concentration against aqueous phase concentration, where q_e is again calculated based on the total mass of copper removed irrespective of mechanism (i.e. the sum of adsorption and

precipitation). Figure 4.7 shows the results of copper single-element batch-equilibrium studies with compost, plotted with polynomial trend lines to illustrate the non-linearity and concavity of the results. In both cases, the rate of change of solid phase metal concentration (q_e) increases as equilibrium aqueous concentration (C_e) increases, demonstrating that the isotherms cannot be characterized by the Langmuir or Freundlich models, which are typical of metal adsorption processes. Instead they appear to follow the model developed by Farley et al. *(Farley et al. 1985)*, where adsorption dominates at low C_e and a combination of adsorption and surface precipitation occurs at higher C_e, resulting in concave up isotherms. For the samples without NOM, the concavity is more pronounced, and thus the effect of precipitation is stronger. However, there is no discernible difference in the two cases at lower copper concentrations. This suggests that NOM has little effect on copper adsorption at a NOM concentration of 0.8 mg/L, but does limit the formation of copper precipitates.
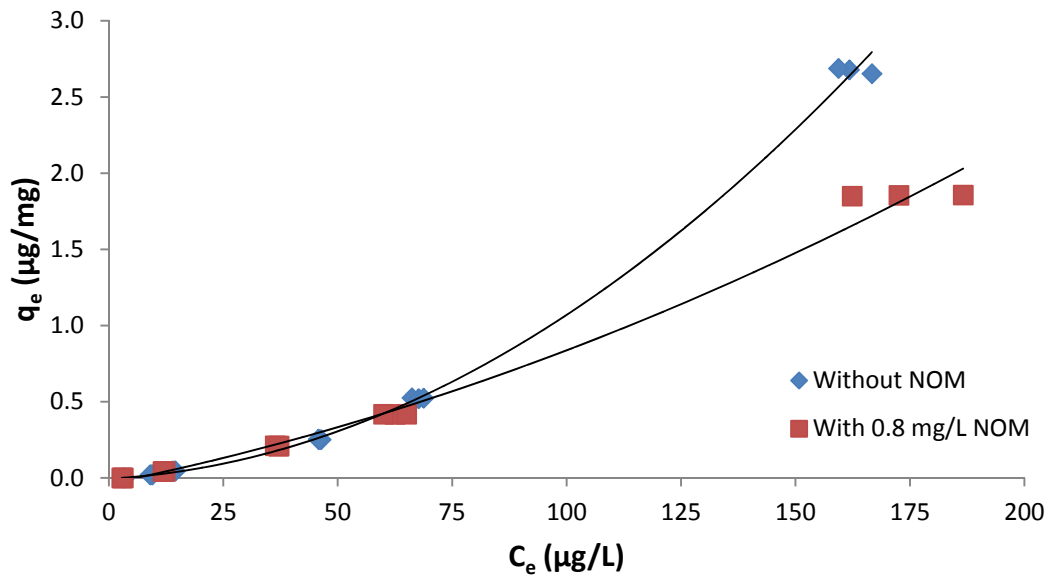
Figure 4.7: Equilibrium copper removal from synthetic stormwater using compost

As with Apatite II™, batch experiments were performed with both copper and zinc in solution to determine how the presence of zinc in stormwater will affect copper removal. For the binary solutions, the copper to zinc concentration ratio was 1:4, which is consistent with values typical for stormwater *(Kayhanian et al. 2007; Nason et al. 2012a)*. The copper results from this experiment are shown in Figure 4.8, as well as results from the single element copper batch test. These results seem to indicate that copper removal is enhanced in binary element systems, which is contrary to what was expected. Similar trends could not be found in the literature, and the difference is likely attributed to heterogeneity in compost material. Irrespective of the mechanism, this result clearly demonstrates that the presence of zinc does not function to diminish the capacity of compost to remove copper from stormwater runoff.
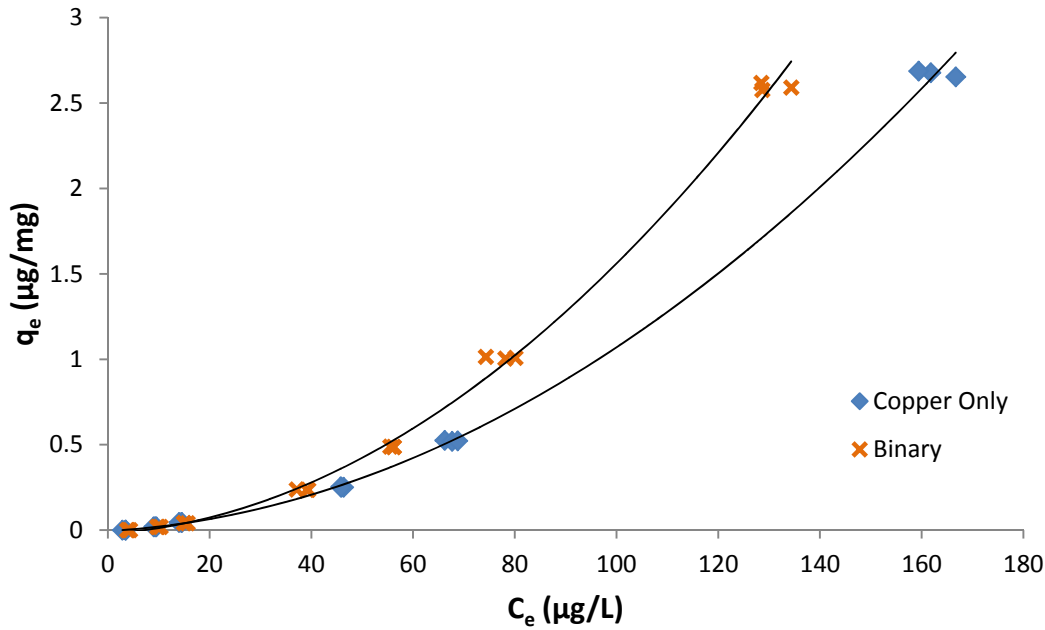
Figure 4.8: Equilibrium copper removal in binary (Cu and Zn) and single element solutions using compost

Similar to experiments with Apatite II™, an isotherm was developed to evaluate the equilibrium capacity of zinc removal using compost. The single element zinc isotherm is shown in Figure 4.9, plotted over the range of zinc concentrations that represent reasonable values for stormwater runoff. Over this range of equilibrium concentrations, zinc removal is best modeled by the Freundlich isotherm (Kf=0.136, n=0.641). To provide a basis of comparison, the single element copper isotherm is also plotted in Figure 4.9, which demonstrates that at equilibrium concentrations less than approximately 200 µg/L zinc removal capacity is greater than copper. This finding indicates that in addition to removing copper, compost is an effective adsorbent for the removal of zinc from solution.
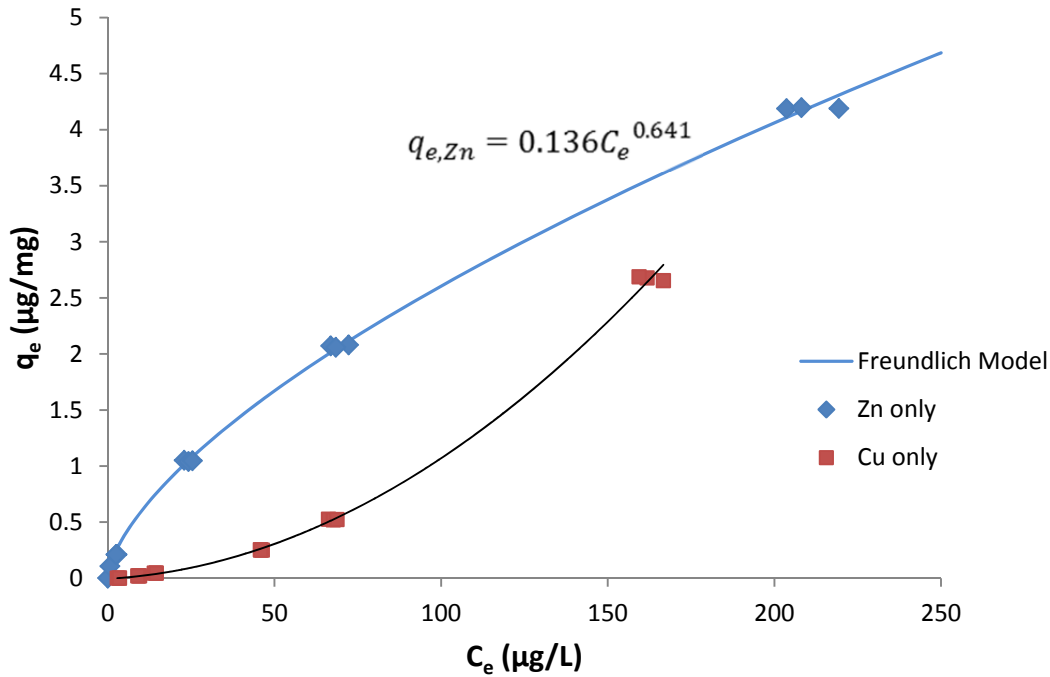
Figure 4.9: Equilibrium copper and zinc removal in single element batch experiments with compost

To gain more perspective into the equilibrium removal capacity of Apatite II™ and compost, the copper and zinc adsorption densities (qe) of these media were compared to those found in the literature for other adsorbents. An equilibrium aqueous concentration of 100 µg/L was chosen as a basis for comparison, and the results of this review are shown in Table 4.3. These studies were conducted at initial pH values ranging from 5.5-6.5, with the exception of oak sawdust, pineapple leaf powder, and activated carbon 1, which were carried out at pH 4, 5, and 7 respectively. This summary demonstrates that both compost and Apatite II™ compare favorably to other adsorbents for the removal of copper and zinc. For each metal, only one adsorbent outperformed compost and Apatite II™, indicating both media types are promising adsorbents at concentrations relevant to stormwater runoff.

Table 4.3: Comparison of copper and zinc adsorption densities (q_e) at equilibrium aqueous metal concentration (C_e) of 100 μg/L using various adsorbents

Adsorbent	Metal	Initial pH	q_e (μg/mg)	Reference
Apatite II™	Cu	6.0	1.3	This study
	Zn		3.4	
Compost	Cu	6.0	1.1	This study
	Zn		2.6	
Pineapple leaf powder	Cu	5.0	0.24	*(Weng and Wu 2012)*
Brown seaweed-*Cystoseira Indica* (CB1)	Cu	6.0	0.07	*(Basha et al. 2009)*
Mixture of Iron hydroxide and zeolite (P4)	Cu	6.5	0.08	*(Wu and Zhou 2009)*
	Zn		0.16	
Activated Carbon 1	Cu	7.0	0.54	*(Moreno-Pirajan and Giraldo 2011)*
Activated Carbon 2	Cu	5.1-5.8	0.07	*(Machida et al. 2005)*
Red mud	Cu	5.5	0.11	*(Nadaroglu et al. 2010)*
Chitosan flakes	Cu	6.0	1.05	*(Bassi et al. 2000)*
	Zn		1.03	
Modified oak sawdust	Cu	4.0	0.30	*(Argun et al. 2007)*
Tea-industry waste	Cu	5.5	0.41	*(Cay et al. 2004)*
Hibiscus dye waste	Zn	6.0	83.85	*(Vankar et al. 2012)*
Activated *Firmiana* simplex leaf	Zn	NA	1.14	*(Tang et al. 2012)*
Potato peels	Cu	6.0	3.79	*(Aman et al. 2008)*

4.3   COPPER AND ZINC REMOVAL MECHANISM

4.3.1 Removal Mechanism with Apatite II™

Simulations using visual MINTEQ and batch precipitation tests without the presence of Apatite II™ were conducted to distinguish the contribution of precipitation and surface complexation (adsorption or ion exchange) towards the removal of copper and zinc by Apatite II™. In these tests, synthetic stormwater with copper or zinc was buffered to an initial pH of 7.3 to replicate the final pH in experiments using Apatite II™, and then reacted on a tumbler for 48 hours. The sample was then filtered with a 0.45 µm filter and a final pH was taken, which was used as an input in the MINTEQ modeling. The results of these tests are shown in Table 4.4 and Table 4.5.

Modeling with MINTEQ revealed that thermodynamically, the precipitate most likely to form in solution is tenorite [CuO]. However, predicted equilibrium concentrations with tenorite as a solid phase were much lower than final copper concentrations measured in the precipitation experiments. A second model run was carried out excluding tenorite as a possible crystal phase, as shown in Table 4.4. These modeling results were closer to batch precipitation tests, suggesting that the initial formation of tenorite may be kinetically unfavorable under these conditions. Exclusion of tenorite resulted in malachite [$Cu_2CO_3(OH)_2$] as the only copper-containing solid phase in equilibrium modeling, but it is also possible that a less soluble amorphous copper oxide/hydroxide formed initially.

The final pH values in the batch precipitation experiments with 20 mg/L of phosphate were relatively constant around 7.3. However, in trials without phosphate the final pH varied from 6.7 to 7.3. This demonstrates that while modeling indicated that phosphate does not directly participate in precipitation reactions, it acts as a pH buffer that allows the solution to remain at an elevated pH where the solubility of malachite and other metal solids is reduced. The result is elevated copper removal in solutions with phosphate. When elevated concentrations of copper were present in the initial solution, high amounts of hydroxide ion were consumed in precipitation, leading to much lower final pH in solutions that were not buffered by phosphate, and resulted in higher concentrations of dissolved copper.

It should be noted that while equilibrium modeling indicated malachite was the likely solid phase, experiments aimed at verifying this assumption using XRD were inconclusive. Additionally, previous work by another group evaluating copper removal using Apatite II™ proposed libethenite [Cu2(PO4)OH] as the solid phase responsible for copper precipitation *(Oliva et al. 2011)*. However, using a solubility product for libethenite obtained from the literature *(Madsen 2005)*, it was determined that at the concentrations of copper, phosphate, and hydroxide present in batch testing, libethenite is unlikely to precipitate.

Both modeling and precipitation experiments demonstrated that copper precipitates form at the same aquatic chemistry and pH as batch experiments with Apatite II™. This is strong indication that precipitation is occurring in experiments with Apatite II™. However, at the lower initial concentrations in Table 4.4, batch experiments with Apatite II™ had lower final copper concentrations than the precipitation experiments and modeling. This suggests that adsorption is likely contributing to copper removal, and is particularly important at low copper concentrations.

At higher copper concentrations, adsorption sites are typically consumed and isotherms become concave down. However, this does not occur with Apatite II™, indicating precipitation is playing a major role at higher copper concentrations.

Zinc, on the contrary, appeared to be more soluble than copper based on the results of modeling and batch precipitation tests (Table 4.5). In the absence of phosphate, modeling and precipitation experiments confirmed that little precipitation occurs. The addition of phosphate stabilized pH at 7.2-7.3 and provided phosphate for the formation of solids, resulting in lower final concentrations. The proposed solid phase based on modeling results is hopeite $[Zn_3(PO_4)_2 4H_2O]$, which agrees with previous work examining the precipitation of zinc using Apatite II™ *(Oliva et al. 2010)*. For the experiments with phosphate, precipitation experiments yielded considerably higher final concentrations than modeling results, likely indicating that the formation of hopeite is limited kinetically. Irrespective, experiments with Apatite II™ resulted in much lower final concentrations than precipitation experiments and modeling, suggesting that adsorption is the dominant removal mechanism with zinc.

Surface complexation of zinc with hydroxyapatite has been suggested to follow the following mechanism: $HAP - OH + Zn^{2+} \rightleftharpoons HAP - O - Zn^+ + H^+$ *(Corami et al. 2007)*. Exchange of calcium with zinc, which can be expressed as $HAP - Ca^{2+} + Zn^{2+} \rightleftharpoons HAP - Zn^{2+} + Ca^{2+}$, has also been suggested *(Suzuki et al. 1981; Corami et al. 2007)*. Ideally, the process controlling zinc removal could be identified based on the increased concentration of calcium or decreased pH. However, Apatite II™ releases high concentrations of calcium through dissolution, even in the absence of copper or zinc. Additionally, both surface complexation and zinc phosphate precipitation result in the release of protons. Consequently, it is difficult to characterize the specific adsorption processes based on the released of calcium or changes in pH.

Table 4.4: Summary of copper equilibrium modeling, precipitation experiments, and batch tests with Apatite II™

Initial Copper Concentration (µg/L)	Precipitation without PO$_4$				Precipitation with 20 mg/L of PO$_4$				Apatite II™ Batch	
	Final pH	Final Cu (µg/L) (experiment)	Final Cu (µg/L) (Model)	Final Cu (µg/L) (Model, no tenorite)	Final pH	Final Cu (µg/L) (experiment)	Final Cu (µg/L) (Model)	Final Cu (µg/L) (Model, no tenorite)	Final pH	Final Cu (µg/L) (experiment)
100	7.2	21.7±9.6	26.8	52.8	7.3	NA[a]	28.7	62.7	7.3	5.6±1.1
400	6.8	224.8±22.0	114.4	155.1	7.3	65.0±9.4	28.7	63.0	7.3	23.9±3.5
1600	6.72	590.7±10.1	156.9	202.8	7.3	78.7±16.7	28.7	63.9	7.3	59.8±11.6
6400	6.68	833.3±32.6	184.2	254.5	7.2	83.2±7.5	40.3	88.3	7.3	213.0±10.2

Table 4.5: Summary of zinc equilibrium modeling and batch tests with and without Apatite II™

Initial Zinc Concentration (µg/L)	Precipitation without PO$_4$			Precipitation with 20 mg/L of PO$_4$			Apatite II™ Batch	
	pH	Final Zn (µg/L) (experimental)	Final Zn (µg/L) (Modeling)	pH	Final Zn (µg/L) (experimental)	Final Zn (µg/L) (Modeling)	pH	Final Zn (µg/L) (experimental)
100	7.1	55.9±6.7	100	7.3	NA[a]	100	7.3	BDL[b]
400	NA	NA	NA	7.3	328.4±32.7	166.7	7.3	BDL
800	6.86	678.9±12.9	800	NA	NA	NA	NA	6.9±2.1
1600	6.75	1519.2±91.4	1600	7.3	1293.2±74.6	171.9	7.3	8.1±2.4
6400	6.6	4340.5±34.7	6400	7.24	1160.7±31.5	225.6	7.3	84.3±6.1

[a]Data not available
[b]BDL: below detection limits

As mentioned previously in section 2.3.3, there have been a number of studies detailing the potential of using bioremediation for copper removal. Accordingly, an assessment of the copper removal mechanisms using Apatite II™ should include a consideration of biological copper removal. This is particularly important in light of the fact that Apatite II™ releases carbon and phosphate, thus creating an environment suitable for microbial growth. To accomplish this, a batch test was carried out with Apatite II™ and a biocide (NaN_3) to determine if the absence of microbes affected copper removal. From Figure 4.10, it is apparent that the addition of NaN_3 did not have an effect on copper removal. This was confirmed statistically with a 95% confidence interval on the slope of the regression lines. These results demonstrate that biological activity does not have a significant impact copper removal using Apatite II™ in batch tests. However, the Apatite II™ used for laboratory experiments was autoclaved and the DDI water that was used for solution preparation is sterile. Therefore, microbial activity could be more pronounced in field experiments, potentially leading to biologically induced copper removal playing a more significant role.
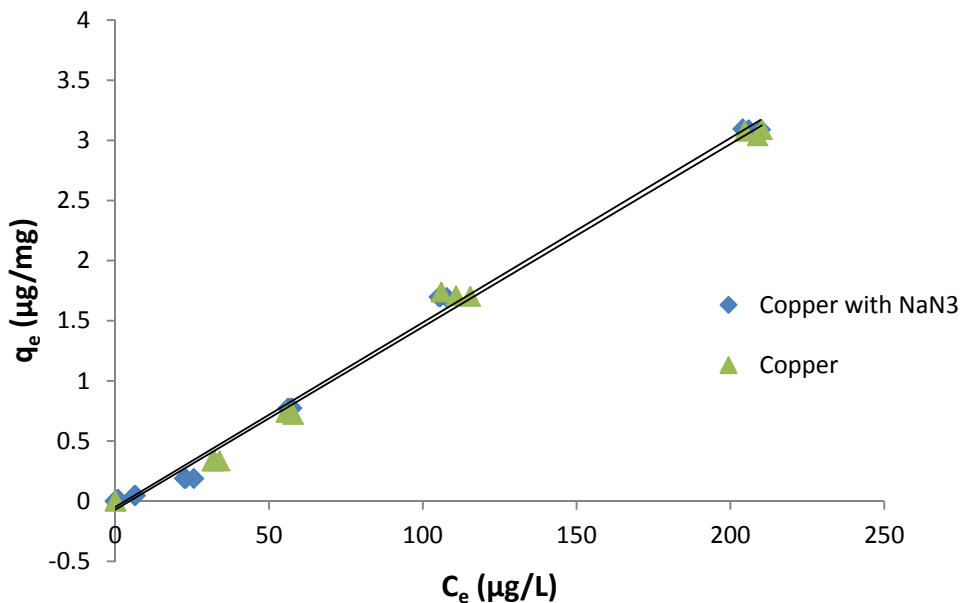
Figure 4.10: Equilibrium copper removal using Apatite II™ in the presence of NaN_3

4.3.2 Removal Mechanism with Compost

In batch experiments with synthetic stormwater and compost solutions that were adjusted to initial pH values of 2, 3, 4, 6, and 8, copper removal remained fairly consistent for final pH values ranging from 3 to 9 (Figure 4.11). In fact, there is no statistical difference ($p > 0.05$) between the cluster of samples just below pH 6 and the cluster just below pH 8. Because copper exists almost entirely in the aqueous phase at pH values below 6, it can be gathered that for samples with a final pH lower than 6, copper removal is not attributable to chemical precipitation. This suggests that adsorption is the dominant mechanism driving copper removal

with compost. Supplementary experiments tested copper removal from synthetic stormwater by buffering the solution from pH 6.0 to 7.3 to induce precipitation. At an initial concentration of 100 µg/L, 78.3% copper removal was observed and ascribed to chemical precipitation. This is well below the percent removal at similar pH values in this experiment, lending further support that copper removal with compost is governed by adsorption processes.

The abrupt drop in removal efficiency around pH 2 is likely due to the abundance of hydronium ions in solution, which compete for binding sites with copper. This phenomenon of sudden decrease in adsorption at a pH threshold is characteristic of metal adsorption processes and is known as the pH-adsorption edge *(Benjamin 2002)*. Similar behavior has been observed in experiments assessing heavy metal removal with other organic adsorbents *(Yu et al. 2001)*.
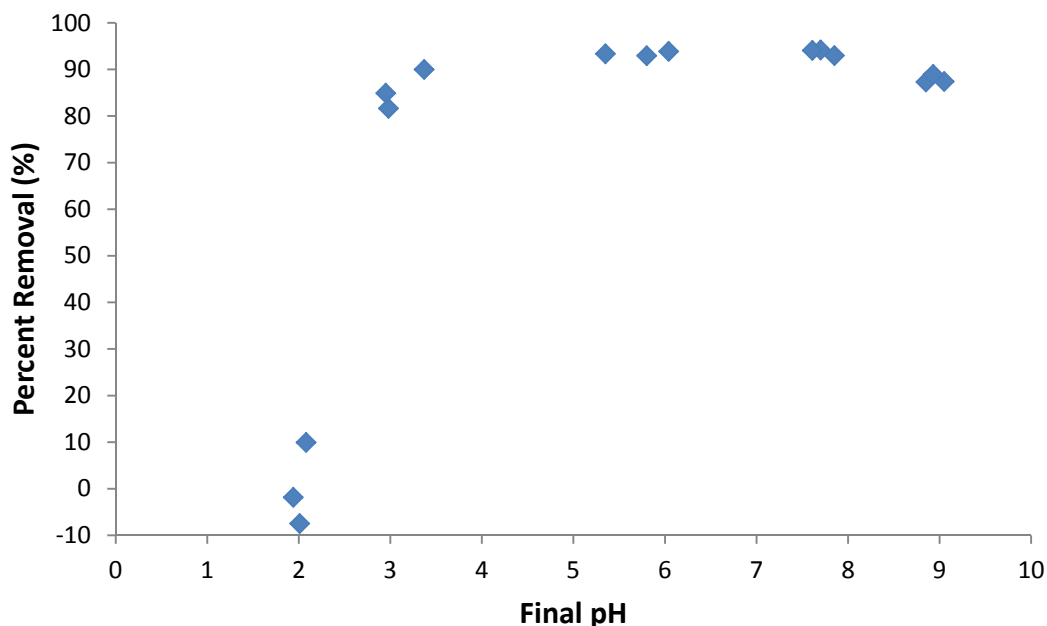
Figure 4.11: Copper removal from synthetic stormwater by compost in batch tests at varying solution pH

4.4 NOM INHIBITION BATCH EXPERIMENTS

As discussed in Section 2.6, NOM can have a profound effect on metal speciation and removal processes. The typical result of NOM in solution is inhibition of metal removal, either by interacting with the adsorbent surface and thereby preventing metal adsorption, or by formation of metal-NOM complexes that have lower adsorption affinities than the metal ion. These processes are represented by the following equations, where NOM is denoted as *L*, copper is represented as a generic metal, *Me*, and the adsorbent is denoted as a solid surface ≡*S*:

$$\equiv S + L \leftrightarrow \ \equiv SL \tag{4.1}$$

$$Me^{+x} + L^{-y} \leftrightarrow \ MeL^{(x-y)} \tag{4.2}$$

Understanding which of these processes are inhibiting copper is important because it lends insight into the impact of variable water quality on process performance. For example, would a pulse of high NOM concentration in stormwater affect copper removal in later storms, or would the high concentration of NOM associated with the first flush inhibit copper removal for the rest of that rainfall event?

4.4.1 Effect of NOM on Copper Removal with Apatite II™

From Figure 4.12 it can be seen that Cu-NOM pretreatment resulted in elevated final concentrations of copper relative to the control, whereas Apatite-NOM pretreatment yielded similar copper concentrations to the control. This demonstrates that Cu-NOM complexes and not Apatite-NOM complexes inhibit copper removal. Simultaneous addition of copper and NOM to Apatite II™ resulted in similar copper concentrations as Cu-NOM pretreatment, suggesting that at concentrations of copper and NOM relevant to stormwater, Cu-NOM complexes will form regardless of the presence of Apatite II™, and these complexes will subsequently govern copper removal. In general, these results indicate that Cu-NOM complexes do not adsorb or precipitate as readily as free copper ion.

Figure 4.12 also seems to demonstrate that there is no recognizable relationship between NOM concentration and final copper concentration. This was unexpected based on the findings of previous work that demonstrated that dissolved copper concentration in stormwater is positively correlated with DOC *(Nason et al. 2012a)*. A possible explanation is that there was experimental error in the Cu-NOM pretreatment case with 1mg/L NOM, causing artificially high final copper concentrations. If this value had been lower, a general pattern of increasing final copper with increasing NOM concentrations would have been present, similar to the simultaneous addition case. It was not surprising that no trend was observed for the Apatite-NOM pretreatment case based on the finding that pretreating Apatite II™ with NOM does not affect copper removal.

Based on the lack of a strong NOM concentration effect, it is reasonable to group each pretreatment type together ignoring NOM concentration in order to test the statistical significance of the different pretreatments. At the 95% confidence level, there was no statistical difference between the control and the Apatite-NOM pretreatment, but the control and the other two pretreatments were statistically different. Additionally, there was no statistical difference between the Cu-NOM pretreatment and simultaneous addition cases.
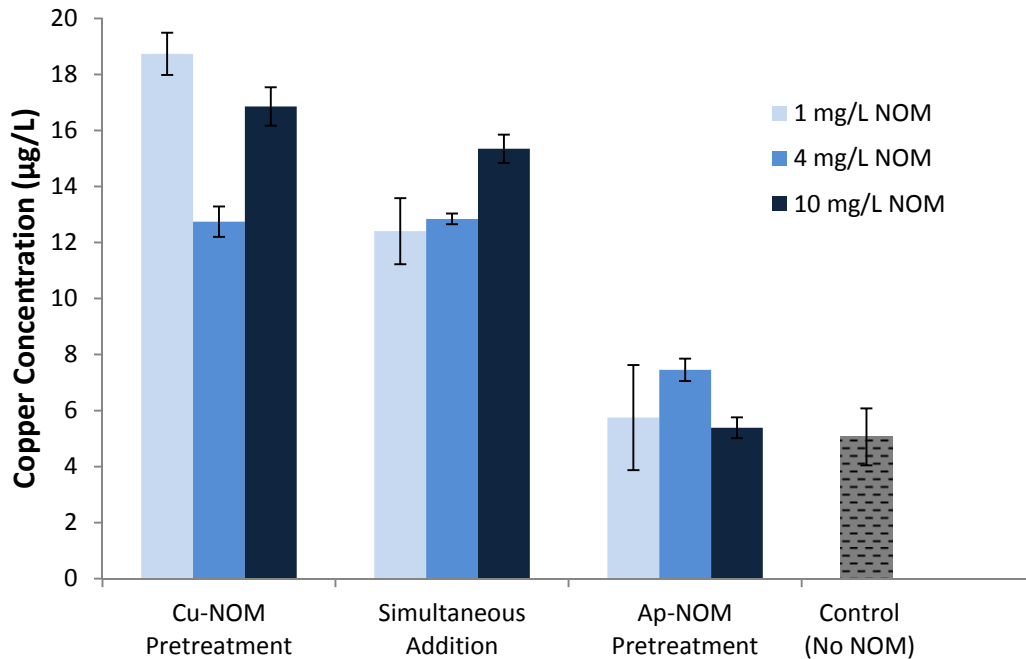
Figure 4.12: Final dissolved copper concentrations of batch experiments with Apatite II™ in synthentic stormwater under different NOM pretreatment scenarios

When Apatite II™ dissolves, Ca^{+2} and PO_4^{-3} that are released into solution will presumably be in proportion to one another based on the chemical formula for Apatite II™. This explains the parallel trends of Ca^{+2} and PO_4^{-3} release in Figure 4.13 and Figure 4.14. It should be noted that in all cases Ca^{+2} and PO_4^{-3} concentrations are higher in solutions with NOM than in the control. This demonstrates that NOM in solution does not inhibit dissolution of Apatite II™, further lending evidence to the conclusion that Cu-NOM complexes (and not Apatite-NOM) inhibit copper removal. For the Apatite-NOM pretreatment case, after the NOM solution was decanted it was replaced by a solution that had been pretreated with Apatite II™. This in effect allowed twice as long for dissolution, which explains the elevated concentrations of Ca and PO_4^{-3} for that case. In kinetic experiments with Apatite II™ in synthetic stormwater without NOM, calcium concentration increased from 6.3 mg/L at 48 hours to 10.2 mg/L at 96 hours. This is a 62% increase, which aligns closely with the 70% increase in calcium over the same time step in this experiment. In Figure 4.13 it can be seen that calcium concentrations increase as NOM concentration increases. This is likely due to the formation of Ca-NOM complexes, which effectively draw calcium into the aqueous phase.
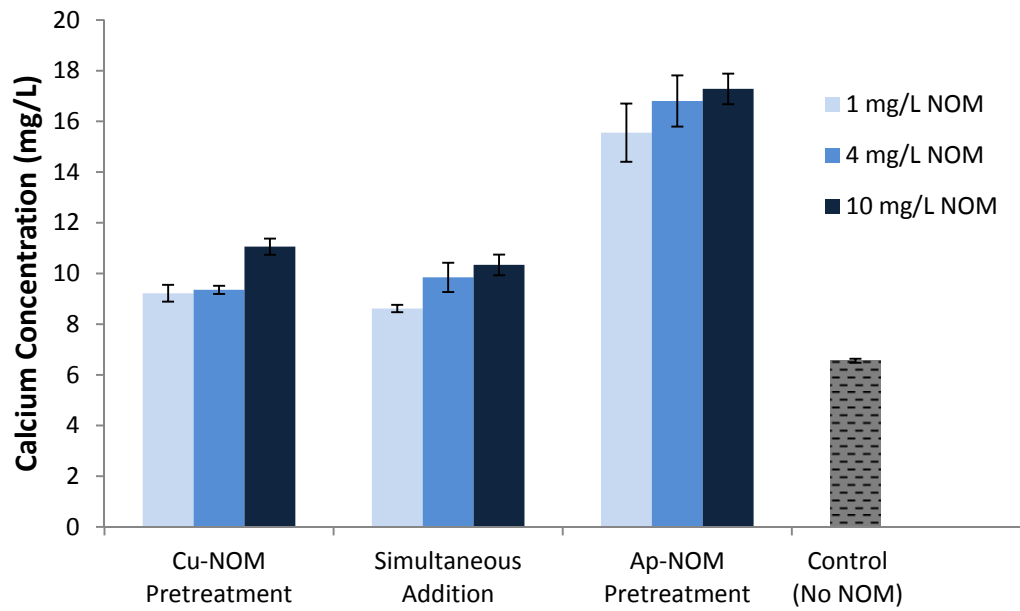
Figure 4.13: Final aqueous calcium concentrations of batch experiments with Apatite II™ in synthentic stormwater under different NOM pretreatment scenarios
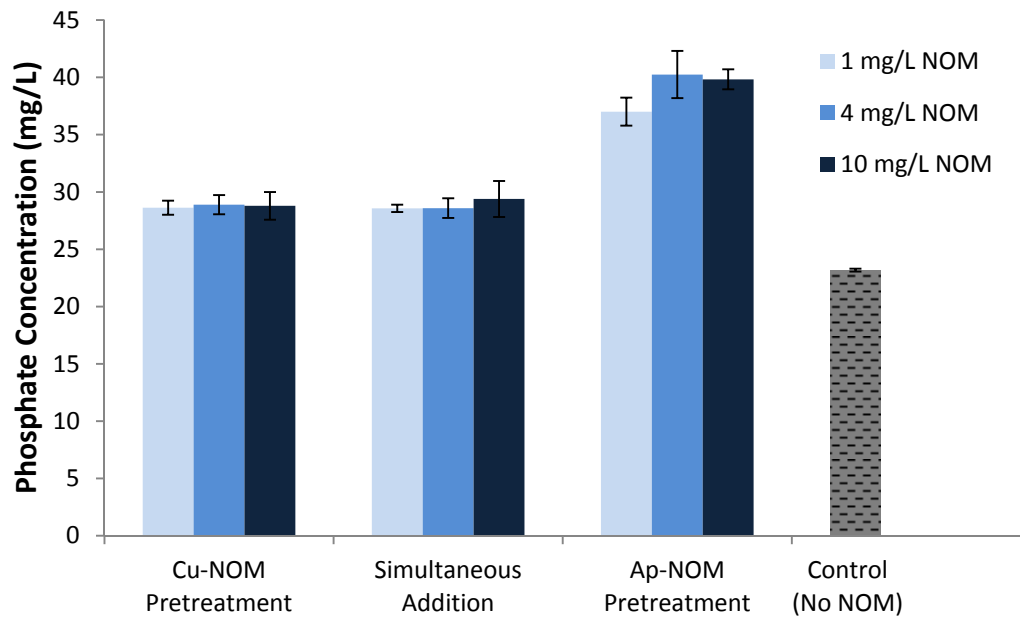
Figure 4.14: Final aqueous phosphate concentrations of batch experiments with Apatite II™ in synthentic stormwater under different NOM pretreatment scenarios

4.4.2 Effect of NOM on Copper Removal with Compost

Experiments were performed to assess the impact of NOM on copper adsorption onto compost, utilizing a similar approach as the experiments with Apatite II™. When comparing the final copper concentration of the control to the Cu-NOM pretreatment case in Figure 4.15, it is apparent that the formation of Cu-NOM complexes inhibits copper removal. Additionally, increases in the NOM concentration in the Cu-NOM pretreatment case produced higher final copper concentrations, demonstrating that the level of inhibition is dependent upon the concentration of NOM in solution. Figure 4.15 also shows that the compost-NOM pretreatment case had lower final concentrations than the control. This is likely a product of how the samples were processed. Namely, after pretreating the compost with synthetic stormwater containing NOM, the liquid was decanted and replaced with synthetic stormwater. Therefore, the control contained fresh compost whereas in the compost-NOM pretreatment case the compost had already been in solution for 48 hours. Because leaching of organic matter from compost is highest during initial contact with solutions *(McLaughlan and Al-Mashaqbeh 2009)*, the control contained higher final DOC concentrations, which likely caused the higher final copper concentrations. Nonetheless, the final copper concentration was independent of the initial NOM concentration in the compost-NOM pretreatment case, indicating that compost-NOM interactions do not inhibit copper removal.
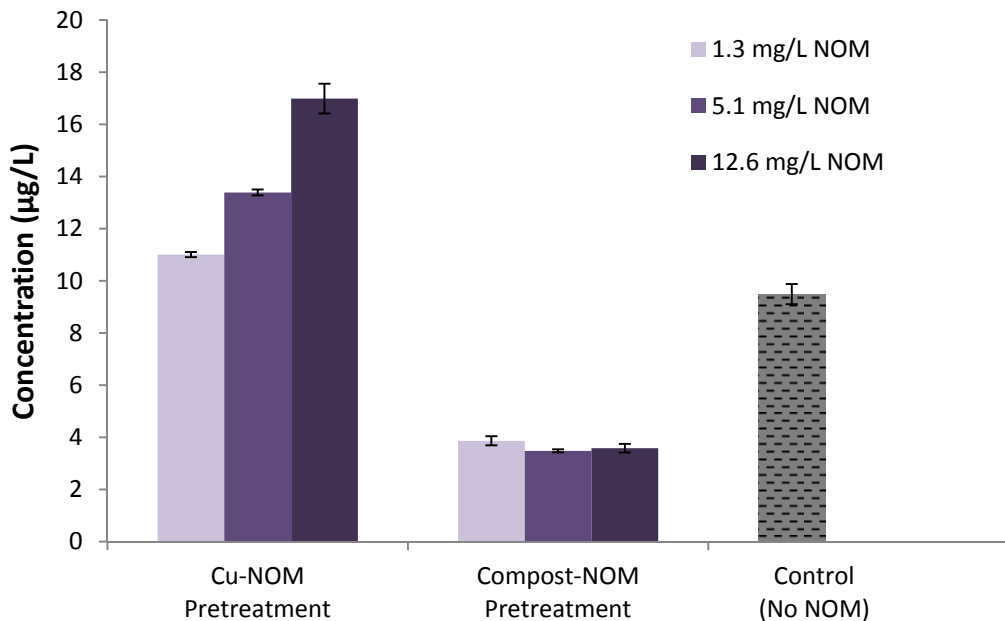
Figure 4.15: Final dissolved copper concentrations in batch experiments with different NOM pretreatment scenarios

4.5   COLUMN EXPERIMENTS

Rapid, small-scale column tests (RSSCTs) were carried out to evaluate the ability of Apatite II™ and compost to remove copper in continuous flow systems. These experiments were designed to mimic flow conditions at the field level to gain insight into copper removal that may be expected with actual stormwater BMPs. For both media types, one column was performed with natural water (river water or stormwater runoff) to more closely model actual field conditions. The characterization of the natural water samples is shown in **Error! Reference source not found.**, where the listed copper concentrations are after the samples were spiked. While each experiment will be discussed individually, **Error! Reference source not found.** shows the results of the four columns using Apatite II™ and two columns using compost to provide an initial comparison of performance.

Table 4.6: Characterization of natural water samples used in column experiments

	Stormwater	River Water
pH	6.77	7.10
Conductivity (µS/cm)	21.4	69.1
DOC (mg/L)	1.54	1.25
Copper (µg/L)	94.8	50.3
Calcium (mg/L)	1.00	4.02
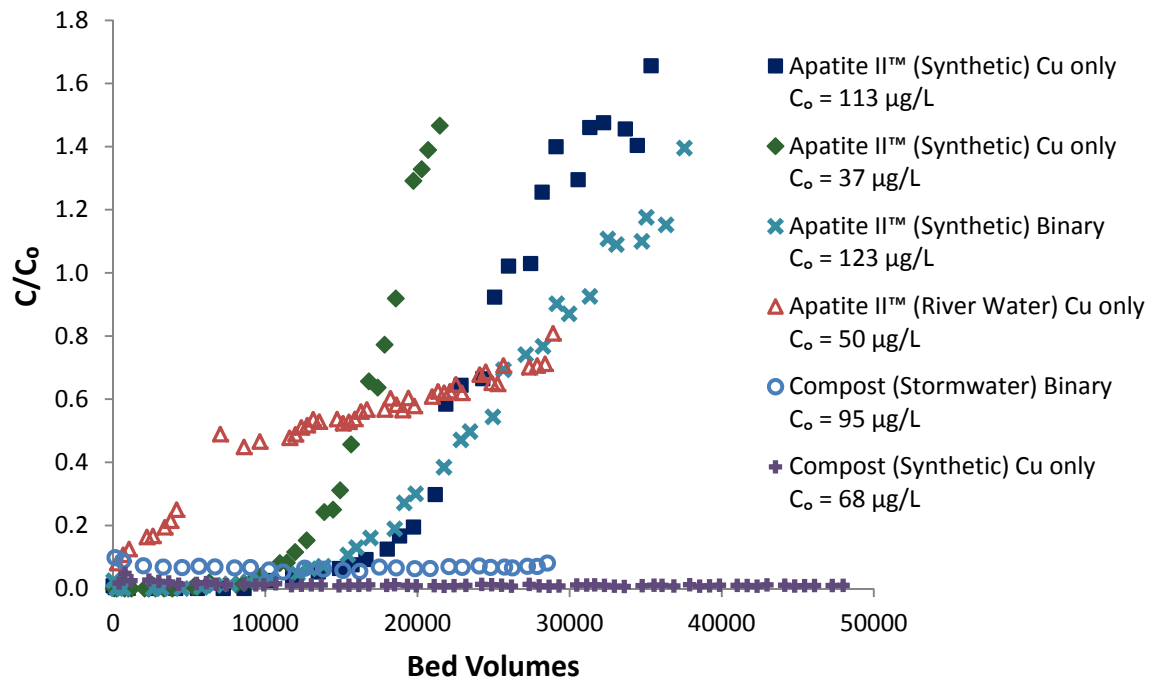
Figure 4.16: Copper breakthrough for all RSSCTs

4.5.1 Apatite II™ Column Experiments

Three RSSCTs were performed using synthetic stormwater and Apatite II™ as media. For two of these experiments, synthetic stormwater solutions were spiked with different levels of copper to determine the effect of influent concentration on copper removal. In Figure 4.16 it can be seen that on a relative basis (C/C_o), the column test with the lower influent copper concentration (37 µg/L) had a faster time to breakthrough than the column with the higher influent copper concentration (113 µg/L). This result was unexpected based on the isotherm results obtained for Apatite II™ in synthetic stormwater. Copper removal with Apatite II™ followed a linear isotherm, so based on equilibrium alone breakthrough was predicted to occur at the same time in the two experiments.

While the relative breakthrough for the two copper only experiments was different, from Figure 4.17 it is apparent that the effluent copper concentrations closely mirror one another. This is likely due to the role precipitation processes play in copper removal. Namely, over the course of the two experiments, the effluent pH from the 37 µg/L copper column remained approximately 0.25 pH units higher (a factor of about 1.8) than the 113 µg/L column (Figure 4.18). Therefore, based on malachite as the proposed solid phase and assuming the effluent carbonate concentrations are approximately equal, the reaction quotient (Q) for the reaction in Equation 4.3 is nearly the same for the two column experiments with only copper. As the pH values for the two experiments converge at higher bed volumes, Q becomes larger for the column with higher influent copper. This could be the reason effluent concentrations for the 37 µg/L column become higher than the effluent concentrations of the 113 µg/L column at higher bed volumes.

$$CuCO_3(OH)_2 \ (s) \leftrightarrow Cu^{+2} + CO_3^{-2} + 2OH^- \qquad\qquad \textbf{(4.3)}$$

From Figure 4.18 it is evident that pH values in all three experiments using Apatite II™ and synthetic stormwater decrease over time, causing increased copper solubility and leading to higher copper concentrations in the effluent. These experiments indicate that effluent pH is the strongest controlling factor on effluent copper concentration. This result lends support to the hypothesis of precipitation processes controlling copper removal, based on the strong role pH has on governing final concentrations in solubility reactions.

Calcium and phosphate leaching trends over the course of all three synthetic stormwater experiments with Apatite II™ are shown in Figure 4.18. Initially, phosphate and calcium concentrations were similar to those measured in equilibrium batch experiments (Table 4.2). As with pH, the concentrations of these ions decrease over the course of the experiment. This demonstrates that the rate of Apatite II™ dissolution decreases over time, resulting in a lower capacity to buffer the solution and fewer available ions for the formation of metal precipitates.

As was discussed in Section 4.3.1, phosphate plays an important role in buffering the solution to a pH where metal precipitates can form. Additionally, previous work indicated that phosphate participates in the metal precipitation reactions responsible for removing copper *(Oliva et al. 2011)*. However, phosphate is a pollutant of concern in stormwater runoff. The negative effects of phosphate on aquatic ecosystems have been well documented, and the concentrations leaching

from Apatite II™ are consistently above 2 mg/L, with concentrations during early operation approaching 20 mg/L. An evaluation of the impact of phosphate loading on receiving waters or some type of phosphate mitigation incorporated into the BMP directly following contact with Apatite II™ should be adopted prior to using Apatite II™ as media.
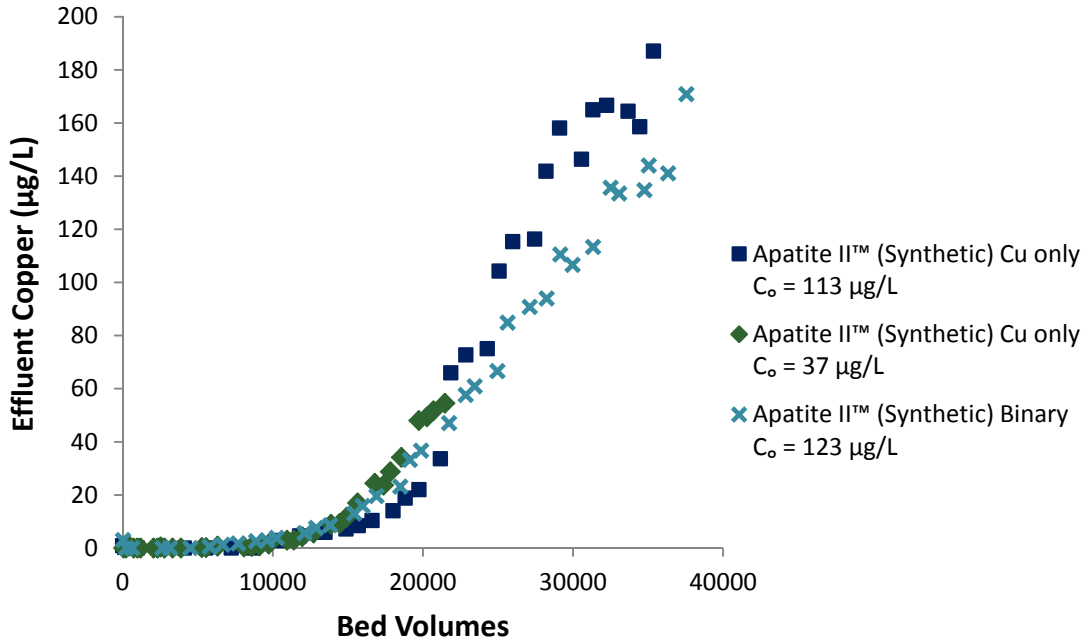
Figure 4.17: Effluent copper for RSSCTs using Apatite II™ and synthetic stormwater

a)

60

b)

c)
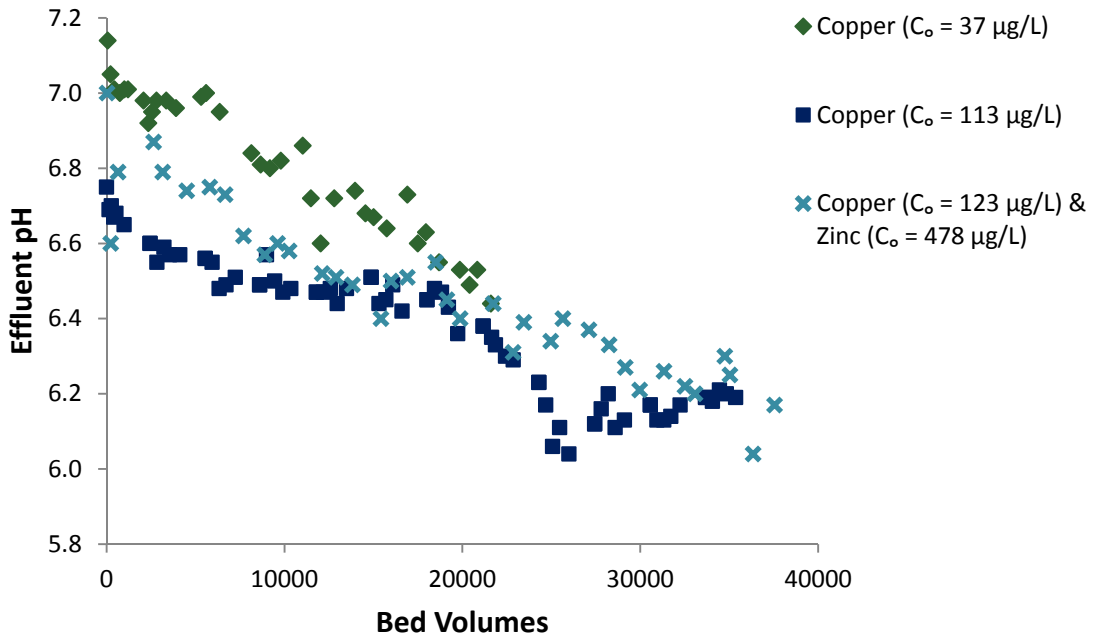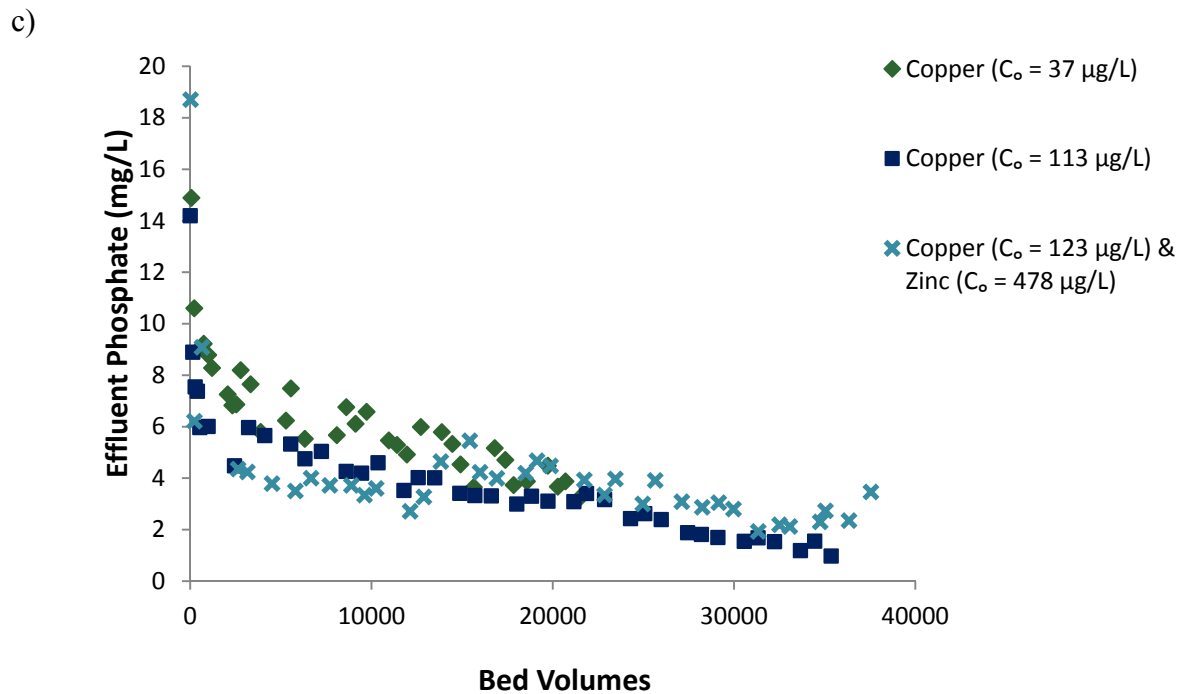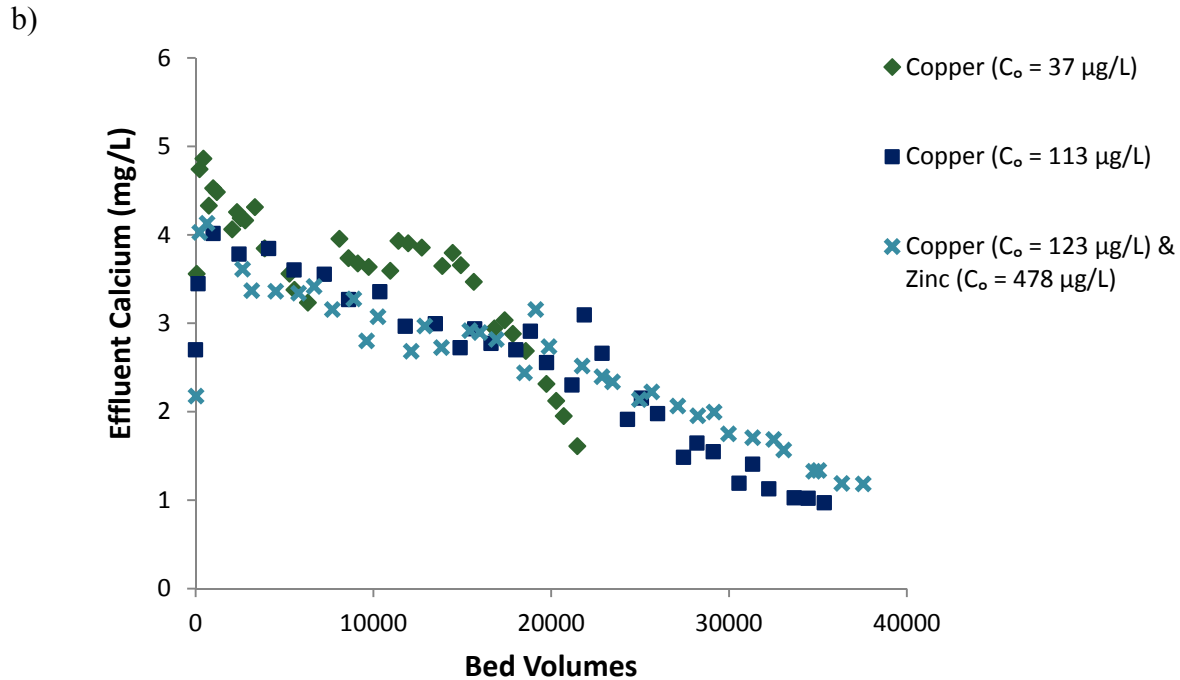
Figure 4.18: Effluent pH, calcium, and phosphate from RSSCTs using Apatite II™ and synthetic stormwater

In addition to the two column experiments with only copper, one RSSCT was performed with both copper and zinc in the influent, and the breakthrough curves from this experiment are shown in Figure 4.19. The influent copper concentration (C_o = 123 µg/L) was chosen to be similar to a previous column with only copper (C_o = 113 µg/L), and the influent zinc (C_o = 478 µg/L) was chosen based on typical copper to zinc ratios found in stormwater runoff *(Kayhanian*

et al. 2007; Nason et al. 2012a). From Figure 4.19, it is apparent that zinc breakthrough occurs prior to copper breakthrough. Therefore, if the treatment goal involves removal of both copper and zinc, the life of the filter will be limited by the removal capacity of zinc.

When defining breakthrough as C/C_o=0.5, the binary column achieved copper breakthrough after approximately 23,400 bed volumes. This is nearly the same as the copper only column (C_o=113 µg/L), which reached breakthrough after approximately 21,700 bed volumes. This similarity indicates that zinc does not have a significant effect on copper removal using Apatite II™, a result that was also observed in batch experiments (Figure 4.5). However, the shapes of the breakthrough curves from the binary and single element experiments are noticeably different, with that of the copper only column appearing to be much closer to a square wave than the binary column (Figure 4.16 and Figure 4.17). This spreading of the copper mass transfer zone in the binary column is likely caused by altered kinetics of copper removal in the presence of zinc. Copper and zinc could be competing for adsorption sites or ions for precipitation, which could in turn cause some resistance to mass transport and lead to the more diffuse breakthrough that is observed in the binary column.
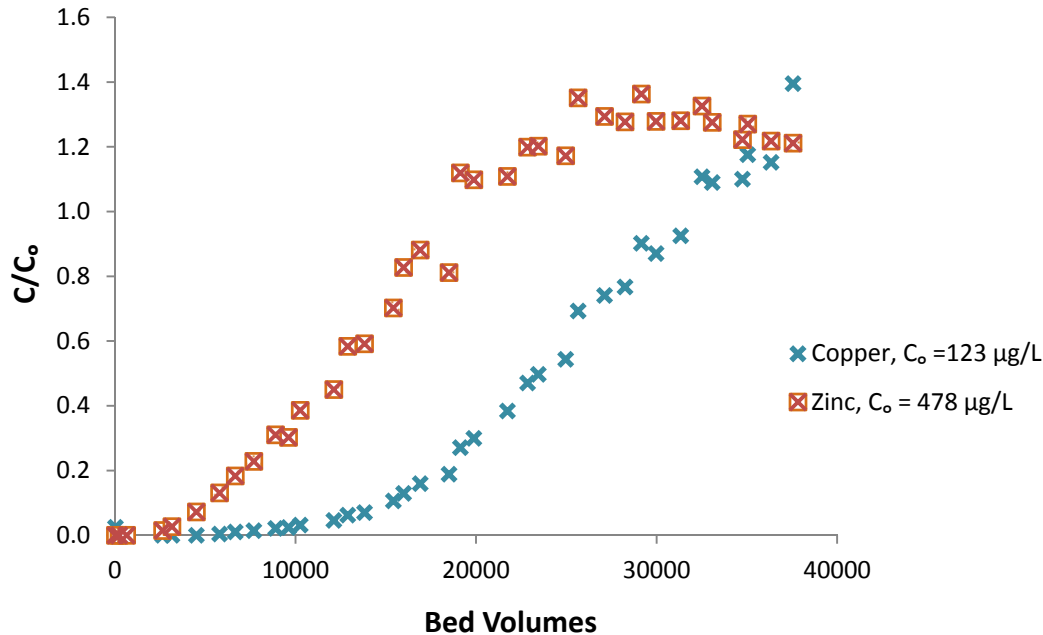
Figure 4.19: Copper and zinc breakthrough in binary element RSSCT with Apatite II™ and synthetic stormwater

In each of the three column experiments with Apatite II™ and synthetic stormwater, C/C_o exceeded one in the later stages of the column, indicating that effluent copper and zinc concentrations exceeded those of the influent (Figure 4.16). This is likely due to the decreasing pH values that are observed at the later stages of the experiments (Figure 4.18), which increases solubility of previous precipitated copper and induces desorption of copper from surface sites. Example reactions for surface complexation (Equation 4.4) and metal hydroxide precipitation (Equation 4.5) both demonstrate this process, where increased hydrogen activity (i.e. lower pH)

drives the reaction to the left. In these equations, *HAP* represents the hydroxyapatite mineral, and *Me* denotes a generic metal ion.

$$\text{HAP-OH} + \text{Me}^{+2} \leftrightarrow \text{HAP-O-Me}^+ + \text{H}^+ \tag{4.4}$$

$$2\text{OH}^- + \text{Me}^{+2} \leftrightarrow \text{Me(OH)}_2 \ (s) \tag{4.5}$$

The release of previously deposited metals is a major drawback to the potential use of Apatite II™. If used, the Apatite II™ would require consistent monitoring to ensure that it was still removing Apatite II™ and not transitioning into a copper source. For widely distributed stormwater BMPs, this would potentially require regular sampling across varied locations and timely removal of used Apatite II™. This would be both costly and time-consuming, and would need to be factored into the cost of using Apatite II™. An ideal media type would remove metals permanently, and based on these column experiments there is strong indication that this is not the case with Apatite II™.

Over the course of the column experiments the color of the media gradually changed from yellow to blue-green, as is shown in Figure 4.20. This lends visual support to the hypothesis that the formation of copper precipitates were driving copper removal, based on the final Apatite II™ color closely resembling the patina color characteristic of many copper precipitates.

SEM-EDS was used to compare the surface structure of used and new Apatite II™ (Figure 4.21), and analyze the chemical composition of the used Apatite II™ (Figure 4.22). As expected, copper was detected at the mineral surface, demonstrating copper removal by the Apatite II™. Additionally, calcium and phosphorus were both detected, although at significantly lower levels than the virgin Apatite II™ (Figure 4.2). This demonstrates that calcium and phosphorus are significantly depleted due to the dissolution of Apatite II™, which is in agreement with Figure 4.18. The elevated carbon content of the used Apatite II™ is most likely due to the preferential dissolution of the mineral phase, leaving the organic materials that originally existed within the pore structure. XRD measurements were also conducted on the used Apatite II™ to determine the crystal phase of the copper precipitates. However, a distinct copper containing phase was not observed, possibly due to its poor crystallinity and low relative concentration.

Figure 4.20: Sieved Apatite II™ before (left) and after (right) a column experiment
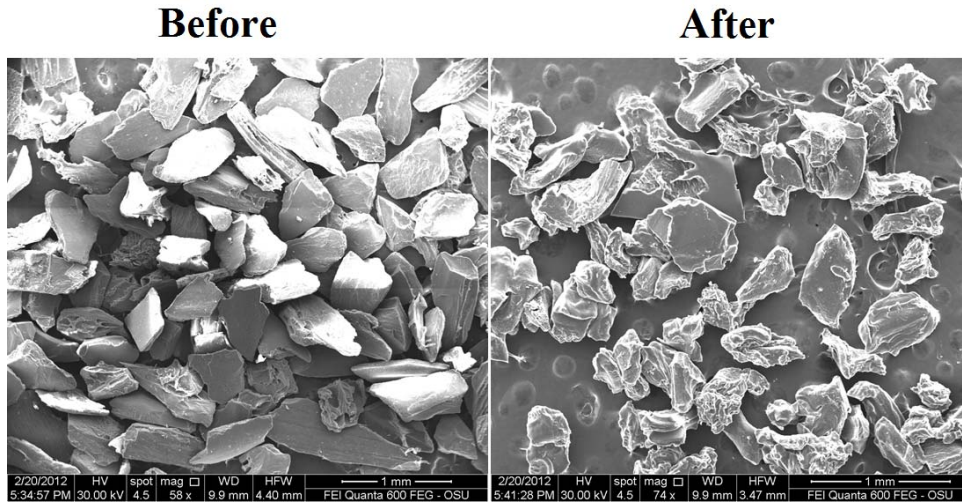
Figure 4.21: SEM Image of Apatite II™ before and after a column experiment with synthetic stormwater (Copper C_o = 113 µg/L)

Element	Molar %
C	80.14
O	18.17
Na	0.31
P	0.25
S	0.41
Ca	0.4
Cu	0.32
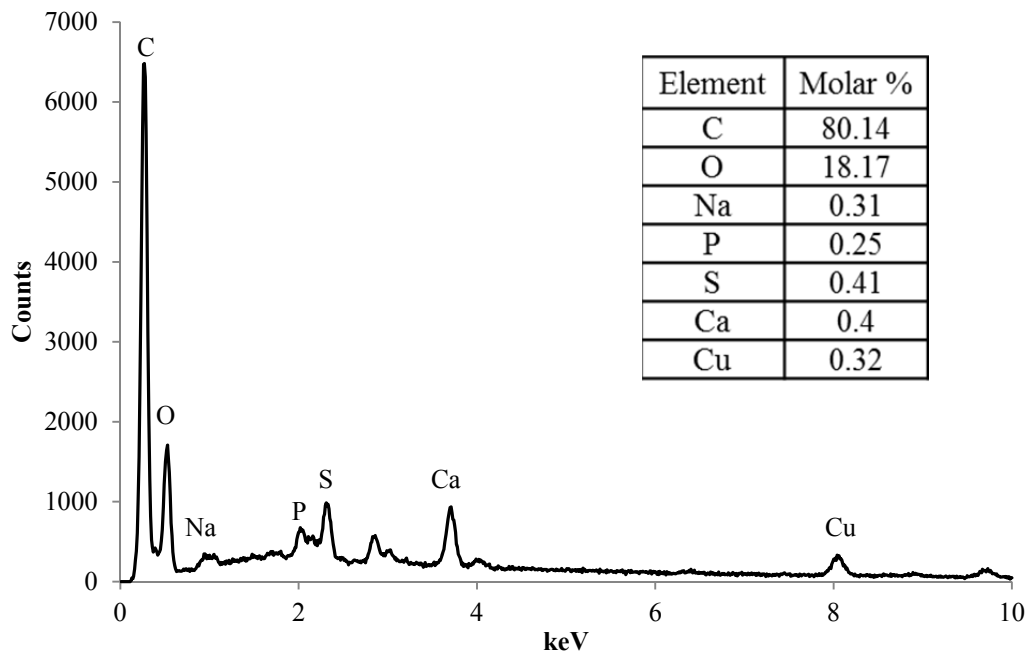
Figure 4.22: EDS spectrum of Apatite II™ after a column experiment with synthetic stormwater (Copper C_o = 113 µg/L)

For the column tests with synthetic stormwater, effective adsorption density ($q_{effective}$) was calculated from the cumulative mass of metal removed at breakthrough normalized by the mass of filter media. For calculations, breakthrough was defined as the time when C/C_o = 0.5, which should correspond to the breakthrough of a column that rapidly reaches equilibrium between the

liquid and solid phases and has no mass transport limitations. These values were then compared to q_e values obtained using the isotherm equations from batch experiments. This comparison makes it possible to evaluate the capability of equilibrium experiments to be used as a predictive tool for estimating media life. The results of these calculations are shown in Table 4.7.

In all cases, the removal capacity of Apatite II™ for copper in column tests was higher than that in batch tests. During column operation, constant influent concentrations were maintained. As a result, the driving force for precipitation (C-C_{sat}) remained at an elevated state. In batch experiments, on the other hand, the concentration decreases over the duration and results in decreasing driving force for precipitation over time. Furthermore, the differences in the solid to liquid ratio within the column and the presence of increased quantities of precipitated copper solids in the column experiments may have enhanced the precipitation process. The surface area to liquid ratio is approximately 500 times larger in the column experiments (18 m^2/L) than in the batch experiments (0.03 m^2/L). This would result in increased available surface area for heterogeneous precipitation or crystal growth on the surface of the media.

Table 4.7: Calculated adsorption densities from column and batch experiments

| | Copper only (C$_o$=37 μg/L) | Copper only (C$_o$=113 μg/L) | Binary | |
			Copper (C$_o$=123 μg/L)	Zinc (C$_o$=478 μg/L)
q$_{effective}$ (column tests)	1.1	4.3	4.7	9.0
q$_e$ (batch tests)	0.49	1.5	1.6	8.0

In addition to the synthetic stormwater column experiments with Apatite II™, a RSSCT was performed using river water spiked with copper (C$_o$ = 50 μg/L). From the very first sample, this column had measureable copper in the effluent, and the concentration steadily increased over the course of the experiment (Figure 4.23). This resulted in a breakthrough curve that was drastically different from the experiments using synthetic stormwater (Figure 4.16). Effluent pH was in the same range for both studies, demonstrating that pH was not the primary cause for the dissimilar curves. The difference in ionic strength of synthetic stormwater and river water is small, and ionic strength has been shown to have little effect on copper partitioning *(Lu and Allen 2001)*. As mentioned in Section 2.6, many studies have demonstrated that NOM has a significant impact on copper speciation and removal. It is hypothesized that NOM in the influent water is complexed with copper, leading to measurable copper concentrations from the very first sample. There has been work demonstrating that organic acids in solution inhibit precipitation of hydroxyapatite, likely due to the blocking of crystal growth sites *(Inskeep and Silvertooth 1988)*. A similar effect could have inhibited copper precipitation, thereby causing the effluent concentrations to slowly rise over the course of the experiment. Furthermore, as was mentioned previously the decreased rate of Apatite II™ dissolution over time results in lower pH values and fewer available ions for precipitation, likely contributing to the increasing effluent concentrations over the course of the experiment.

Due to the variability of copper concentrations in stormwater from first-flush and seasonal effects, along with previous work in synthetic stormwater columns demonstrating the potential for desorption/dissolution of copper from Apatite II™, it is important to understand how Apatite II™ will behave when exposed to varying copper concentrations. Figure 4.23 demonstrates that when influent copper concentration was switched from 50 to 2 µg/L, copper was leached at concentrations that appear to level off at around 10 µg/L. This demonstrates that some of the copper that was removed is released back into solution, albeit at lower concentrations than the original influent. In practice, stormwater filters are deployed in the field and receive infrequent maintenance during their service life. This makes the impermanence of copper removal especially problematic, because if a filter is left out too long it will eventually leach copper. Additionally, storm-to-storm variability in influent copper concentrations could lead to a scenario where the filter removes copper from one storm only to release it the following storm.
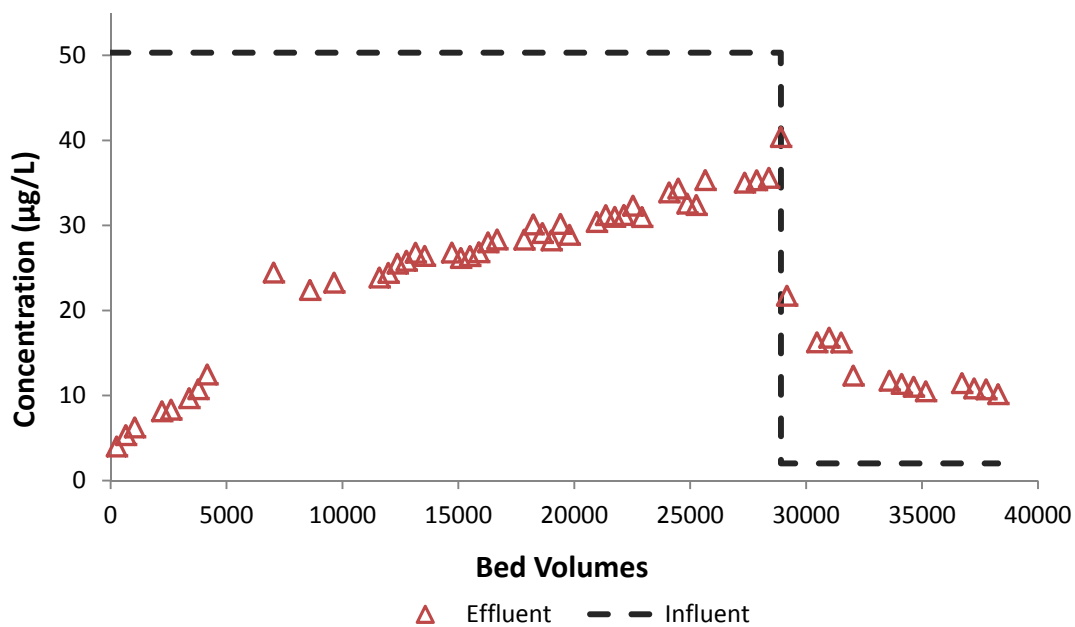
Figure 4.23: Effluent copper for column with Apatite II™ in river water that was spiked with copper for the first 28,000 bed volumes

4.5.2 Compost Column Experiments

To facilitate comparison between the two media types, column experiments with synthetic stormwater and actual stormwater were conducted using compost as media. From Figure 4.16, it can be seen that for the synthetic stormwater column ($C_o = 68$ µg/L) effluent concentration remained nearly zero for the duration of the experiment. With the exception of one data point, every effluent sample contained less than 2 µg/L of copper, which has been shown to be a threshold for inhibitory effects on coho salmon *(Sandahl et al. 2007)*. The complete lack of breakthrough is especially impressive when compared to the breakthrough curves for Apatite II™ in synthetic stormwater. Defining breakthrough as $C/C_o=0.5$, the Apatite II™ columns achieved breakthrough after approximately 16,000, 21,700, and 23,400 bed volumes, whereas

the compost column was still removing copper to below 2 µg/L after 48,000 bed volumes. Additionally, each of the Apatite II™ columns began to exceed the 2 µg/L threshold after approximately 10,000 bed volumes. These results indicate that at concentrations relevant to stormwater runoff, compost will have a much longer media life than Apatite II™.

Similar to the compost column with synthetic stormwater, copper breakthrough was not achieved for the RSSCT using compost and stormwater runoff (Figure 4.24). In spite of the lack of breakthrough, this column proved useful in again demonstrating superior copper removal when using compost as opposed to Apatite II™ (Figure 4.16). Removal efficiency was lower as compared to the synthetic stormwater test with compost, which is likely due to the presence of NOM in solution. As was discussed previously, NOM readily complexes with copper, which in turn diminishes adsorption capacity.

While copper did not achieve breakthrough, Figure 4.24 shows that full breakthrough of zinc occurred toward the end of the column experiment with stormwater runoff. This demonstrates that zinc did not outcompete copper for adsorption sites. This agrees with batch experiments that revealed that the presence of zinc did not inhibit copper removal (Section 4.2.2). It is important to note that zinc is normally present at concentrations considerably higher than copper, whereas in this experiment the reverse is true. Understanding the effects of elevated levels of zinc with respect to copper in column experiments may be a worthwhile future investigation to fully understand copper removal with compost. However, effluent copper concentration remained constant regardless of effluent zinc, indicating that elevated levels of zinc would not likely have an effect on the fraction of copper removal.

Due to concern over ion leaching from compost, cation leaching was measured for the compost column with stormwater, and the results are shown in Figure 4.25. Cation leaching was observed in the early stages of the column, but quickly decreased and appeared to stabilize at very low levels. While nitrate and phosphate are more of a concern with respect to ion leaching, cations can be detected at lower concentrations using the techniques employed in this study (i.e. ICP-OES for cations and IC for anions), and therefore can more accurately display leaching trends at concentrations below 1 mg/L. While these trends do not lend direct insight into the leaching concentrations of nitrate and phosphate, they do demonstrate the time frame over which the initial flush of nutrients occurs, and potentially can serve as a surrogate measurement for anions.

It should be noted that in both RSSCTs with compost, experiments were terminated due to pressure buildup to a point that exceeded the limitations of the column setup, eventually causing leaks at tubing joints. This is thought to be the result of the migration of small particles that subsequently plugged up pore spaces. While it would be optimal to achieve breakthrough in order to calculate the column adsorption capacity ($q_{effective}$) and to formulate preliminary estimations of media life at the field scale, these experiments were useful in forming a basis of comparison with Apatite II™ for evaluating a proposed media type.
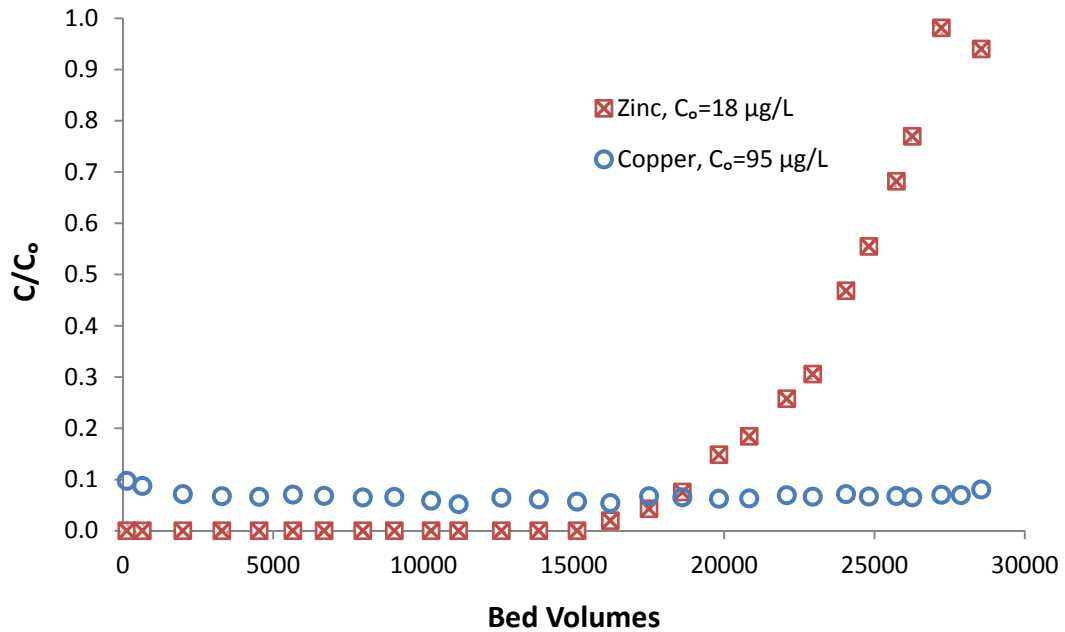
Figure 4.24: Copper and zinc breakthrough curves for RSSCT with compost in stormwater runoff spiked with copper
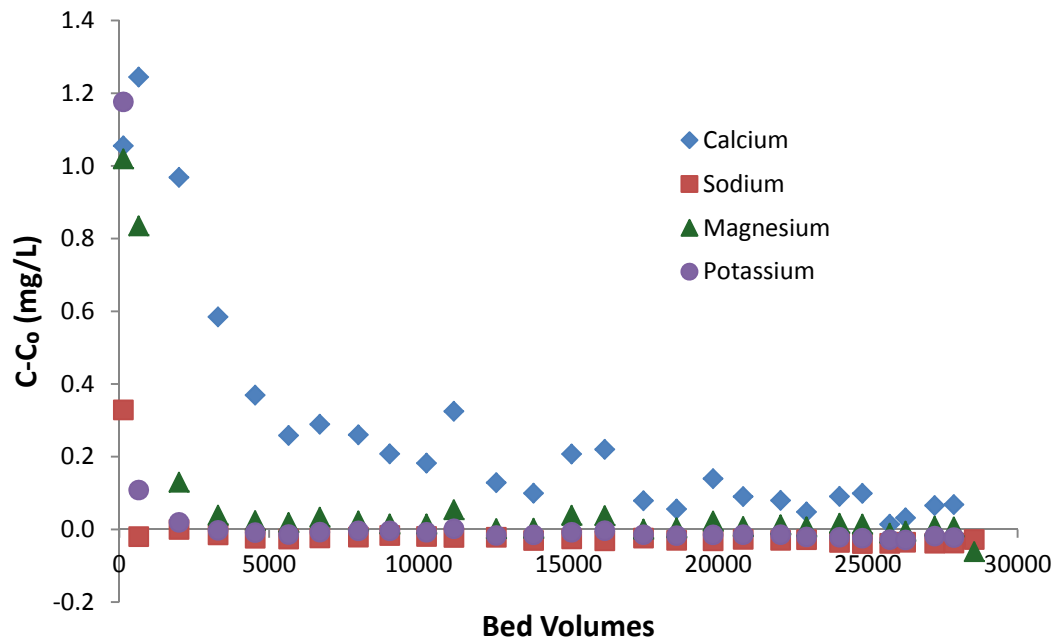
Figure 4.25: Cation leaching from compost in RSSCT with stormwater runoff

5.0   FIELD RESULTS AND DISCUSSION

Seven storms were sampled using Apatite II™ as filter media, and five storms were sampled using compost. In each case, rainfall data was recorded from NOAA.gov, flow and sampling data was downloaded from ISCO autosamplers, and influent and effluent composite samples were analyzed in the lab for complete water quality characterization. Flow rate was variable over the course of the storms, with typical values ranging from 2 to 6 gpm. This corresponds to loading rates of 0.13 to 0.38 gpm/ft^2 (0.51 to 1.53 cm/min), and hydraulic residence times of 6.6 to 20 minutes. Full data sets for each of the twelve storms are available in the Appendix (section 8.5), along with hydrographs of flow through the filter (section 8.6).

5.1   FIELD RESULTS WITH APATITE II™ AS MEDIA

Figure 5.1 displays influent and effluent dissolved copper over the seven storms with Apatite II™, as well as the cumulative flow through the filter during those storms. For the first storm, 59.8% of dissolved copper was removed, reducing the influent concentration from 25.2 μg/L to 10.1 μg/L. While this initial removal efficiency was considerably lower than in the column test with synthetic stormwater, it was not unexpected based on the effect NOM has on removal, as demonstrated by batch experiments and the natural water RSSCT. The second sampling event demonstrated a similar trend, where copper removal occurred but at a mere 16.1% efficiency. In the third storm, however, copper concentration in the effluent was higher than in the influent by a factor of 3.1. Copper release back into the aqueous phase upon switching from high to low influent concentrations was observed previously in the natural water column test with Apatite II™ (Figure 4.23), demonstrating this is not an isolated occurrence. On this basis, copper removal from stormwater using Apatite II™ cannot be viewed as permanent; based on the influent characteristics, the filter could shift from acting as a copper sink to serving as a copper source. This is especially problematic due to the nature of stormwater runoff, which exhibits temporal fluctuations in dissolved copper concentration. In the remaining storms there was little to no copper removal, providing ample evidence that Apatite II™ was ineffective at removing dissolved copper at the field scale.

In RSSCTs with Apatite II™, breakthrough occurred between 12,000 and 23,400 bed volumes, depending on the experimental conditions (Figure 4.16). Because column experiments and the field site were designed to mimic one another based on scaling relationships, theoretically breakthrough should occur after the same amount of bed volumes. Through seven storms, the Apatite II™ filter had treated 20,000 gallons (Figure 5.1), which equates to 500 bed volumes. At that point, the column experiments had not even begun to break through, indicating that the high effluent concentrations are likely a product of inefficacy of the media type in field conditions as opposed to filter breakthrough.
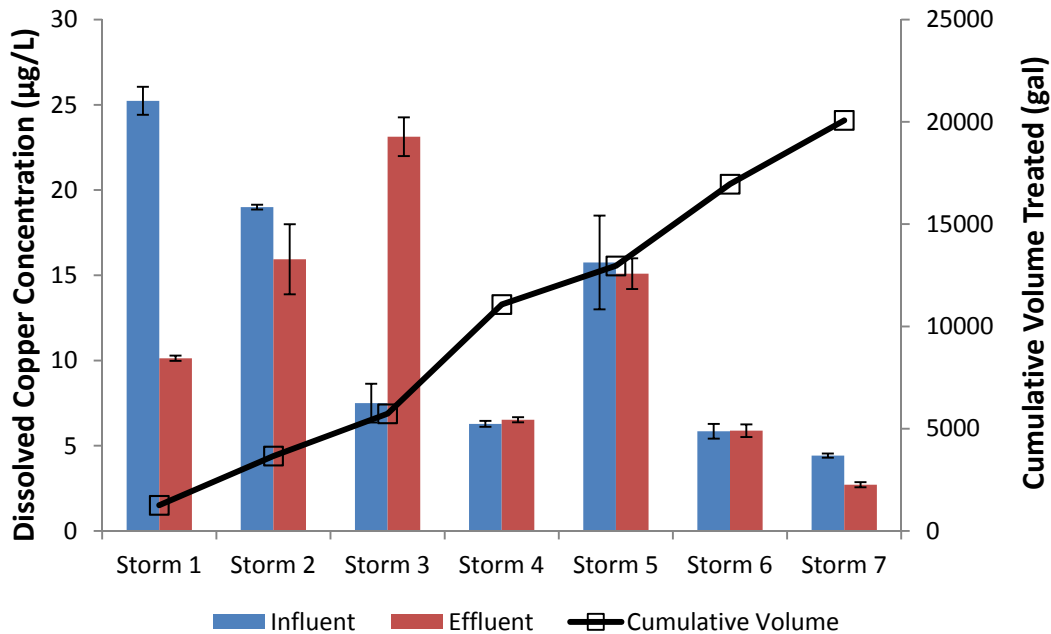
Figure 5.1: Influent and effluent dissolved copper, with error bars representing standard deviations and cumulative volume plotted on the secondary axis

In addition to dissolved copper, it is important to monitor total copper due to the potential for partitioning of solid phase copper into the aqueous phase. Influent and effluent total copper concentrations are shown in Figure 5.2. This figure illustrates that, similar to dissolved copper, total copper removal using the Apatite II™ filter was somewhat unpredictable. In the first, fourth, and seventh runoff events, the filter exhibited favorable removal, with efficiencies of 89.5%, 43.3%, and 61.4 % respectively. For the remaining storms, however, there was either minimal removal or release of total copper back into solution. This could be attributable to variable TSS removal, a hypothesis that is further discussed in section 5.2.
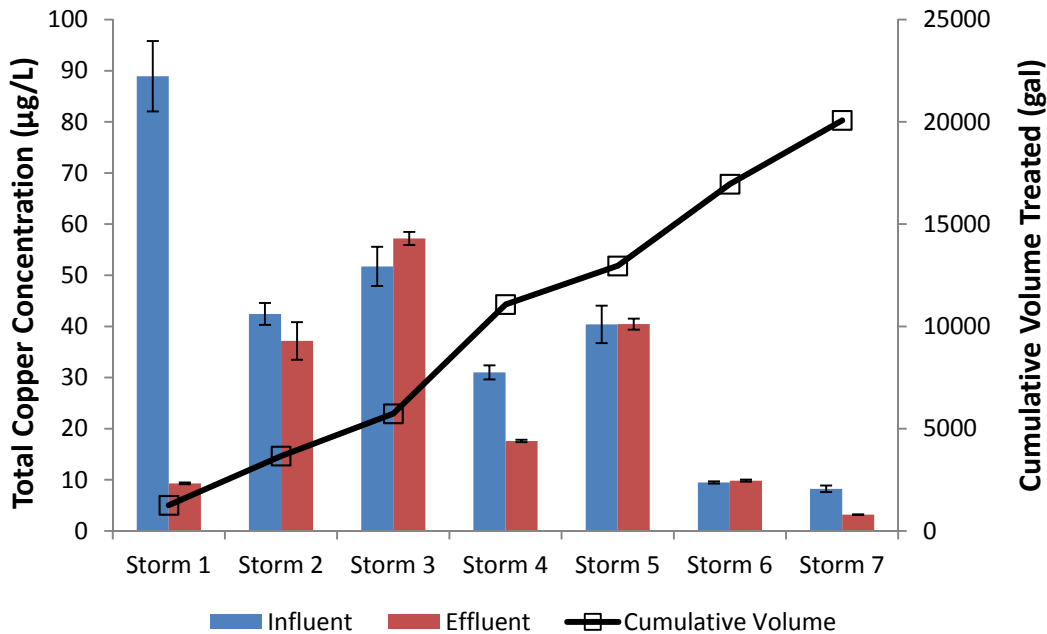
Figure 5.2: Influent and effluent total copper, with error bars representing standard deviations and cumulative volume plotted on the secondary axis

Several studies have demonstrated that zinc is commonly present in stormwater runoff, typically at concentrations several times higher than copper *(Kayhanian et al. 2007; Nason et al. 2012a)*. This is particularly important based on recent work demonstrating that zinc can cause acute toxicity to aquatic organisms, with median lethal concentrations as low as 166 μg/L for Rio Grande cutthroat trout *(Brinkman and Johnston 2012)*. It is therefore important to monitor the impact the media filter will have on zinc. Figure 5.3 contains influent and effluent dissolved zinc concentrations for the seven storms with Apatite II™. Unlike dissolved copper, removal is fairly consistent for zinc, with removal efficiencies ranging from 19.1% to 47.4%. This demonstrates that there is far less storm-to-storm performance variability with zinc, and suggests that zinc removal is permanent. Modeling with Visual MINTEQ revealed that zinc is less likely to form metal-NOM complexes than copper, resulting in larger fractions of Zn^{+2} in solution. It is hypothesized that this is the mechanism leading to increased removal fractions with zinc, but further laboratory experiments are needed for verification.

In the binary element column study with Apatite II™, zinc breakthrough occurred prior to copper breakthrough (Figure 4.19). Based on that result it would be expected that zinc would break through before copper in field-testing as well. The fact that the fraction of zinc removal does not decrease over the course of the seven field experiments indicates that zinc breakthrough has not been reached, suggesting that copper breakthrough has not likely occurred. This is further evidence that poor copper removal can be attributed to the media itself as opposed to filter breakthrough.
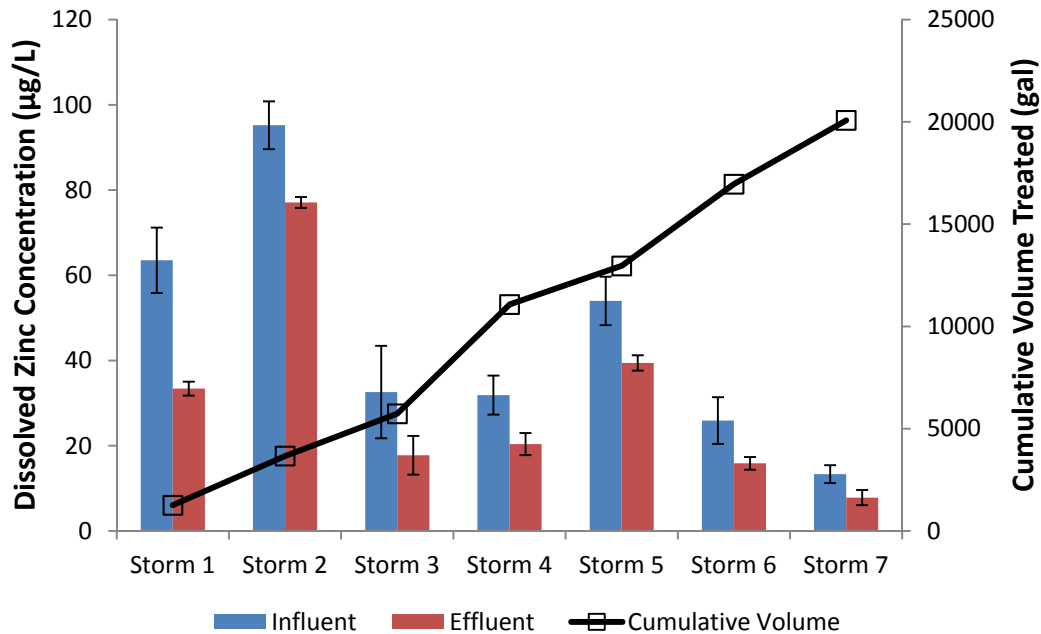
Figure 5.3: Influent and effluent dissolved zinc, with error bars representing standard deviations and cumulative volume plotted on the secondary axis

In addition to monitoring metals, it is important to understand the effect filter media will have on other water quality parameters. This is particularly relevant in light of previous studies that have documented release of DOC and phosphate from Apatite II™ *(Conca and Wright 2006; Martin et al. 2008)*. Accordingly, the leaching trends for DOC, phosphate, sulfate, and alkalinity over the seven runoff events are plotted in Figure 5.4. These trends demonstrate that following high initial leaching, equilibrium levels appear to be achieved after roughly 8,000 gallons of flow through the filter. This reveals that poor copper removal cannot be attributed to an initial flush phase, as the final four sampling events were within the equilibrated phase of the filter. Additionally, Figure 5.4 demonstrates that equilibrium leaching values of phosphate are approximately 1.5 mg/L. This is potentially troublesome due to phosphorous being the most common cause of eutrophication in receiving waters *(Correll 1998)*. Eutrophication can lead to anoxic zones, thereby making it impossible for aquatic species to inhabit those regions. Any use of Apatite II™ should therefore contain a downstream phosphate mitigation strategy to avoid creating a negative environmental impact.
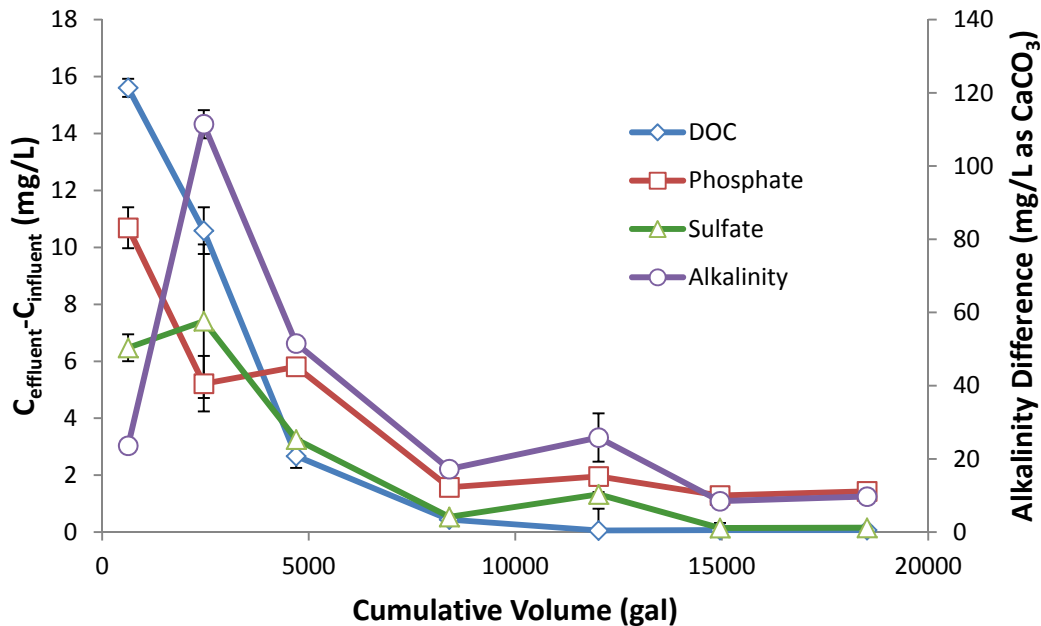
Figure 5.4: Leaching trends over seven storms for DOC, phosphate, sulfate, and alkalinity

5.2   FIELD RESULTS WITH COMPOST AS MEDIA

Influent and effluent dissolved copper concentrations from field samples using compost as filter media are shown in Figure 5.5. As with Apatite II™, removal efficiency in the field was considerably lower than in laboratory settings. In the first two storms, there was only a 0.7 µg/L difference between the influent and effluent, indicating the filter had essentially no impact on dissolved copper for those storms. Copper removal improved for the final three runoff events, with efficiencies of 45.2%, 24.7%, and 25.4% respectively, but was still much lower than the >90% efficiencies observed in column and batch experiments.

Dimensions for the filter were chosen based on relationships derived for scaling RSSCTs into full-scale operations *(Crittenden et al. 1986)*, which suggests there should not be any difference in behavior in the field and laboratory columns. This model assumes a constant diffusivity, which based on the results of kinetic tests comparing sieved and whole compost (Figure 8.3) should be a valid assumption. To determine the effect of the stormwater solution on copper removal, influent samples from Storm 4 were tested in batch and compared with results from synthetic stormwater equilibrium tests. Three 100 mL aliquots of influent stormwater were added to 200 mg of sieved compost and tumbled for 48 hours, and then filtered and tested for dissolved copper. The resulting copper concentrations were 13.2, 14.1, and 14.2 µg/L. Using the isotherms determined from equilibrium batch experiments, the predicted final copper concentration for an initial concentration of 17.1 µg/L was calculated to be 5.2 µg/L in synthetic stormwater and 6.8 µg/L in synthetic stormwater containing 0.8 mg/L SRNOM. This suggests that the composition of the stormwater is causing lower than expected removal efficiencies, a conclusion that is analyzed in more detail in section 5.3. Additionally, the measured effluent concentrations from Storm 4 ranged from 12.0 to 13.4 µg/L, which overlap with the values

obtained from the equilibrium batch testing of the influent samples. This suggests removal at the field level was not limited by kinetics, lending further support to the conclusion that it is the aquatic matrix, and not the filter design, that is limiting copper removal.
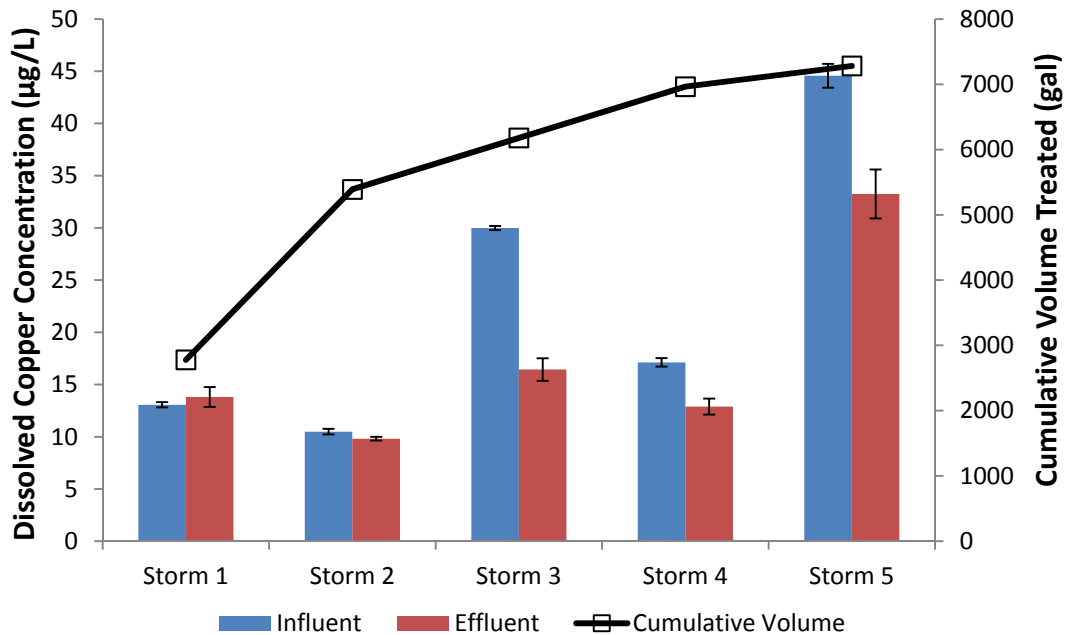
Figure 5.5: Influent and effluent dissolved copper, with error bars representing standard deviations and cumulative volume plotted on the secondary axis

Removal of total copper follows the same general trend as dissolved copper over the five runoff events, as shown in Figure 5.6. However, in each case removal efficiency for total copper is slightly higher than dissolved copper. The increased efficiency is likely attributable to the removal of particulates by the filter. TSS has been shown to be correlated with total copper *(Bloomquist 2009)*, and Figure 5.7 demonstrates that there appears to be some correlation between the fractions of TSS and particulate copper removed by the filter. Grouping the media types together, the correlation coefficient (*r*) was found to be 0.78 using Equation 3.3, which suggests there is some correlation. However, the correlation is not particularly strong and more data is needed to solidify this trend. TSS removal efficiencies were never greater than 55.8% for the compost filter, which is much lower than many other stormwater BMPs *(Barrett 2005)*. In practice, it would be useful to have a pre-filtration step for removal of solids. Along with increasing total copper removal, this would have the added effect of preventing clogging of the media filter, thereby extending its service life.
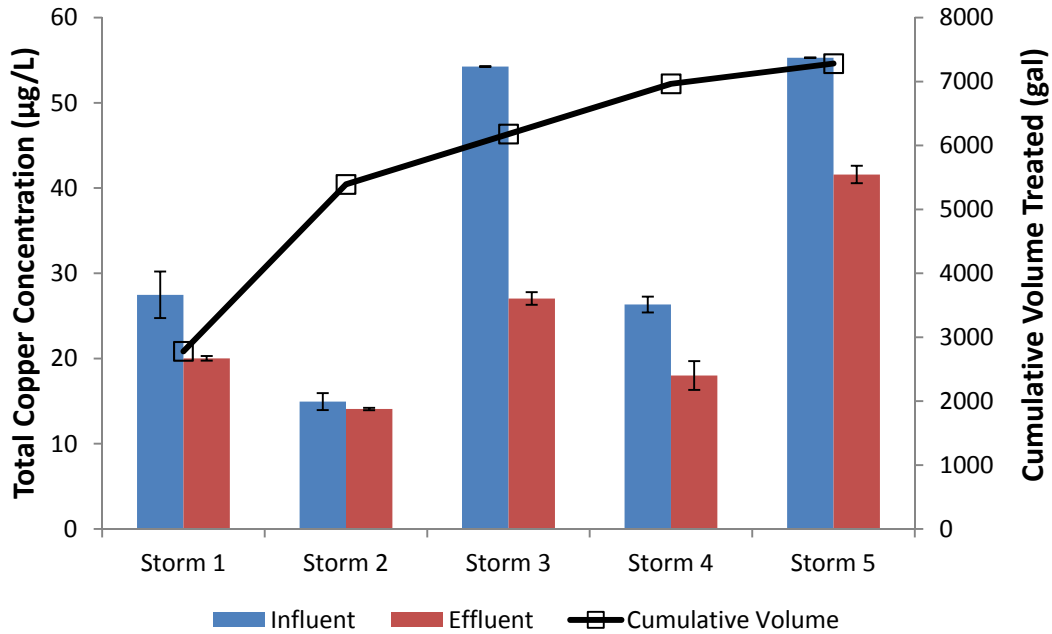
Figure 5.6: Influent and effluent total copper, with error bars representing standard deviations and cumulative volume plotted on the secondary axis
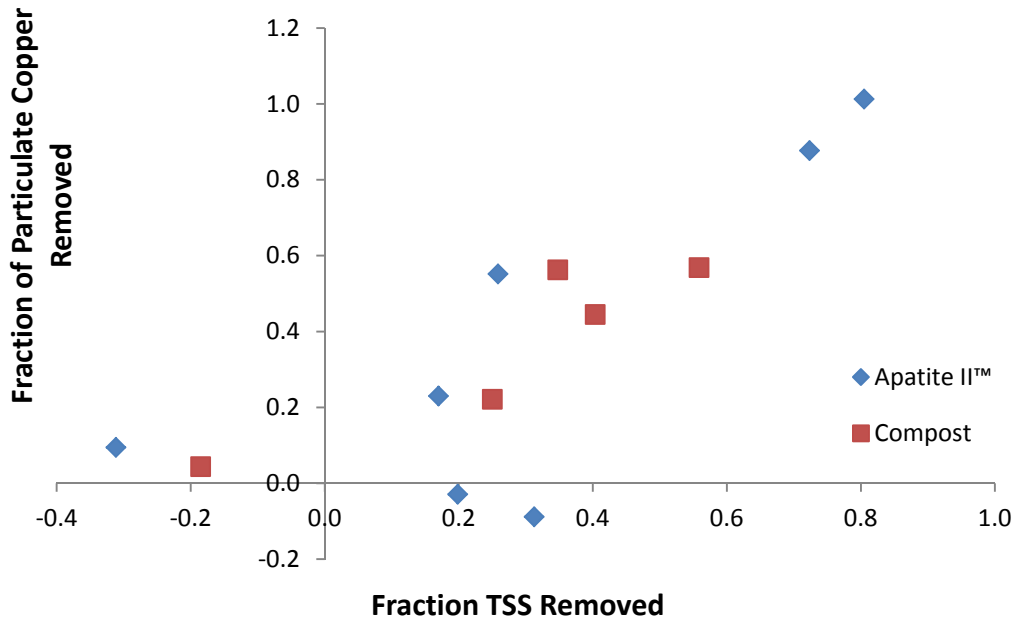
Figure 5.7: Correlation of TSS removal and particulate copper removal

As with Apatite II™, the compost filter removed zinc at a higher rate than copper. Zinc removal was also more consistent among sampling events, with efficiencies ranging from 34.3% to 58.2%

(Figure 5.8). Again, this is thought to be a product of zinc having a lower affinity for metal-NOM complexation, thereby leading to more Zn^{+2} adsorbed to the compost.
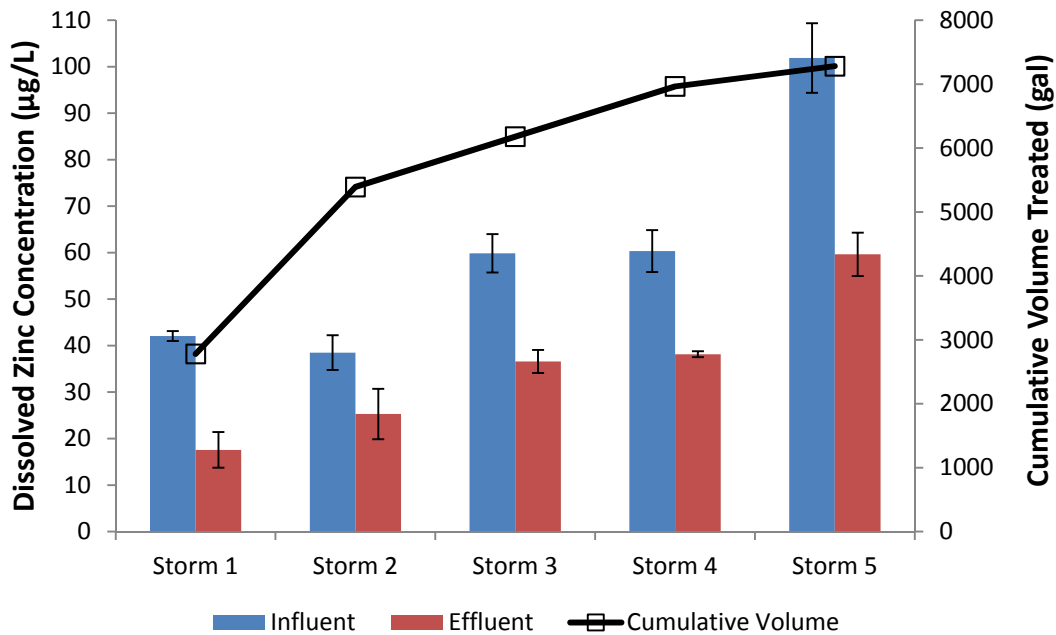
Figure 5.8: Influent and effluent dissolved zinc, with error bars representing standard deviations and cumulative volume plotted on the secondary axis

Similar to Apatite II™, there is reason for concern over leaching of carbon and other nutrients from compost *(McLaughlan and Al-Mashaqbeh 2009)*. Consequently, leaching trends for DOC, phosphate, sulfate, and nitrate are plotted in Figure 5.9. The trends in this case are less defined than with Apatite II™, but aside from nitrate, there is a general decrease in leaching over time. The cumulative volume through the compost filter was 7280 gallons, and it likely requires more total volume to reach steady state. In laboratory column tests with compost, there was no statistical difference between influent and effluent nitrate and phosphate concentrations, indicating that after the initial flushing phase these ions will likely stop leaching. However, based solely on the trends shown in Figure 5.9, there is concern over nitrate and phosphate release. As with phosphorus, heavy nitrogen loading into receiving waters can have negative effects such as eutrophication, and reducing nitrogen loading from stormwater is in itself a challenging task *(Passeport et al. 2013)*. Further investigation should be performed to see if these nutrients would continue to leach as more volume flows through the filter, and this should be factored into any decision regarding using compost in stormwater BMPs.
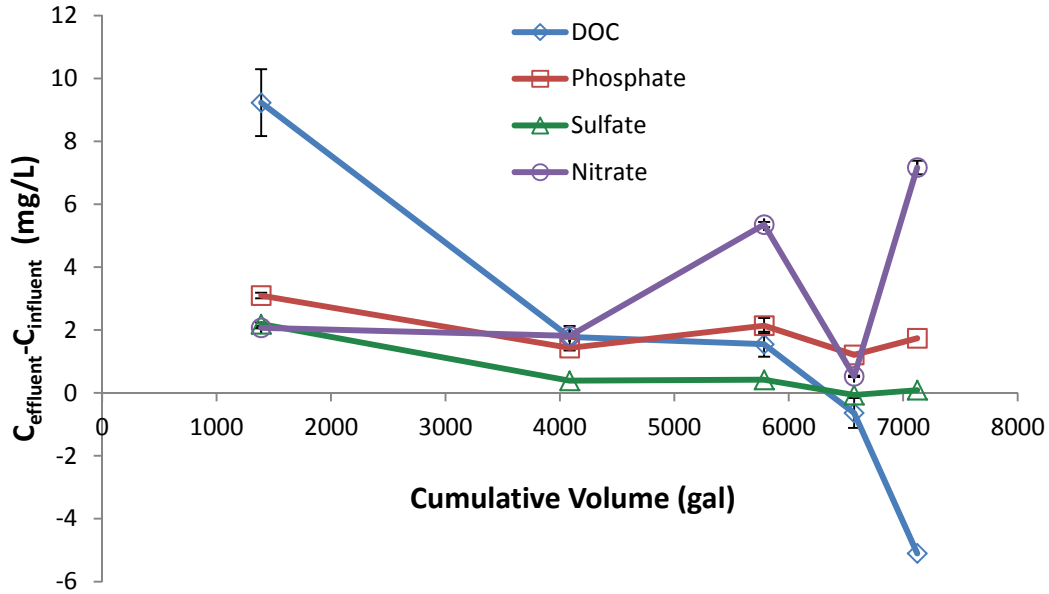
Figure 5.9: Leaching trends of DOC, phosphate, sulfate, and nitrate over five storms using compost as filter media

5.3   MODELING THE EFFECT OF DOC ON EFFLUENT COPPER

It was demonstrated in sections 4.4.1 and 4.4.2 that Cu-NOM complexes inhibit copper removal. It is therefore important to predict the fraction of copper that complexes with organic molecules. An empirical relationship between stormwater DOC concentration and the concentration of copper binding ligands (L) as measured by competitive ligand exchange adsorptive cathodic stripping voltammetry is presented in Equation 4.3, where *DOC* and *L* are in M *(Nason et al. 2012b)*. Formation of CuL complexes occurs through the equilibrium reaction shown in Equation 4.4, and previous work has demonstrated that the stability constant (K_{CuL}) is large enough that it reasonable to assume that the reaction will proceed forward until one of the reactants is >99% consumed *(Nason et al. 2012b)*. From the mass balance on the organic ligand (Equation 4.5), it can be seen that when L^{-2} is the limiting reactant in Equation 4.4, L≈CuL. From the mass balance on copper (Equation 4.6), it can be seen that when copper is the limiting reactant in Equation 4.4, Cu$_T$≈CuL. It should be noted that Equation 4.6 assumes that inorganic complexes with copper are insignificant, which was confirmed by a sensitivity test with typical α values for inorganic copper complexes in solutions containing organic ligands.

$$\log[L] = 0.5 \log[DOC] - 5.22 \tag{4.3}$$

$$Cu^{+2} + L^{-2} \leftrightarrow CuL \tag{4.4}$$

$$L = CuL + L^{-2} \tag{4.5}$$

$$Cu_T = Cu^{+2} + CuL \tag{4.6}$$

Using the measured DOC values from effluent samples (or final concentrations in batch experiments), values for *L* were calculated for each experiment using Equation 4.3. Using the measured influent (or initial) copper concentrations and the calculated value for *L*, a theoretical *CuL* concentration was estimated. In both laboratory and field experiments, that theoretical *CuL* concentration closely resembled the measured effluent (or final) copper concentration. This is shown in Figure 5.10 for Apatite II™ experiments and Figure 5.11 for compost. The data point for the column tests refers to the first effluent sample, with DOC concentrations shown in Table 4.6. In both figures, the experimental data is scattered around the 1:1 line, indicating direct correlation between measured effluent copper and organically complexed copper. This suggests that the copper that is not removed by the media is complexed with organic matter. The relationship also lends explanation as to why removal efficiencies in the lab were far greater than in the field. Namely, the relatively high DOC and low dissolved copper concentrations in the field resulted in a higher fraction of organically complexed copper and hence a lower removal efficiency.
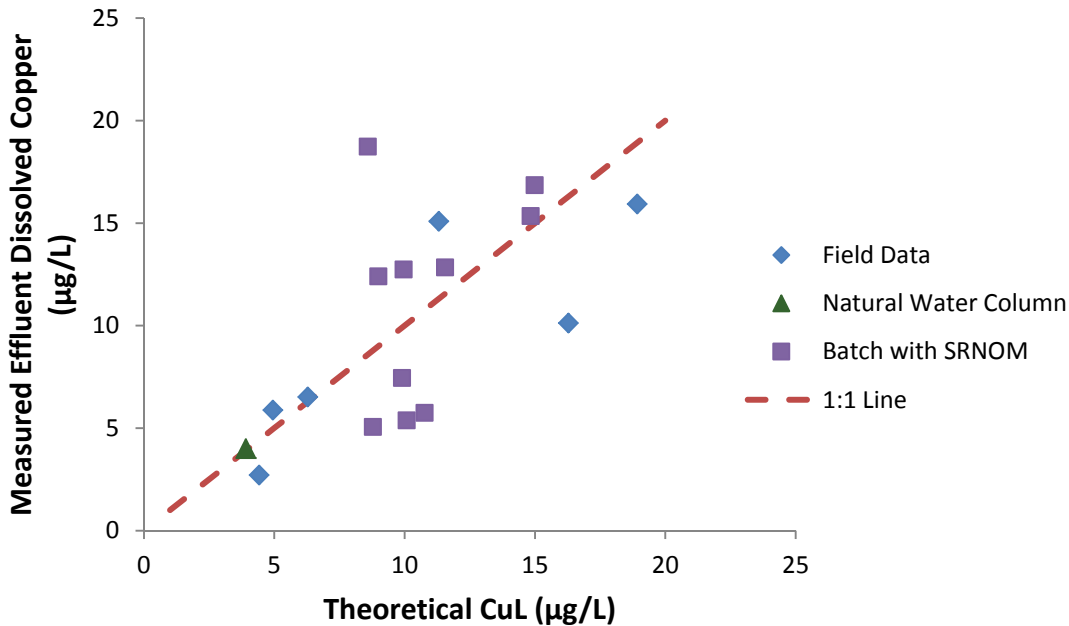
Figure 5.10: Comparison of measured effluent dissolved copper concentrations and predicted concentrations of CuL complexes in experiments using Apatite II™
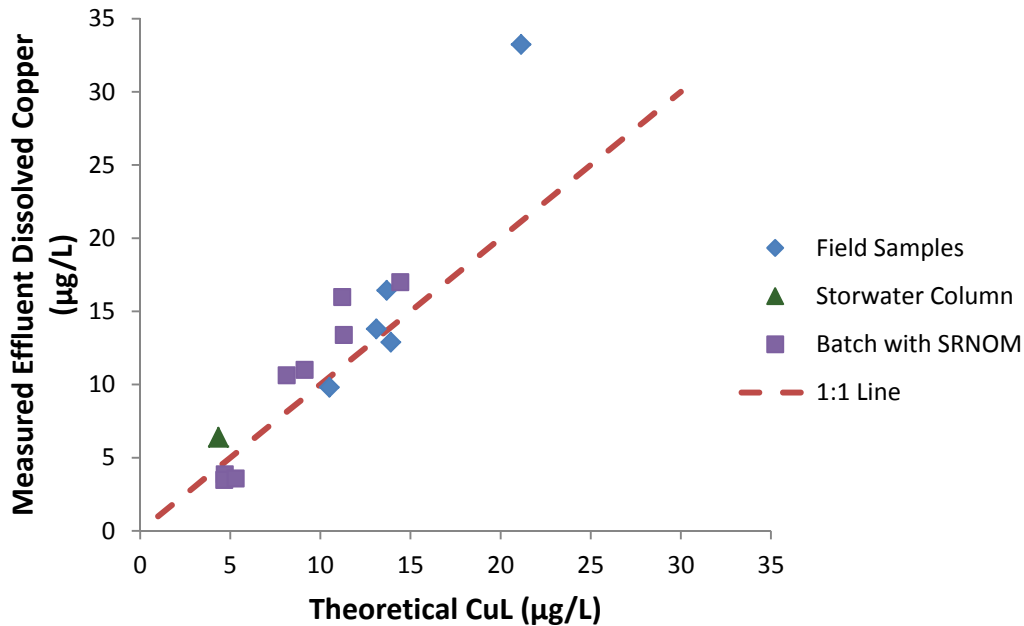
Figure 5.11: Comparison of measured effluent dissolved copper concentrations and predicted concentrations of CuL complexes in experiments using compost

It is widely known that Cu^{+2} is more bioavailable than Cu-NOM complexes (i.e. *CuL*). Therefore, while effluent concentrations are greater than the desired 2 μg/L threshold, there is evidence to suggest that Cu^{+2} is being removed and the more environmentally benign Cu-NOM complexes are passing through the filter. However, the fate and transport of those Cu-NOM complexes upon reaching receiving waters is not well understood, and it remains unclear whether or not Cu^{+2} will eventually be released into solution.

It is unlikely that the phenomenon of Cu-NOM complexes passing through the media filter will be limited to Apatite II™ and compost. NOM is ubiquitous in stormwater runoff, and recent work has demonstrated that the majority of dissolved copper in highway stormwater runoff is complexed with NOM *(Nason et al. 2012b)*. These complexes will likely have the same effect on removal efficiency in other adsorption or precipitation processes using different media types, although additional research would be needed to confirm this assumption. This should be kept in mind when considering media types for filtration, especially in cases where solutions were tested in the absence of NOM. In light of these issues, any adsorbent capable of efficiently removing Cu-NOM complexes would be promising for application with stormwater runoff.

6.0   CONCLUSIONS

The primary goal of this project was to assess whether Apatite II™ and compost are viable options for copper removal in stormwater BMPs. Within this overarching framework, specific objectives included:

- evaluating the state of science with respect to copper removal from stormwater runoff,

- understanding the mechanisms of copper removal using Apatite II™ and compost,

- assessing the ability of Apatite II™ and compost to remove copper in bench and field scale applications, and

- understanding the overall effect that Apatite II™ and compost will have on the quality of stormwater runoff.

The major findings of this work are as follows:

1. There are currently no well-documented methods for treatment of stormwater runoff that consistently achieve effluent copper concentrations below the 2 μg/L threshold that is desired to prevent olfactory impairment in salmonid species. Of the available treatment technologies for metals removal, adsorption shows the most promise for application in stormwater BMPs. This is based on the high removal efficiencies many adsorption processes have demonstrated, as well as the low relative cost and infrequent maintenance required to operate these systems.

2. Compost removes copper primarily through adsorption processes, whereas copper removal using Apatite II™ occurs through a combination of adsorption and precipitation. This precipitation process is driven by the dissolution of Apatite II™, which releases phosphate and carbonate ions into solution and buffers the pH to levels that promote the formation of copper precipitates.

3. At equilibrium, both compost and Apatite II™ have demonstrated the ability to remove copper and zinc to trace levels, and compare favorably to other adsorbent media that have been tested in studies found in the literature. Additionally, for both media types removal of copper was uninhibited by the presence of zinc.

4. Column tests revealed that both Apatite II™ and compost have the ability to remove copper and zinc to trace levels in continuous flow applications. For Apatite II™, effluent copper concentration was independent of influent concentration, and the presence of zinc did not affect copper breakthrough. Compost outperformed Apatite

II™ in column experiments, removing copper to trace levels long after complete breakthrough had occurred in the Apatite II™ columns.

5. NOM inhibits copper removal through the formation of Cu-NOM complexes, which do not adsorb or precipitate as readily as Cu^{+2}. This caused lower copper removal in both batch and column experiments, although for column experiments the effect was more pronounced with Apatite II™. There is indication that this effect is also driving copper removal in the field, based largely on the strong agreement of theoretical CuL values and measured effluent copper concentrations.

6. Copper removal efficiency was much lower at the field scale using both compost and Apatite II™. For Apatite II™, copper removal was only observed for three of the seven storms with efficiencies ranging from 16.1% to 59.8%. Compost removed copper in three of the five storms sampled, with efficiencies ranging from 24.7% to 45.4%. Additionally, Apatite II™ demonstrated the potential for release of previously removed copper back into solution, an effect that was also observed in all four RSSCTs using Apatite II™.

7. Ion leaching was observed for both media types. For Apatite II™, phosphate leaching was documented in batch, column, and field experiments. At the field level, steady state phosphate release of approximately 1.5 mg/L was observed. For compost, leaching of phosphate was observed in batch experiments, but column experiments indicated that low levels of ion leaching could be expected. However, at the field level, leaching of nitrate and phosphate was observed, and leaching trends had not yet stabilized after approximately 7,300 gallons of flow through the filter.

6.1   PRACTICAL IMPLICATIONS

The favorable comparison of compost and Apatite II™ to other potential adsorbents demonstrated that both media types showed initial promise for copper removal from stormwater. This was further exemplified by the high removal efficiencies observed in the synthetic stormwater column tests. However, the introduction of NOM significantly altered removal characteristics, rendering both adsorbents less effective in equilibrium and continuous flow scenarios. This is problematic due to the ubiquitous nature of NOM in stormwater runoff. A manifestation of this issue was observed at the field scale, where removal efficiencies were much lower than in the laboratory. However, there was indication that dissolved copper in the effluent was fully complexed with NOM. This suggests the filter effectively removed the bioavailable free copper (Cu^{+2}), and consequently could be seen as effective at reducing the toxicological impacts of copper from stormwater. Due to the superior performance of compost in RSSCTs, as well as the documented steady state leaching of phosphate from Apatite II™ and the potential for Apatite II™ to release copper back into solution, compost is viewed as the more promising adsorbent for stormwater applications.

Several issues persist that need to be addressed before media filters are implemented in stormwater BMPs. Leaching of nitrate and phosphate was observed in field experiments, and a more complete understanding of steady state leaching is needed to fully quantify the effects compost will have on downstream water quality. If release of nitrate and phosphate continues,

compost should only be used if an analysis is performed on the sensitivity of receiving waters to pulses of these nutrients. Sediment deposition was observed in both filters, and an accumulation of solids will eventually cause clogging of pore spaces and increased head loss. This could potentially cause filter failure prior to reaching the adsorbent's capacity for removing heavy metals. For improved flow characteristics and longer filter life, some type of pre-filtration of solids is recommended. Potential ideas for this include a sedimentation basin or a sand filter.

It is important to understand that with this work, a certain amount of uncertainty exists due to the variability of compost and stormwater runoff. Compost is heterogeneous in nature, and different batches will vary somewhat depending on source material, time of year, and composting practices. Even when the same vendor is used, copper removal characteristics could potentially change from batch to batch. Additionally, stormwater runoff is highly variable based on location, antecedent dry period, time within the rainfall event, and time of year. These are all factors that could potentially influence copper removal characteristics, and it would be very difficult to control for these factors in field-based testing. Accordingly, this inherent variability should be kept in mind when considering application of these results in the design of stormwater BMPs.

6.2   FUTURE WORK

As mentioned previously, there are still unresolved issues that should be explored in future work to form a more comprehensive understanding of the effect media filtration will have on stormwater runoff. The following is a summary of future research topics that would build upon this project:

1. Speciation of dissolved copper in the filter effluent. This will determine if, as proposed in this work, effluent dissolved copper is almost entirely comprised of Cu-NOM complexes. Knowing with certainty that any copper released from the filter is complexed with NOM will give engineers and regulators a better understanding of the effect the treated stormwater will have on receiving waters.

2. Fate and transport of Cu-NOM complexes upon reaching receiving waters. The stability of Cu-NOM complexes upon mixing with different water bodies containing variable concentrations of NOM is not well understood, and it is unclear if free copper ion will be released into solution. Additionally, exposure to UV radiation has been shown to diminish the copper complexing capacity of NOM from mountain streams *(Brooks et al. 2007)*. An investigation should be performed to determine if similar photochemical processes occur with NOM from stormwater runoff. A better understanding of these processes will have strong implications on copper toxicity and whether stormwater treatment is deemed successful.

3. Further work with compost at the field scale to understand the leaching characteristics over time. This will allow for a more complete analysis of the impact compost will have on downstream water quality, especially with respect to effluent nitrate and phosphate concentrations.

4. Varying of the flow delivered to the filter to determine the maximum loading rate that can be treated by this system. This would enable engineers to design the most efficient system possible while still effectively treating the stormwater runoff.

Experiments with other promising adsorbents to determine if there is a more effective and economical alternative to compost. Specifically, any adsorbent that is capable of removing Cu-NOM complexes would be especially promising given the nature of stormwater runoff.

7.0   REFERENCES

Al-Asheh, S., F. Banat, and F. Mohai. Sorption of Copper and Nickel by Spent Animal Bones. *Chemosphere,* Vol. 39, No. 12, 1999, pp. 2087-96.

Aman, T., A.A. Kazi, M.U. Sabri, and Q. Bano. Potato Peels as Solid Waste for the Removal of Heavy Metal Copper(II) from Waste Water/Industrial Effluent. *Colloids and Surfaces B-Biointerfaces*, Vol. 63, No. 1, 2008, pp. 116-21.

APHA, AWWA, and WEF. Standard Methods for the Examination of Water and Wastewater. An American Public Health Association (APHA), American Water Works Association (AWWA), and Water Environment Federation (WEF), Washington, D.C., 2005.

Argun, M.E., S. Dursun, C. Ozdemir, and M. Karatas. Heavy Metal Adsorption by Modified Oak Sawdust: Thermodynamics and Kinetics. *Journal of Hazardous Materials*, Vol. 141, No. 1, 2007, pp. 77-85.

Backstrom, M. (2003). Grassed Swales for Stormwater Pollution Control During Rain and Snowmelt. *Water Science and Technology*, Vol. 48, No. 9, 2003, pp. 123-34.

Baldwin, D.H., J.F. Sandahl, J.S. Labenia, and N.L. Scholz. Sublethal Effects of Copper on Coho Salmon: Impacts on Nonoverlapping Receptor Pathways in the Peripheral Olfactory Nervous System. *Environmental Toxicology and Chemistry*, Vol. 22, No. 10, 2003, pp. 2266-74.

Baldwin, D.H., C.P. Tatara, and N.L. Scholz. Copper-Induced Olfactory Toxicity in Salmon and Steelhead: Extrapolation Across Species and Rearing Environments. *Aquatic Toxicology*, Vol. 101, No. 1, 2011, pp. 295-7.

Barrett, M., L. Katz, S. Taylor, J. Sansalone, and M. Stevenson. Measuring and Removing Dissolved Metals from Stormwater in Highly Urbanized Areas. *National Cooperative Highway Research Program*, No. 767, Transportation Research Board, Washington, D.C., 2014.

Barrett, M.E. Performance Comparison of Structural Stormwater Best Management Practices. *Water Environment Research*, Vol. 77, No. 1, 2005, pp. 78-86.

Basha, S., Z.V.P. Murthy, and B. Jha. Removal of Cu(II) and Ni(II) from Industrial Effluents by Brown Seaweed, Cystoseira Indica. *Industrial and Engineering Chemistry Research*, Vol. 48, No. 2, 2009, pp. 961-75.

Bassi, R., S.O. Prasher, and B.K. Simpson. Removal of Selected Metal Ions from Aqueous Solutions using Chitosan Flakes. *Separation Science and Technology*, Vol. 35, No. 4, 2000, pp. 547-60.

Benjamin, M.M. *Water Chemistry*. McGraw-Hill, Boston, MA, 2002.

Bettini, S., F. Ciani, and V. Franceschini. Recovery of the Olfactory Receptor Neurons in the African Tilapia Mariae Following Exposure to Low Copper Level. *Aquatic Toxicology*, Vol. 76, No. 3, 2006, pp. 321-8.

Beyers, D.W., and M.S. Farmer. Effects of Copper on Olfaction of Colorado Pikeminnow. *Environmental Toxicology and Chemistry*, Vol. 20, No. 4, 2001, pp. 907-12.

Bhavsar, S.P., M.L. Diamond, L.J. Evans, N. Gandhi, J. Nilsen, and P. Antunes. Development of a Coupled Metal Speciation-Fate Model for Surface Aquatic Systems. *Environmental Toxicology and Chemistry*, Vol. 23, No. 6, 2004, pp. 1376-85.

Bloomquist, D.J. *Statistical Analysis and Speciation Modeling of Copper in Oregon Highway Runoff.* Thesis/Dissertation. Oregon State University, Corvallis, OR. 2009.

Bogya, E.S., R. Barabas, A. Csavdari, V. Dejeu, and I. Baldea. (2009). Hydroxyapatite Modified with Silica used for Sorption of Copper(II). *Chemical Papers*, Vol. 63, No. 5, 2009, pp. 568-73.

Brinkman, S.F., and W.D. Johnston. Acute Toxicity of Zinc to Several Aquatic Species Native to the Rocky Mountains. *Archives of Environmental Contamination and Toxicology*, Vol. 62, No. 2, 2012, pp. 272-81.

Brooks, M.L., D.M. McKnight, and W.H. Clements. Photochemical Control of Copper Complexation by Dissolved Organic Matter in Rocky Mountain Streams, Colorado. *Limnology and Oceanography*, Vol. 52, No. 2, 2007, pp. 766-79.

Buck, K.N., and K.W. Bruland. Copper Speciation in San Francisco Bay: A Novel Approach Using Multiple Analytical Windows. *Marine Chemistry*, Vol. 96, No. 1, 2005, pp. 185-98.

Buerge-Weirich, D., R. Hari, H. Xue, P. Behra, and L. Sigg. Adsorption of Cu, Cd, and Ni on Goethite in the Presence of Natural Groundwater Ligands. *Environmental Science and Technology*, Vol. 36, No. 3, 2002, pp. 328-36.

Carreau, N.D., and G.G. Pyle. Effect of Copper Exposure during Embryonic Development on Chemosensory Function of Juvenile Fathead Minnows (Pimephales Promelas). *Ecotoxicology and Environmental Safety*, Vol. 61, No. 1, 2005, pp. 1-6.

Castro, R.S.D., L. Caetano, G. Ferreira, P.M. Padilha, M.J. Saeki, L.F. Zara, M.A.U. Martines, and G.R. Castro. Banana Peel Applied to the Solid Phase Extraction of Copper and Lead from River Water: Preconcentration of Metal Ions with a Fruit Waste. *Industrial and Engineering Chemistry Research*, Vol. 50, No. 6, 2011, pp. 3446-51.

Cay, S., A. Uyanik, and A. Ozasik. Single and Binary Component Adsorption of Copper(II) and Cadmium(II) from Aqueous Solutions using Tea-Industry Waste. *Separation and Purification Technology*, Vol. 38, No. 3, 2004, pp. 273-80.

Champagne, P., and C. Li. Use of Sphagnum Peat Moss and Crushed Mollusk Shells in Fixed-Bed Columns for the Treatment of Synthetic Landfill Leachate. *Journal of Material Cycles and Waste Management*, Vol. 11, No. 4, 2009, pp. 339-47.

Chatterjee, S., G.B. Sau, and S.K. Mukherjee. Bioremediation of Cr(VI) from Chromium-Contaminated Wastewater by Free and Immobilized Cells of Cellulosimicrobium Cellulans KUCr3. *Bioremediation Journal*, Vol. 15, No. 3, 2011, pp. 173-80.

Chen, C.W., D. Leva, and A. Olivieri. Modeling the Fate of Copper Discharged to San Francisco Bay. *Journal of Environmental Engineering*, Vol. 122, No. 10, 1996, pp. 924-34.

Christl, I., and R. Kretzschmar. Interaction of Copper and Fulvic Acid at the Hematite-Water Interface. *Geochimica et Cosmochimica Acta*, Vol. 65, No. 20, 2001, pp. 3435-42.

Chu, C.F., and K.M. Ng. Flow in Packed Tubes with a Small Tube to Particle Diameter Ratio. *AIChE Journal*, Vol. 35, No. 1, 1989, pp. 148-58.

Conca, J.L., and J. Wright. An Apatite II Permeable Reactive Barrier to Remediate Groundwater Containing Zn, Pb and Cd. *Applied Geochemistry*, Vol. 21, No. 8, 2006, pp. 1288-300.

Corami, A., S. Mignardi, and V. Ferrini. Copper and Zinc Decontamination from Single- and Binary-Metal Solutions using Hydroxyapatite. *Journal of Hazardous Materials*, Vol. 146, No. 1-2, 2007, pp. 164-70.

Correll, D.L. The Role of Phosphorus in the Eutrophication of Receiving Waters: A Review. *Journal of Environmental Quality*, Vol. 27, No. 2, 1998, pp. 261-6.

Crittenden, J.C., J.K. Berrigan, and D.W. Hand. (1986). Design of Rapid Small-Scale Adsorption Tests for a Constant Diffusivity. *Journal (Water Pollution Control Federation)*, 1998, pp. 312-9.

Czupyrna, G., R.D. Levy, A.O. Maclean, and H. Gold. *In Situ Immobilization of Heavy-Metal-Contaminated Soils*. Noyes Data Corporation. 1989.

Dabrowski, A., Z. Hubicki, P. Podkoscielny, and E. Robens. (2004). Selective Removal of the Heavy Metal Ions from Waters and Industrial Wastewaters by Ion-Exchange Method. *Chemosphere*, Vol. 56, No. 2, 2004, pp. 91-106.

Davis, A.P., M. Shokouhian, and S. Ni. Loading Estimates of Lead, Copper, Cadmium, and Zinc in Urban Runoff from Specific Sources. *Chemosphere*, Vol. 44, No. 5, 2001, pp. 997-1009.

Davis, A.P., M. Shokouhian, H. Sharma, C. Minami, and D. Winogradoff. Water Quality Improvement through Bioretention: Lead, Copper, and Zinc Removal. *Water Environment Research*, Vol. 75, No. 1, 2003, pp. 73-82.

Farley, K.J., D.A. Dzombak, and F.M.M. Morel. A Surface Precipitation Model for the Sorption of Cations on Metal Oxides. J*ournal of Colloid and Interface Science*, Vol. 106, No. 1, 1985, pp. 226-42.

Farm, C. Evaluation of the Accumulation of Sediment and Heavy Metals in a Storm-Water Detention Pond. *Water Science and Technology*, Vol. 45, No. 7, 2002, pp. 105-12.

Faust, S.D., and O.M. Aly. *Adsorption Processes for Water Treatment*. Butterworth London. 1987.

Fu, F.L., and Q. Wang. Removal of Heavy Metal Ions from Wastewaters: A Review. *Journal of Environmental Management*, Vol. 92, No. 3, 2011, pp. 407-18.

Gao, Y., and G. Korshin. Effects of NOM Properties on Copper Release from Model Solid Phases. *Water Research,* Vol. 47, No. 14, 2013, pp. 4843-52.

Genc-Fuhrman, H., P.S. Mikkelsen, and A. Ledin. Simultaneous Removal of As, Cd, Cr, Cu, Ni and Zn from Stormwater: Experimental Comparison of 11 Different Sorbents. *Water Research*, Vol. 41, No.3, 2007, pp. 591-602.

Genz, A., B. Baumgarten, M. Goernitz, and M. Jekel. NOM Removal by Adsorption onto Granular Ferric Hydroxide: Equilibrium, Kinetics, Filter and Regeneration Studies.*Water Research*, Vol. 42, No. 1, 2008, pp. 238-48.

Grimes, S.M., G.H. Taylor, and J. Cooper. The Availability and Binding of Heavy Metals in Compost Derived from Household Waste. *Journal of Chemical Technology and Biotechnology*, Vol. 74, No. 12, 1999, pp. 1125-30.

Hansen, J.A., J.D. Rose, R.A. Jenkins, K.G. Gerow, and H.L. Bergman. Chinook Salmon (Oncorhynchus Tshawytscha) and Rainbow Trout (Oncorhynchus Mykiss) Exposed to Copper: Neurophysiological and Histological Effects on the Olfactory System. *Environmental Toxicology and Chemistry*, Vol. 18, No. 9, 1999, pp. 1979-91.

Hossain, M.A., M. Alam, D.R. Yonge, and P. Dutta. Efficiency and Flow Regime of a Highway Stormwater Detention Pond in Washington, USA. *Water Air and Soil Pollution*, Vol. 164, No. 1-4, 2005, pp. 79-89.

Hsieh, C.-h., A.P. Davis, and B.A. Needelman. Bioretention Column Studies of Phosphorus Removal from Urban Stormwater Runoff. *Water Environment Research*, Vol. 79, No. 2, 2007, pp. 177-84.

Imani, S., S. Rezaei-Zarchi, M. Hashemi, H. Borna, A. Javid, A.M. Zand, and H.B. Abarghouei. Hg, Cd and Pb Heavy Metal Bioremediation by Dunaliella Alga. *Journal of Medicinal Plants Research,* Vol. 5, No. 13, 2011, pp. 2775-80.

Inskeep, W.P., and J.C. Silvertooth. Inhibition of Hydroxyapatite Precipitation in the Presence of Fulvic, Humic, and Tannic Acids. *Soil Science Society of America Journal*, Vol. 52, No. 4, 1988, pp. 941-6.

Jang, A., Y. Seo, and P.L. Bishop. The Removal of Heavy Metals in Urban Runoff by Sorption on Mulch. *Environmental Pollution*, Vol, 133, No. 1, 2005, pp. 117-27.

Jiang, M.Q., X.Y. Jin, X.Q. Lu, and Z. L. Chen. Adsorption of Pb(II), Cd(II), Ni(II) and Cu(II) onto Natural Kaolinite Clay. *Desalination*, Vol. 252, No. 1-3, 2010, pp. 33-9.

Johir, M.A.H., J.J. Lee, S. Vigneswaran, J. Kandasamy, and K. Shaw. Treatment of Stormwater using Fibre Filter Media. *Water, Air, and Soil Pollution: Focus*, Vol. 9, No. 5-6, 2009, pp. 439-47.

Johnson, P.D., R. Pitt, S.R. Durrans, M. Urrutia, and S. Clark. *Metals Removal Technologies for Urban Stormwater*. Water Environment Federation. 2003.

Joshi, P.K., A. Swarup, S. Maheshwari, R. Kumar, and N. Singh. Bioremediation of Heavy Metals in Liquid Media through Fungi Isolated from Contaminated Sources. *Indian Journal of Microbiology*, Vol. 51, No. 4, 2011, pp. 482-7.

Joshi, U.M., and R. Balasubramanian. Characteristics and Environmental Mobility of Trace Elements in Urban Runoff. *Chemosphere*, Vol. 80, No. 3, 2010, pp. 310-8.

Julliard, A.K., D. Saucier, and L. Astic. Time-Course of Apoptosis in the Olfactory Epithelium of Rainbow Trout Exposed to a Low Copper Level. *Tissue and Cell*, Vol. 28, No. 3, 1996, pp. 367-77.

Kannan, N., and T. Veemaraj. Green and Economical Adsorbent for Zinc (II) Ions Removal by Adsorption from Water Environment using Batch Mode and Fixed Bed Column Experiments. *Electronic Journal of Environmental, Agricultural and Food Chemistry*, Vol. 9, No. 7, 2010, pp. 1156-67.

Kayhanian, M., and M.K. Stenstrom. Mass Loading of First Flush Pollutants with Treatment Strategy Simulations. *Transportation Research Record: Journal of the Transportation Research Board,* No. 1904, (1), Transportation Research Board of the National Academies, Washington, D.C., 2005, pp. 133-4.

Kayhanian, M., C. Suverkropp, A. Ruby, and K. Tsay. Characterization and Prediction of Highway Runoff Constituent Event Mean Concentration. *Journal of Environmental Management*, Vol. 85, No. 2, 2007, pp. 279-95.

Kim, W.G., M.N. Kim, S.M. Lee, and J.K. Yang. Removal of Cu(II) with Hydroxyapatite (Animal Bone) as an Inorganic Ion Exchanger. *Desalination and Water Treatment*, Vol. 4, No. 1-3, 2009, pp. 269-73.

Krejzler, J., and J. Narbutt. Adsorption of Strontium, Europium and Americium(III) Ions on a Novel Adsorbent Apatite II. *Nukleonika*, Vol. 48, No. 4, 2003, pp. 171-5.

Lee, S.M., and A.P. Davis. Removal of Cu(II) and Cd(II) from Aqueous Solution by Seafood Processing Waste Sludge. *Water Research*, Vol. 35, No. 2, 2001, pp. 534-40.

Lee, Y.J., E.J. Elzinga, and R.J. Reeder. Cu (II) Adsorption at the Calcite–Water Interface in the Presence of Natural Organic Matter: Kinetic Studies and Molecular-Scale Characterization. *Geochimica et Cosmochimica Acta*, Vol. 69, No. 1, 2005, pp. 49-61.

Leecaster, M.K., K. Schiff, and L.L. Tiefenthaler. Assessment of Efficient Sampling Designs for Urban Stormwater Monitoring. *Water Research*, Vol. 36, No. 6, 2002, pp. 1556-64.

Legret, M., and C. Pagotto. Evaluation of Pollutant Loadings in the Runoff Waters from a Major Rural Highway. *Science of the Total Environment*, Vol. 235, No. 1, 1999, pp. 143-50.

Li, H., and A.P. Davis. Water Quality Improvement through Reductions of Pollutant Loads Using Bioretention. *Journal of Environmental Engineering-ASCE*, Vol. 135, No. 8, 2009, pp. 567-76.

Liu, Z.G., and F.S. Zhang. Removal of Copper (II) and Phenol from Aqueous Solution using Porous Carbons Derived from Hydrothermal Chars. *Desalination*, Vol. 267, No. 1, 2011, pp. 101-6.

Lu, Y., and H.E. Allen. Partitioning of Copper onto Suspended Particulate Matter in River Waters. *Science of the Total Environment*, Vol. 277, No. 1, 2001, pp. 119-32.

Luoma, S.N. Bioavailability of Trace Metals to Aquatic Organisms—A Review. *Science of the Total Environment*, Vol. 28, No. 1, 1983, pp. 1-22.

Ma, Q.Y., S.J. Traina, T.J. Logan, and J.A. Ryan. Effects of Aqueous Al, Cd, Cu, Fe (II), Ni, and Zn on Pb Immobilization by Hydroxyapatite. *Environmental Science and Technology*, Vol. 28, No. 7, 1994, pp. 1219-28.

Machida, M., M. Aikawa, and H. Tatsumoto. Prediction of Simultaneous Adsorption of Cu(II) and Pb(II) onto Activated Carbon by Conventional Langmuir Type Equations. *Journal of Hazardous Materials*, Vol. 120, No. 1-3, 2005, pp. 271-5.

Madsen, H.E.L. Crystal Growth Kinetics of Copper Phosphate from Acid Solution at 37° C. *Journal of Crystal Growth*, Vol. 275, No. 1, 2005, pp. e191-e6.

Malandrino, M., O. Abollino, A. Giacomino, M. Aceto, and E. Mentasti. Adsorption of Heavy Metals on Vermiculite: Influence of pH and Organic Ligands. *Journal of Colloid and Interface Science*, Vol. 299, No. 2, 2006, pp. 537-46.

Martin, W.A., S.L. Larson, D.R. Felt, J. Wright, C.S. Griggs, M. Thompson, J.L. Conca, and C.C. Nestler. The Effect of Organics on Lead Sorption onto Apatite II™. *Applied Geochemistry*, Vol. 23, No. 1, 2008, pp. 34-43.

Martínez-Villegas, N., and C.E. Martínez. Solid-and Solution-Phase Organics Dictate Copper Distribution and Speciation in Multicomponent Systems Containing Ferrihydrite, Organic Matter, and Montmorillonite. *Environmental Science and Technology*, Vol. 42, No. 8, 2008, pp. 2833-8.

McElmurry, S.P., D.T. Long, and T.C. Voice. Stormwater Dissolved Organic Matter: Influence of Land Cover and Environmental Factors. *Environmental Science and Technology*, Vol. 48, No. 1, 2013, pp. 45-53.

McIntyre, J.K., D.H. Baldwin, J.P. Meador, and N.L. Scholz. Chemosensory Deprivation in Juvenile Coho Salmon Exposed to Dissolved Copper Under Varying Water Chemistry Conditions. *Environmental Science and Technology*, Vol. 42, No. 4, 2008, pp. 1352-8.

McLaughlan, R.G., and O. Al-Mashaqbeh. Simple Models for the Release Kinetics of Dissolved Organic Carbon from Woody Filtration Media. *Bioresource Technology*, Vol. 100, No. 9, 2009, pp. 2588-93.

Moran, D.T., J.C. Rowley, G.R. Aiken, and B.W. Jafek. Ultrastructural Neurobiology of the Olfactory Mucosa of the Brown Trout, Salmo Trutta. *Microscopy Research and Technique*, Vol. 23, No. 1, 1992, pp. 28-48.

Moreno-Pirajan, J.C., and L. Giraldo. Activated Carbon Oobtained by Pyrolysis of Potato Peel for the Removal of Heavy Metal Copper (II) from Aqueous Solutions. *Journal of Analytical and Applied Pyrolysis*, Vol. 90, No. 1, 2011, pp. 42-7.

Morley, M.C., J.L. Henke, and G.E. Speitel Jr. Adsorption of RDX and HMX in Rapid Small-Scale Column Tests: Implications for Full-Scale Adsorbers. *Journal of Environmental Engineering*, Vol. 131, No. 1, 2005, pp. 29-37.

Nadaroglu, H., E. Kalkan, and N. Demir. Removal of Copper from Aqueous Solution Using Red Mud. *Desalination*, Vol. 251, No. 1-3, 2010, pp. 90-5.

Nason, J.A., D.J. Bloomquist, and M.S. Sprick. Factors Influencing Dissolved Copper Concentrations in Oregon Highway Storm Water Runoff. *Journal of Environmental Engineering-ASCE*, Vol. 138, No. 7, 2012a, pp. 734-42.

Nason, J.A., M.S. Sprick, and D.J. Bloomquist. Determination of Copper Speciation in Highway Stormwater Runoff Using Competitive Ligand Exchange–Adsorptive Cathodic Stripping Voltammetry. *Water Research*, Vol. 46, No. 17, 2012b, pp. 5788-98.

ODOT. 2012 Transportation Volume Tables. In, Oregon Department of Transportation, 2012, p. 90.

Oliva, J., J. De Pablo, J.-L. Cortina, J. Cama, and C. Ayora. The Use of Apatite II™ to Remove Divalent Metal Ions Zinc (II), Lead (II), Manganese (II) and Iron (II) from Water in Passive Treatment Systems: Column Experiments. *Journal of Hazardous Materials*, Vol. 184, No. 1, 2010, pp. 364-74.

Oliva, J., J. De Pablo, J.-L. Cortina, J. Cama, and C. Ayora. Removal of Cadmium, Copper, Nickel, Cobalt and Mercury from Water by Apatite II™: Column Experiments. *Journal of Hazardous Materials*, Vol. 194, 2011, pp. 312-23.

Paradelo, R., and M.T. Barral. Evaluation of the Potential Capacity as Biosorbents of Two MSW Composts with Different Cu, Pb and Zn Concentrations. *Bioresource Technology*, Vol. 104, 2012, pp. 810-3.

Passeport, E., P. Vidon, K.J. Forshay, L. Harris, S.S. Kaushal, D.Q. Kellogg, J. Lazar, P. Mayer, and E.K. Stander. Ecological Engineering Practices for the Reduction of Excess Nitrogen in Human-Influenced Landscapes: A Guide for Watershed Managers. *Environmental Management*, Vol. 51, No. 2, 2013, pp. 392-413.

Pitcher, S.K., R.C.T. Slade, and N.I. Ward. Heavy Metal Removal from Motorway Stormwater Using Zeolites. *Science of the Total Environment*, Vol. 334, 2004, pp. 161-6.

Ramirez-Paredes, F.I., T. Manzano-Munoz, J.C. Garcia-Prieto, G.G. Zhadan, V.L. Shnyrov, J.F. Kennedy, and M.G. Roig. Biosorption of Heavy Metals from Acid Mine Drainage onto Biopolymers (Chitin and Alpha (1,3) Beta-D-Glucan) from Industrial Biowaste Exhausted Brewer's Yeasts (Saccharomyces Cerevisiae L.). *Biotechnology and Bioprocess Engineering*, Vol. 16, No. 6, 2011, pp. 1262-72.

Sandahl, J.F., D.H. Baldwin, J.J. Jenkins, and N.L. Scholz. A Sensory System at the Interface between Urban Stormwater Runoff and Salmon Survival. *Environmental Science and Technology*, Vol. 41, No. 8, 2007, pp. 2998-3004.

Sansalone, J.J., and S.G. Buchberger. Partitioning and First Flush of Metals in Urban Roadway Storm Water. *Journal of Environmental Engineering*, Vol. 123, No. 2, 1997, pp. 134-43.

Seelsaen, N., R. McLaughlan, S. Moore, and R.M. Stuetz. Influence of Compost Characteristics on Heavy Metal Sorption from Synthetic Stormwater. *Water Science and Technology*, Vol. 55, No. 4, 2007.

Singh, G., and N.S. Rawat. Removal of Trace Elements from Acid Mine Drainage. *International Journal of Mine Water*, Vol. 4, No. 1, 1985, pp. 17-23.

Speth, T.F. Evaluating Capacities of GAC Preloaded with Natural Water. *Journal of Environmental Engineering*, Vol. 117, No. 1, 1991, pp. 66-79.

Sun, X., and A.P. Davis. Heavy Metal Fates in Laboratory Bioretention Systems. *Chemosphere*, Vol. 66, No. 9, 2007, pp. 1601-9.

Suzuki, T., T. Hatsushika, and Y. Hayakawa. Synthetic Hydroxy Apatites Employed As Inorganic Cation-Exchangers. *Journal of the Chemical Society-Faraday Transactions I*, Vol. 77, 1981, pp. 1059-62.

Swami, D., and D. Buddhi. Removal of Contaminants from Industrial Wastewater through Various Non-conventional Technologies: A Review. *International Journal of Environment and Pollution*, Vol. 27, No. 4, 2006, pp. 324-46.

Tang, Q., X.W. Tang, Z.Z. Li, Y. Wang, M.M. Hu, X.J. Zhang, and Y.M. Chen. Zn(II) Removal with Activated Firmiana Simplex Leaf: Kinetics and Equilibrium Studies. *Journal of Environmental Engineering-ASCE*, Vol. 138, No. 2, 2012, pp. 190-9.

Tipping, E., J.R. Griffith, and J. Hilton. The Effect of Adsorbed Humic Substances on the Uptake of Copper (II) by Goethite. *Croatica Chemica Acta*, Vol. 56, No. 4, 1983, pp. 613-21.

USEPA. *Results of the Nationwide Urban Runoff Program*. Water Planning Division, Washington, D.C., 1982.

Vankar, P.S., R. Sarswat, and R. Sahu. Biosorption of Zinc Ions from Aqueous Solutions onto Natural Dye Waste of Hibiscus Rosa Sinensis: Thermodynamic and Kinetic Studies. *Environmental Progress and Sustainable Energy*, Vol. 31, No. 1, 2012, pp. 89-99.

Vijayaraghavan, K., U.M. Joshi, and R. Balasubramanian. Removal of Metal Ions from Storm-Water Runoff by Low-Cost Sorbents: Batch and Column Studies. *Journal of Environmental Engineering-ASCE*, Vol. 136, No. 10, 2010, pp. 1113-8.

Wachinski, A.M., and J.E. Etzel. *Environmental Ion Exchange: Principles and Design*. CRC Press. 1997.

Washington State Dept. of Ecology. *Guidance for Evaluating Emerging Stormwater Treatment Technologies, Technology Assessment Protocol-Ecology (TAPE)*. Washington State Department of Ecology, Olympia, WA. 2008.

Weng, C.-H., and Y.-C. Wu. Potential Low-Cost Biosorbent for Copper Removal: Pineapple Leaf Powder. *Journal of Environmental Engineering-ASCE*, Vol. 138, No. 3, 2012, pp. 286-92.

Wright, J., and J. Conca. Remediation of Groundwater and Soil Contaminated with Metals and Radionuclides using Apatite II, a Biogenic Apatite Mineral. Preprints of Extended Abstracts presented at the ACS National Meeting, American Chemical Society, Division of Environmental Chemistry, Vol. 42, No. 2, 2002, pp. 117-22.

Wright Water Engineers and Geosyntec Consultants. *Pollutant Category Summary: Metals*. International Stormwater Best Management Practices (BMP) Database. 2011.

Wu, P., and Y.S. Zhou. Simultaneous Removal of Coexistent Heavy Metals from Simulated Urban Stormwater using Four Sorbents: A Porous Iron Sorbent and Its Mixtures with Zeolite and Crystal Gravel. *Journal of Hazardous Materials*, Vol. 168, No. 2-3, 2009, pp. 674-80.

Wu, X., H.P. Wang, N.S. Deng, and F. Wu. Feasibility Study on Heavy Metal Removal from Mine Water by using Geological Material. *Fresenius Environmental Bulletin*, Vol. 12, No. 11, 2003, pp. 1400-6.

Yu, B., Y. Zhang, A. Shukla, S.S. Shukla, and K.L. Dorris. The Removal of Heavy Metals from Aqueous Solutions by Sawdust Adsorption - Removal of Lead and Comparison of Its Adsorption with Copper. *Journal of Hazardous Materials*, Vol. 84, No. 1, 2001, pp. 83-94.

APPENDIX A

8.0   APPENDICES

8.1   APATITE II™ SORPTION KINETICS

Understanding sorption kinetics lends insight into how to design residence times for treatment and how long to react samples for equilibrium testing. Accordingly, copper sorption experiments were conducted for both Apatite II™ and compost. In each case, 'sorption' refers to copper removal from solution regardless of removal mechanism (i.e. the sum of adsorption and precipitation). For Apatite II™, 100 mL solution of synthetic stormwater with 3 mg/L copper were reacted with 200 mg of sieved media, and samples were taken every hour for the first 6 hours and then three times per day from the second day until the fifth day. The results from this experiment are shown in Figure 8.1. Greater than 90% of the copper removal occurred within the first 10 hours, after which copper removal occurred at a much slower rate. While aqueous copper continued to decrease slightly over the entire 120-hour span of the experiment, more than 98% of the copper removal occurred over the first 48 hours, which was chosen as the reaction time for equilibrium experiments.
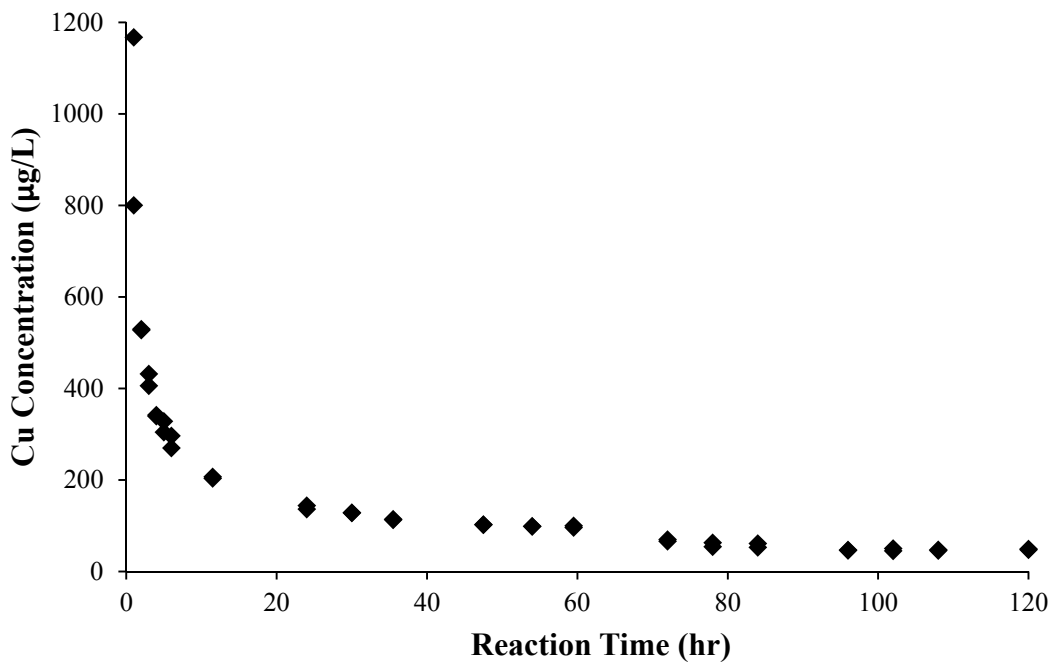
Figure 8.1: Copper sorption kinetics with sieved Apatite II™ in synthetic stormwater

8.2   COMPOST SORPTION KINETICS

For compost, an initial copper concentration of 95 µg/L was chosen for sorption kinetic experiments, and samples were taken over the same 5-day span as with Apatite II™. Figure 8.2

demonstrates that copper adsorption occurs primarily over the first few hours of contact, and is nearly complete after 48 hours. While copper concentrations did drop slightly from 48 hours to 120 hours, this drop represented a tiny fraction of the total copper removed, and 48 hours was chosen as the reaction time for batch testing.
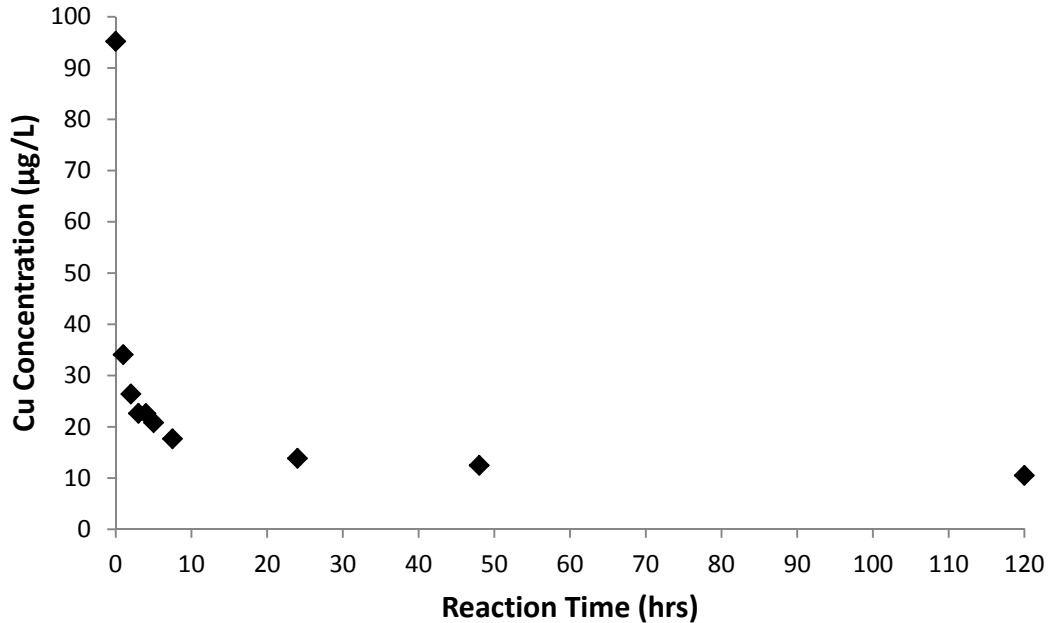
Figure 8.2: Copper sorption kinetics with sieved compost in synthetic stormwater

Previous studies have demonstrated that adsorption kinetics can be a function of particle size, which in turn affects the scalability of RSSCTs *(Summers et al. 2013)*. To address the potential for dependency of kinetics on particle size, parallel kinetic tests were performed with whole and sieved compost. From Figure 8.3 it can be seen that whole compost actually has slightly faster adsorption kinetics than sieved compost. While the cause for this is unknown, it demonstrates that increase in particle size won't likely lead to slower copper removal kinetics at the field scale, indicating that the constant diffusivity approach for scaling is likely appropriate. It should be noted that this experiment was performed in batch, which is a fundamentally different process than column experiments. However, previous work utilized batch kinetic tests and column experiments to test the effect of particle size on removal kinetics, and found the two approaches yielded the same conclusion *(Summers et al. 2013)*.
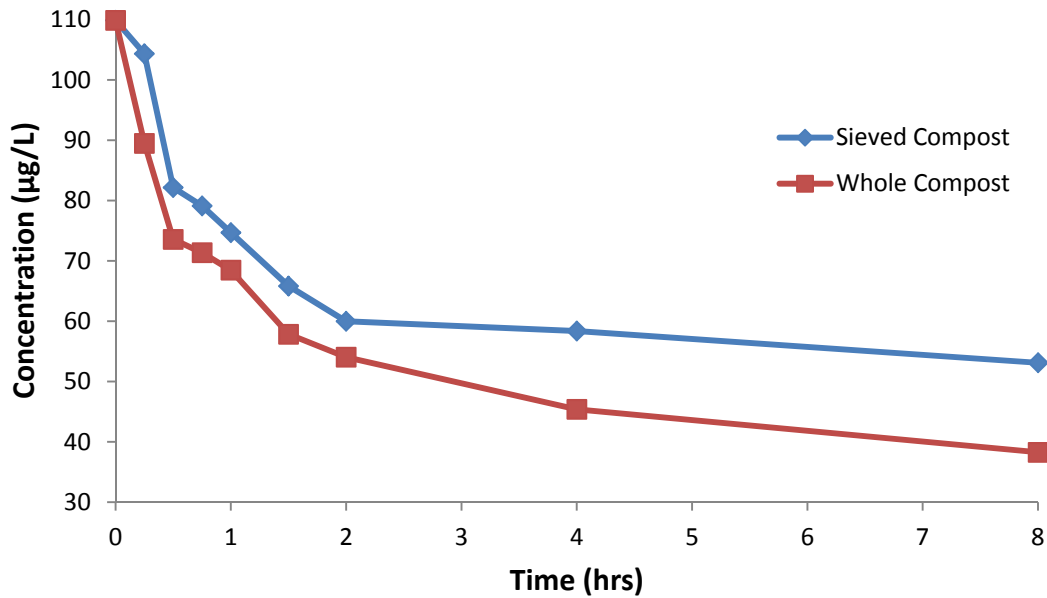
Figure 8.3: Comparison of copper adsorption kinetics with whole and sieved compost

8.3 INFLUENT CHARACTERISTICS IN COLUMN EXPERIMENTS

In section 4.5, influent pH and metals concentrations were reported as constant values, and these constant values were used for C/C_o calculations. However, the reported influent concentration was actually an average of all measured influent values. These influent values varied slightly over the course of the column experiments, as shown in Figure 8.4, Figure 8.5, and Figure 8.6.
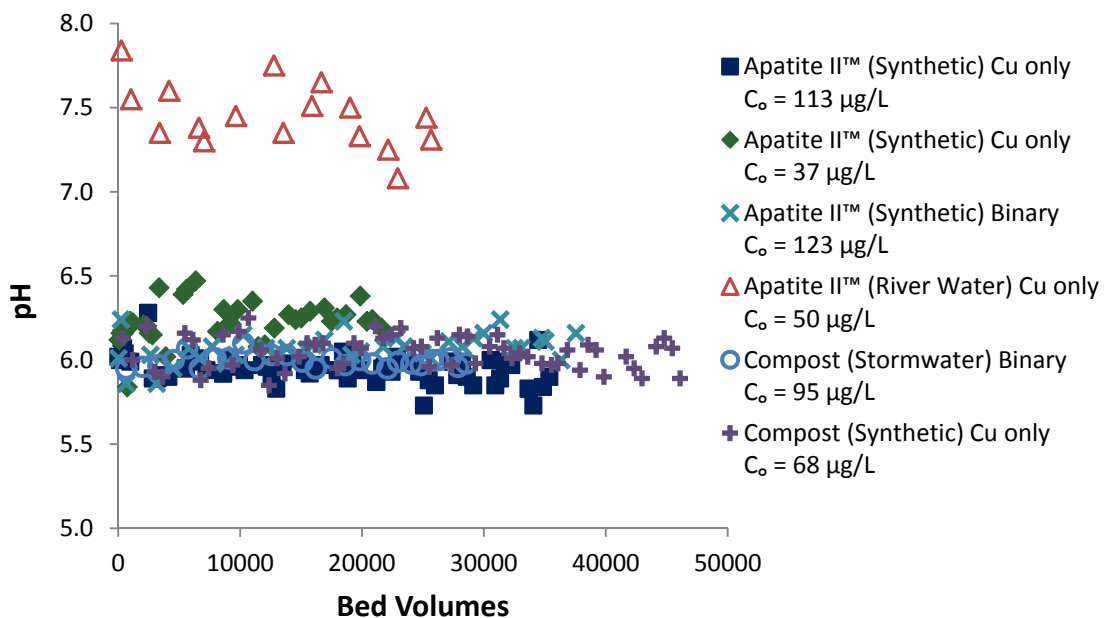
Figure 8.4: Influent pH values from column experiments

A-3
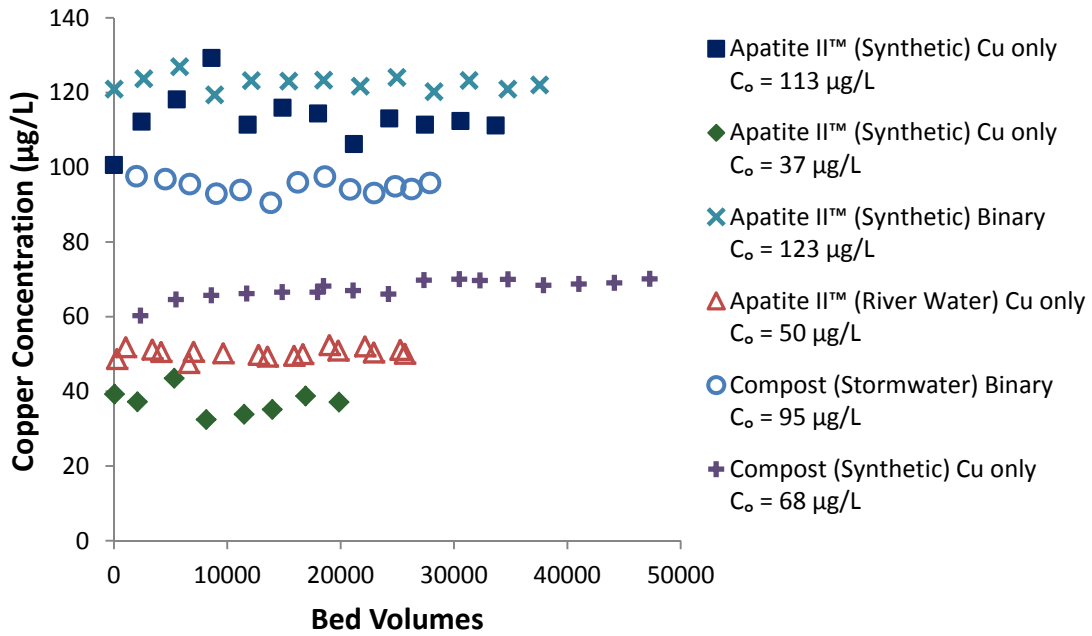
Figure 8.5: Influent copper concentrations from column experiments
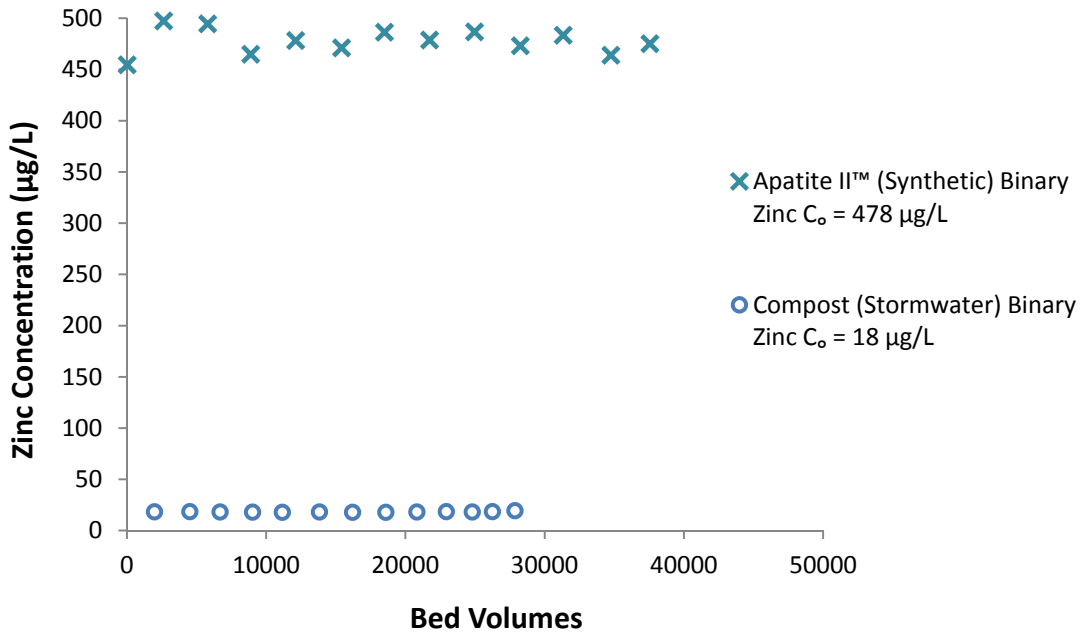
Figure 8.6: Influent zinc concentrations from binary element column experiments

8.4   WHOLE COMPOST HYDRAULIC CONDUCTIVITY

To assess the head loss that could be expected through the filter in field experiments, a constant head permeability test was performed in accordance with the standard method for assessing hydraulic conductivity of granular soils (ASTM-D 2434). In this method, water is pumped at a constant flow rate into a packed column with a fixed elevation outlet point until equilibrium is achieved, at which point measurements of flow rate and hydraulic head are recorded. A schematic of this setup is shown in Figure 8.7.
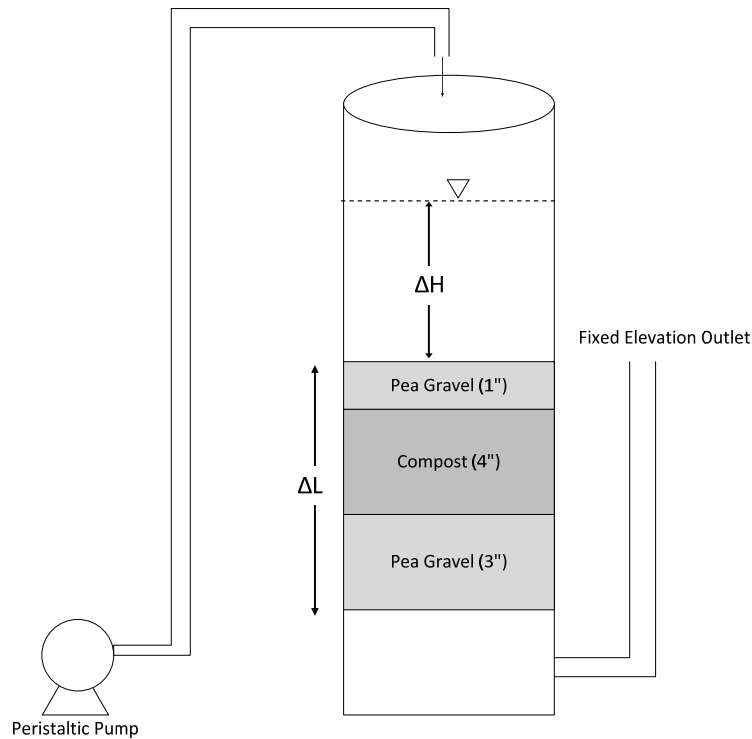
Figure 8.7: Setup for the constant head permeability test

A 7.75-inch inner-diameter, polycarbonate column was used to house the filter media, which was arranged to mimic the depths of each packing material in the field. A peristaltic pump was used to deliver water at a flow rate (Q) of 540-2250 mL/min, and the outlet was fixed at the top of the pea gravel to allow for measurement of hydraulic head (ΔH). Several combinations of flow rate and resulting hydraulic head were tested, and the results were plotted with Q/A on the ordinate and $\Delta H/\Delta L$ on the abscissa (Figure 8.8). The hydraulic conductivity was obtained from the slope of the best-fit line of these points, based on the following form of Darcy's Law:

$$\frac{Q}{A} = K \frac{\Delta H}{\Delta L} \tag{8-1}$$

Initial installation of media at the field site involved shoveling compost or Apatite II™ into the open filter bed, a process that is similar to tilling soil. It has been shown that following soil tillage, successive wetting and drying events will reduce saturated hydraulic conductivity, with the greatest decrease observed after the first wetting and drying cycle *(Mapa et al. 1986)*. Due to the structural similarity of compost and organic soils, there was concern over the potential effect drying and rewetting may have on the hydraulic conductivity of the compost. Accordingly, the experiment was repeated over four wetting and drying events spanning 6 days. The first day the hydraulic conductivity was found to be 8.09 in/min. For a flow rate of 10 gpm at the field site, this corresponds to a head loss of 1.0 inches. The hydraulic conductivity decreased sharply after the compost was drained and dried, resulting in a value of 3.75 in/min. The conductivity continued to decrease over the final two experiments, but the decrease was much less drastic than following the first drying event (Table 8.1). This suggests that filter permeability will decrease substantially after the initial wetting and drying cycle, but after a few wetting events the head loss will likely stabilize. However, in addition to wetting and drying, clogging of pore spaces with particulates could decrease filter permeability over time. It is therefore important to monitor head loss periodically at the field level, especially in instances with high solids concentrations in the influent. It should be noted that in Figure 8.8 the best-fit linear trend lines pass through non-zero values, whereas in accordance with Darcy's Law they should all go through the origin. It is hypothesized that the mechanism causing this is compaction of the compost at higher *ΔH* values, which in turn lowers hydraulic conductivity and causes nonlinearity.

Similar hydraulic conductivity experiments were performed using whole Apatite II™. However, these tests indicated that Apatite II™ and pea gravel offered little resistance to flow, and would cause negligible head loss at the field level.

Table 8.1: Hydraulic conductivity and the expected head loss in the field based on a predicted flow rate of 10 gpm

	K (in/min)	Field ΔH (in)
First Test	7.46	1.0
Second Test	3.01	2.6
Third Test	2.25	3.5
Fourth Test	2.16	3.6
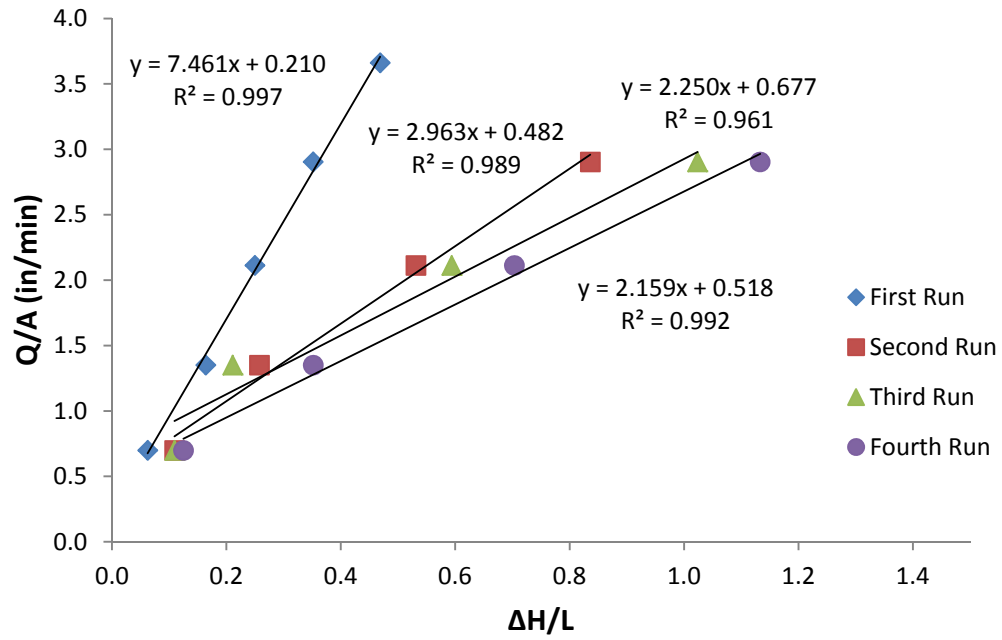
Figure 8.8: Results from the constant head permeability test for compost

8.5 FIELD DATASET TABLES

Table 8.2: Apatite II™ Storm 1 dataset

Total Precipitation	0.40	inches				
Volume Through Filter	1258	gal				
Samples Taken	9					
	Average Value			**Standard Deviations**		
	Influent	**Effluent**		**Influent**	**Effluent**	**Change**
pH	6.78	6.89		0.12	0.06	0.13
Conductivity (µS/cm)	189	394		8.33	16.20	18.21
TSS (mg/L)	143	28.0		7.51	3.61	8.33
TDS (mg/L)	74.7	235		4.16	6.11	7.39
Alkalinity (mg/L CaCO$_3$)	15.0	39		N/A	0.39	0.39
DOC (mg/L)	6.1	21.7		0.22	0.23	0.32
Anions						
Cl$^-$ (mg/L)	40.3	85.0		6.43	1.03	6.52
NO$_3^-$ (mg/L)	1.4	1.1		0.19	0.02	0.19
PO$_4^{-3}$ (mg/L)	BDL	10.7		N/A	0.72	0.72
SO$_4^{-2}$ (mg/L)	3.6	10.1		0.47	0.07	0.47
Major Cations - Dissolved						
Ca^{+2} (mg/L)	8.83	8.24		0.01	0.05	0.05
Mg^{+2} (mg/L)	10.23	10.56		0.03	0.13	0.13
Na^{+1} (mg/L)	7.72	37.41		0.00	0.33	0.33
K^{+1} (mg/L)	1.88	11.93		0.04	0.06	0.07
Fe^{+2} (mg/L)	BDL	BDL		N/A	N/A	N/A
Trace Metals-Dissolved						
Copper (µg/L)	25.2	10.1		0.00	0.00	0.00
Zinc (µg/L)	63.5	33.4		7.68	1.64	7.85
Lead (µg/L)	BDL	BDL		1.09	0.71	1.30
Nickel (µg/L)	2.0	2.3		0.09	0.35	0.36
Cadmium (µg/L)	2.1	BDL		0.47	0.08	0.47
Trace Metals-Total						
Copper (µg/L)	88.9	9.3		0.00	0.00	0.00
Zinc (µg/L)	165.4	32.5		11.61	0.37	11.62
Lead (µg/L)	9.7	BDL		0.98	0.26	1.01
Nickel (µg/L)	6.9	2.6		0.73	1.06	1.29
Cadmium (µg/L)	2.1	BDL		0.64	0.08	0.64

Table 8.3: Apatite II™ Storm 2 dataset

Total Precipitation	0.41	inches				
Volume Through Filter	2404	gal				
Samples Taken	19					
	Average Value			**Standard Deviations**		
	Influent	**Effluent**		**Influent**	**Effluent**	**Change**
pH	7.37	7.63		0.07	0.05	0.09
Conductivity (µS/cm)	563	801		11.37	2.00	11.55
TSS (mg/L)	97.3	128		3.21	3.79	4.97
TDS (mg/L)	593	613		11.02	6.43	12.75
Alkalinity (mg/L CaCO₃)	26.5	138		1.14	3.69	3.86
DOC (mg/L)	18.7	29.3		0.41	0.71	0.82
DIC (mg/L)	7.2	32.8		0.32	0.26	0.42
Anions						
Cl⁻ (mg/L)	155.3	164.1		3.74	2.21	4.35
NO₃⁻ (mg/L)	3.1	BDL		0.05	N/A	0.05
PO₄⁻³ (mg/L)	BDL	5.2		N/A	0.97	0.97
SO₄⁻² (mg/L)	8.3	15.7		0.14	2.70	2.70
Major Cations - Dissolved						
Ca⁺² (mg/L)	29.42	25.35		0.49	2.16	2.22
Mg⁺² (mg/L)	18.72	18.16		0.17	0.66	0.68
Na⁺¹ (mg/L)	11.22	17.24		0.21	1.66	1.68
K⁺¹ (mg/L)	4.02	4.34		0.10	0.51	0.52
Fe⁺² (mg/L)	BDL	BDL		N/A	N/A	N/A
Trace Metals-Dissolved						
Copper (µg/L)	19.0	15.9		0.14	2.06	2.06
Zinc (µg/L)	95.2	65.9		5.62	1.28	5.76
Lead (µg/L)	BDL	BDL		N/A	N/A	N/A
Nickel (µg/L)	5.6	5.3		0.17	0.72	0.74
Cadmium (µg/L)	BDL	BDL		N/A	N/A	N/A
Trace Metals-Total						
Copper (µg/L)	42.4	37.2		2.14	3.68	4.25
Zinc (µg/L)	209.6	125.0		8.95	11.99	14.97
Lead (µg/L)	BDL	BDL		N/A	N/A	N/A
Nickel (µg/L)	9.4	7.7		0.37	0.58	0.69
Cadmium (µg/L)	BDL	BDL		N/A	N/A	N/A

Table 8.4: Apatite II™ Storm 3 dataset

	Average Value			Standard Deviations		
Total Precipitation	0.76	inches				
Volume Through Filter	2069	gal				
Samples Taken	17					
	Influent	**Effluent**		**Influent**	**Effluent**	**Change**
pH	6.81	7.38		0.08	0.04	0.09
Conductivity (μS/cm)	59	188		2.77	4.93	5.66
TSS (mg/L)	283	235		4.04	0.58	4.08
TDS (mg/L)	47	58		6.11	2.00	6.43
Alkalinity (mg/L CaCO$_3$)	13.8	65.3		0.12	1.71	1.71
DOC (mg/L)	3.2	5.8		0.22	0.35	0.42
DIC (mg/L)	4.0	16.8		0.35	0.75	0.82
Anions						
Cl$^-$ (mg/L)	7.4	7.8		0.12	0.03	0.13
NO$_3^-$ (mg/L)	0.9	0.8		0.13	0.02	0.13
PO$_4^{-3}$ (mg/L)	BDL	5.8		N/A	0.30	0.30
SO$_4^{-2}$ (mg/L)	1.1	4.4		0.01	0.02	0.03
Major Cations - Dissolved						
Ca^{+2} (mg/L)	3.79	3.27		0.06	0.12	0.13
Mg^{+2} (mg/L)	3.50	3.75		0.11	0.19	0.22
Na^{+1} (mg/L)	1.37	2.22		0.06	0.06	0.09
K^{+1} (mg/L)	0.69	1.09		0.24	0.30	0.39
Fe^{+2} (mg/L)	0.2	0.1		0.01	0.00	0.01
Trace Metals-Dissolved						
Copper (μg/L)	7.5	23.1		1.14	1.13	1.61
Zinc (μg/L)	32.6	17.8		10.86	4.55	11.77
Lead (μg/L)	BDL	BDL		N/A	N/A	N/A
Nickel (μg/L)	2.0	2.1		0.43	0.12	0.44
Cadmium (μg/L)	BDL	BDL		N/A	N/A	N/A
Trace Metals-Total						
Copper (μg/L)	51.7	57.2		3.84	1.28	4.04
Zinc (μg/L)	185.3	136.3		13.00	3.99	13.60
Lead (μg/L)	17.1	13.0		0.86	0.57	1.03
Nickel (μg/L)	12.0	10.0		1.11	0.64	1.28
Cadmium (μg/L)	BDL	BDL		N/A	N/A	N/A

Table 8.5: Apatite II™ Storm 4 dataset

	Average Value			Standard Deviations		
Total Precipitation*:	0.84	inches				
Volume Through Filter	5340	gal				
Samples Taken	68					
	Average Value			**Standard Deviations**		
	Influent	**Effluent**		**Influent**	**Effluent**	**Change**
pH	6.99	7.30		0.05	0.02	0.05
Conductivity (µS/cm)	72	110		1.07	2.52	2.73
TSS (mg/L)	126	94		8.33	15.04	17.19
TDS (mg/L)	43	52		4.16	9.17	10.07
Alkalinity (mg/L CaCO$_3$)	13.9	31.1		0.16	0.05	0.17
DOC (mg/L)	3.7	4.1		0.05	0.08	0.09
DIC (mg/L)	3.9	8.3		0.12	0.21	0.24
Anions						
Cl$^-$ (mg/L)	10.6	10.8		0.10	0.03	0.10
NO$_3^-$ (mg/L)	1.0	1.0		0.04	0.03	0.06
PO$_4^{-3}$ (mg/L)	BDL	1.6		N/A	0.05	0.05
SO$_4^{-2}$ (mg/L)	1.9	2.5		0.02	0.01	0.02
Major Cations - Dissolved						
Ca^{+2} (mg/L)	5.21	5.63		0.07	0.15	0.17
Mg^{+2} (mg/L)	2.33	2.56		0.07	0.15	0.17
Na^{+1} (mg/L)	2.33	2.56		0.06	0.05	0.08
K^{+1} (mg/L)	0.87	1.02		0.11	0.10	0.15
Fe^{+2} (mg/L)	0.16	0.12		0.01	0.01	0.01
Trace Metals-Dissolved						
Copper (µg/L)	6.3	6.5		0.17	0.15	0.23
Zinc (µg/L)	31.9	20.4		4.57	2.59	5.25
Lead (µg/L)	BDL	BDL		N/A	N/A	N/A
Nickel (µg/L)	BDL	BDL		N/A	N/A	N/A
Cadmium (µg/L)	BDL	BDL		N/A	N/A	N/A
Trace Metals-Total						
Copper (µg/L)	31.0	17.6		1.37	0.24	1.39
Zinc (µg/L)	88.6	21.6		4.45	1.04	4.57
Lead (µg/L)	BDL	BDL		N/A	N/A	N/A
Nickel (µg/L)	5.8	3.3		0.31	0.47	0.56
Cadmium (µg/L)	BDL	BDL		N/A	N/A	N/A

*Data was missing from 4AM to 11AM; this total reflects the sum of the available data

Table 8.6: Apatite II™ Storm 5 dataset

Total Precipitation	0.17	inches				
Volume Through Filter	1889	gal				
Samples Taken	36					
	Average Value			**Standard Deviation**		
	Influent	**Effluent**		**Influent**	**Effluent**	**Change**
pH	7.05	7.34		0.07	0.03	0.08
Conductivity (µS/cm)	121	180		1.53	5.51	5.72
TSS (mg/L)	131	105		2.00	1.41	2.45
TDS (mg/L)	200	216		14.00	2.00	14.14
Alkalinity (mg/L CaCO$_3$)	24.4	50.2		1.93	6.30	6.59
DOC (mg/L)	10.4	10.5		0.37	0.67	0.77
Anions						
Cl$^-$ (mg/L)	22.0	23.2		0.25	0.35	0.43
NO$_3^-$ (mg/L)	1.6	1.7		0.03	0.00	0.03
PO$_4^{-3}$ (mg/L)	BDL	2.0		N/A	0.16	0.16
SO$_4^{-2}$ (mg/L)	3.4	4.7		0.04	0.07	0.08
Major Cations - Dissolved						
Ca^{+2} (mg/L)	9.44	9.48		0.06	0.03	0.07
Mg^{+2} (mg/L)	7.57	8.13		0.02	0.02	0.03
Na^{+1} (mg/L)	6.24	6.67		0.03	0.02	0.04
K^{+1} (mg/L)	1.56	1.66		0.02	0.01	0.02
Fe^{+2} (mg/L)	BDL	BDL		N/A	N/A	N/A
Trace Metals-Dissolved						
Copper (µg/L)	15.8	15.1		2.75	0.90	2.90
Zinc (µg/L)	54.0	39.4		5.69	1.80	5.97
Lead (µg/L)	BDL	BDL		N/A	N/A	N/A
Nickel (µg/L)	2.7	3.0		0.10	0.30	0.32
Cadmium (µg/L)	BDL	BDL		N/A	N/A	N/A
Trace Metals-Total						
Copper (µg/L)	40.4	40.4		3.67	1.07	3.82
Zinc (µg/L)	180.9	156.6		0.27	4.22	4.23
Lead (µg/L)	BDL	BDL		N/A	N/A	N/A
Nickel (µg/L)	7.9	8.0		1.00	0.06	1.00
Cadmium (µg/L)	BDL	BDL		N/A	N/A	N/A

Table 8.7: Apatite II™ Storm 6 dataset

	Average Value			Standard Deviation		
Total Precipitation	0.79	inches				
Volume Through Filter	3996	gal				
Samples Taken	55					
	Influent	**Effluent**		**Influent**	**Effluent**	**Change**
pH	6.61	6.88		0.06	0.05	0.08
Conductivity (µS/cm)	30.4	47.8		0.61	1.88	1.98
TSS (mg/L)	40.0	27.5		7.55	5.51	9.35
TDS (mg/L)	37.3	42.0		5.03	5.29	7.30
Alkalinity (mg/L CaCO$_3$)	7.6	16.1		0.15	0.16	0.22
DOC (mg/L)	1.9	2.0		0.24	0.07	0.25
Anions						
Cl$^-$ (mg/L)	3.4	3.4		0.01	0.03	0.04
NO$_3^-$ (mg/L)	0.7	0.5		0.25	0.04	0.25
PO$_4^{-3}$ (mg/L)	BDL	1.3		N/A	0.09	0.09
SO$_4^{-2}$ (mg/L)	0.8	1.0		0.01	0.00	0.01
Major Cations - Dissolved						
Ca^{+2} (mg/L)	2.56	3.44		0.17	0.23	0.29
Mg^{+2} (mg/L)	1.28	1.92		0.09	0.01	0.09
Na^{+1} (mg/L)	1.64	1.62		0.08	0.10	0.13
K^{+1} (mg/L)	0.53	0.51		0.02	0.02	0.03
Fe^{+2} (mg/L)	BDL	BDL		N/A	N/A	N/A
Trace Metals-Dissolved						
Copper (µg/L)	5.8	5.9		0.43	0.37	0.57
Zinc (µg/L)	25.9	15.9		5.47	1.49	5.67
Lead (µg/L)	BDL	BDL		N/A	N/A	N/A
Nickel (µg/L)	1.8	2.0		0.47	0.20	0.52
Cadmium (µg/L)	BDL	BDL		N/A	N/A	N/A
Trace Metals-Total						
Copper (µg/L)	9.5	9.8		0.21	0.21	0.29
Zinc (µg/L)	22.5	24.8		0.89	2.82	2.96
Lead (µg/L)	BDL	BDL		N/A	N/A	N/A
Nickel (µg/L)	2.8	2.5		0.34	0.08	0.35
Cadmium (µg/L)	BDL	BDL		N/A	N/A	N/A

Table 8.8: Apatite II™ Storm 7 dataset

Total Precipitation	0.84	inches				
Volume Through Filter	3120	gal				
Samples Taken	34					
	Average Value			**Standard Deviation**		
	Influent	**Effluent**		**Influent**	**Effluent**	**Change**
pH	6.89	6.98		0.04	0.02	0.04
Conductivity (µS/cm)	25	41		3.47	2.34	4.19
TSS (mg/L)	27	7.3		2.29	0.69	2.39
TDS (mg/L)	22	28		1.53	2.00	2.52
Alkalinity (mg/L CaCO$_3$)	8.5	18.2		0.13	0.49	0.51
DOC (mg/L)	1.6	1.7		0.07	0.12	0.14
Anions						
Cl$^-$ (mg/L)	1.7	1.7		0.00	0.03	0.03
NO$_3^-$ (mg/L)	0.8	0.6		0.16	0.04	0.16
PO$_4^{-3}$ (mg/L)	BDL	1.4		BDL	0.09	0.09
SO$_4^{-2}$ (mg/L)	0.5	0.7		0.00	0.01	0.01
Major Cations - Dissolved						
Ca^{+2} (mg/L)	2.10	3.18		0.03	0.11	0.11
Mg^{+2} (mg/L)	1.03	1.56		0.03	0.06	0.07
Na^{+1} (mg/L)	0.70	0.81		0.01	0.04	0.04
K^{+1} (mg/L)	0.44	0.51		0.01	0.00	0.01
Fe^{+2} (mg/L)	BDL	BDL		0.00	0.00	0.00
Trace Metals-Dissolved						
Copper (µg/L)	4.4	2.7		0.12	0.15	0.20
Zinc (µg/L)	13.3	7.8		2.11	1.79	2.77
Lead (µg/L)	BDL	BDL		N/A	N/A	N/A
Nickel (µg/L)	2.0	2.1		0.33	0.17	0.37
Cadmium (µg/L)	BDL	BDL		N/A	N/A	N/A
Trace Metals-Total						
Copper (µg/L)	8.2	3.2		0.63	0.03	0.63
Zinc (µg/L)	23.0	6.5		1.87	0.54	1.95
Lead (µg/L)	BDL	BDL		N/A	N/A	N/A
Nickel (µg/L)	2.7	1.8		0.20	0.15	0.25
Cadmium (µg/L)	BDL	BDL		N/A	N/A	N/A

Table 8.9: Compost Storm 1 dataset

	Average Value			Standard Deviation		
Total Precipitation	0.35	inches				
Volume Through Filter	2779	gal				
Samples Taken	49					
	Average Value			**Standard Deviation**		
	Influent	**Effluent**		**Influent**	**Effluent**	**Change**
pH	7.05	8.21		0.04	0.04	0.05
Conductivity (µS/cm)	84.7	178		2.56	12.34	12.60
TSS (mg/L)	77	34		2.00	1.53	2.52
TDS (mg/L)	93	180		4.16	3.46	5.42
Alkalinity (mg/L CaCO$_3$)	13.2	41.7		0.11	0.32	0.33
DOC (mg/L)	11.4	20.6		0.65	0.84	1.06
Anions						
Cl$^-$ (mg/L)	12.0	16.4		0.11	0.15	0.19
NO$_3^-$ (mg/L)	1.6	3.7		0.01	0.01	0.01
PO$_4^{-3}$ (mg/L)	BDL	3.1		N/A	0.09	0.09
SO$_4^{-2}$ (mg/L)	2.6	4.8		0.01	0.05	0.05
Major Cations - Dissolved						
Ca^{+2} (mg/L)	6.44	3.45		0.27	0.22	0.34
Mg^{+2} (mg/L)	4.04	2.11		0.18	0.15	0.24
Na^{+1} (mg/L)	2.72	7.93		0.09	0.61	0.62
K^{+1} (mg/L)	1.23	33.15		0.05	2.46	2.46
Fe^{+2} (mg/L)	0.10	0.21		0.00	0.01	0.01
Trace Metals-Dissolved						
Copper (µg/L)	13.1	13.8		0.26	0.95	0.98
Zinc (µg/L)	42.1	17.6		1.06	3.85	3.99
Lead (µg/L)	BDL	BDL		N/A	N/A	N/A
Nickel (µg/L)	2.5	2.9		0.08	0.45	0.46
Cadmium (µg/L)	BDL	BDL		N/A	N/A	N/A
Trace Metals-Total						
Copper (µg/L)	27.5	20.0		2.73	0.28	2.75
Zinc (µg/L)	109.9	41.3		10.74	0.80	10.77
Lead (µg/L)	BDL	BDL		N/A	N/A	N/A
Nickel (µg/L)	4.5	3.8		0.22	0.22	0.31
Cadmium (µg/L)	BDL	BDL		N/A	N/A	N/A

Table 8.10: Compost Storm 2 dataset

	Average Value			Standard Deviation		
Total Precipitation	0.25	inches				
Volume Through Filter	2612	gal				
Samples Taken	50					
	Average Value			**Standard Deviation**		
	Influent	**Effluent**		**Influent**	**Effluent**	**Change**
pH	7.16	7.43		0.06	0.03	0.07
Conductivity (µS/cm)	86.9	113		6.70	5.51	8.67
TSS (mg/L)	18.0	21.3		1.73	3.21	3.65
TDS (mg/L)	68.0	86.7		2.00	1.15	2.31
Alkalinity (mg/L CaCO$_3$)	21.2	31.0		0.43	0.76	0.87
DOC (mg/L)	8.2	10.0		0.21	0.29	0.35
Anions						
Cl$^-$ (mg/L)	9.6	9.9		0.06	0.05	0.08
NO$_3^-$ (mg/L)	2.1	3.9		0.00	0.02	0.02
PO$_4^{-3}$ (mg/L)	BDL	1.4		N/A	0.08	0.08
SO$_4^{-2}$ (mg/L)	2.4	2.8		0.00	0.02	0.02
Major Cations - Dissolved						
Ca^{+2} (mg/L)	8.66	9.54		0.20	0.08	0.22
Mg^{+2} (mg/L)	4.22	5.55		0.10	0.08	0.12
Na^{+1} (mg/L)	2.96	3.47		0.07	0.06	0.09
K^{+1} (mg/L)	1.31	5.81		0.06	0.10	0.12
Fe^{+2} (mg/L)	0.18	0.31		0.01	0.02	0.02
Trace Metals-Dissolved						
Copper (µg/L)	10.5	9.8		0.27	0.18	0.33
Zinc (µg/L)	38.5	25.3		3.73	5.43	6.58
Lead (µg/L)	BDL	BDL		N/A	N/A	N/A
Nickel (µg/L)	3.0	2.4		0.13	0.34	0.36
Cadmium (µg/L)	BDL	BDL		N/A	N/A	N/A
Trace Metals-Total						
Copper (µg/L)	14.9	14.1		0.99	0.14	1.00
Zinc (µg/L)	54.1	40.0		3.10	0.17	3.10
Lead (µg/L)	BDL	BDL		N/A	N/A	N/A
Nickel (µg/L)	3.4	3.1		0.47	0.05	0.48
Cadmium (µg/L)	BDL	BDL		N/A	N/A	N/A

Table 8.11: Compost Storm 3 dataset

	Total Precipitation	0.40	inches				
	Volume Through Filter	787	gal				
	Samples Taken	9					
		Average Value			**Standard Deviation**		
		Influent	Effluent		Influent	Effluent	Change
pH		7.50	7.68		0.07	0.05	0.08
Conductivity (µS/cm)		74.6	113		4.40	1.53	4.66
TSS (mg/L)		54.7	35.7		1.15	0.58	1.29
TDS (mg/L)		87.3	120.7		1.15	4.62	4.76
Alkalinity (mg/L CaCO₃)		19.7	30.9		0.02	0.00	0.02
DOC (mg/L)		13.8	15.3		0.40	0.02	0.40
Anions							
Cl⁻ (mg/L)		5.8	6.2		0.04	0.05	0.06
NO₃⁻ (mg/L)		2.2	7.5		0.08	0.02	0.08
PO₄⁻³ (mg/L)		BDL	2.1		N/A	0.24	0.24
SO₄⁻² (mg/L)		2.4	2.9		0.01	0.03	0.03
Major Cations - Dissolved							
Ca⁺² (mg/L)		6.68	9.63		0.11	0.74	0.75
Mg⁺² (mg/L)		3.24	5.39		0.06	0.42	0.43
Na⁺¹ (mg/L)		2.58	2.67		0.04	0.22	0.22
K⁺¹ (mg/L)		1.69	3.12		0.01	0.25	0.25
Fe⁺² (mg/L)		0.23	0.22		0.01	0.01	0.01
Trace Metals-Dissolved							
Copper (µg/L)		30.0	16.4		0.20	1.08	1.10
Zinc (µg/L)		59.9	36.6		4.13	2.48	4.82
Lead (µg/L)		BDL	BDL		N/A	N/A	N/A
Nickel (µg/L)		3.4	2.9		0.04	0.39	0.39
Cadmium (µg/L)		BDL	BDL		N/A	N/A	N/A
Trace Metals-Total							
Copper (µg/L)		54.3	27.0		0.06	0.74	0.74
Zinc (µg/L)		117.7	67.8		0.13	1.45	1.46
Lead (µg/L)		BDL	BDL		N/A	N/A	N/A
Nickel (µg/L)		5.0	4.3		0.48	0.42	0.64
Cadmium (µg/L)		BDL	BDL		N/A	N/A	N/A

Table 8.12: Compost Storm 4 dataset

	Average Value			Standard Deviation		
Total Precipitation	0.41	inches				
Volume Through Filter	786	gal				
Samples Taken	15					
	Average Value			**Standard Deviation**		
	Influent	**Effluent**		**Influent**	**Effluent**	**Change**
pH	7.43	7.52		0.05	0.04	0.06
Conductivity (µS/cm)	101.4	130		2.95	12.86	13.19
TSS (mg/L)	19.0	11.3		1.73	2.08	2.71
TDS (mg/L)	93.3	99.3		6.11	2.31	6.53
Alkalinity (mg/L $CaCO_3$)	28.0	33.5		0.27	0.17	0.32
DOC (mg/L)	16.5	15.8		0.21	0.43	0.47
Anions						
Cl^- (mg/L)	10.3	9.7		0.03	0.02	0.04
NO_3^- (mg/L)	2.3	2.8		0.02	0.01	0.02
PO_4^{-3} (mg/L)	BDL	1.2		N/A	0.00	0.00
SO_4^{-2} (mg/L)	2.9	2.8		0.01	0.01	0.01
Major Cations - Dissolved						
Ca^{+2} (mg/L)	10.47	11.00		0.28	0.84	0.89
Mg^{+2} (mg/L)	5.05	5.71		0.14	0.42	0.44
Na^{+1} (mg/L)	3.62	3.39		0.05	0.27	0.27
K^{+1} (mg/L)	2.65	2.96		0.06	0.24	0.25
Fe^{+2} (mg/L)	0.40	0.38		0.01	0.02	0.02
Trace Metals-Dissolved						
Copper (µg/L)	17.1	12.9		0.40	0.76	0.86
Zinc (µg/L)	60.3	38.2		4.52	0.64	4.57
Lead (µg/L)	BDL	BDL		N/A	N/A	N/A
Nickel (µg/L)	4.3	3.5		0.31	0.37	0.48
Cadmium (µg/L)	BDL	BDL		N/A	N/A	N/A
Trace Metals-Total						
Copper (µg/L)	26.3	18.0		0.92	1.69	1.93
Zinc (µg/L)	77.0	48.8		4.67	0.92	4.76
Lead (µg/L)	BDL	BDL		N/A	N/A	N/A
Nickel (µg/L)	4.9	3.9		0.09	0.16	0.18
Cadmium (µg/L)	BDL	BDL		N/A	N/A	N/A

Table 8.13: Compost Storm 5 dataset

	Average Value			Standard Deviation		
Total Precipitation	0.37	inches				
Volume Through Filter	317	gal				
Samples Taken	7					
	Average Value			**Standard Deviation**		
	Influent	**Effluent**		**Influent**	**Effluent**	**Change**
pH	7.55	7.67		0.05	0.03	0.06
Conductivity (µS/cm)	165	194		11.00	4.16	11.76
TSS (mg/L)	41.3	31.0		0.58	1.00	1.15
TDS (mg/L)	202.0	236.0		3.46	2.00	4.00
Alkalinity (mg/L $CaCO_3$)	37.1	56.8		0.43	0.45	0.62
DOC (mg/L)	41.7	35.6		0.70	1.76	1.89
Anions						
Cl^- (mg/L)	18.2	17.1		0.14	0.30	0.33
NO_3^- (mg/L)	3.0	10.1		0.01	0.21	0.21
PO_4^{-3} (mg/L)	BDL	1.7		N/A	0.15	0.15
SO_4^{-2} (mg/L)	5.9	6.0		0.04	0.10	0.10
Major Cations - Dissolved						
Ca^{+2} (mg/L)	17.04	21.71		0.23	1.83	1.84
Mg^{+2} (mg/L)	7.28	10.47		0.09	0.85	0.85
Na^{+1} (mg/L)	6.00	6.15		0.09	0.02	0.09
K^{+1} (mg/L)	7.83	7.63		0.25	0.11	0.28
Fe^{+2} (mg/L)	0.62	0.59		0.00	0.03	0.03
Trace Metals-Dissolved						
Copper (µg/L)	44.6	33.2		1.14	2.34	2.61
Zinc (µg/L)	101.9	59.6		7.49	4.65	8.82
Lead (µg/L)	BDL	BDL		N/A	N/A	N/A
Nickel (µg/L)	8.0	6.9		0.31	0.38	0.49
Cadmium (µg/L)	BDL	BDL		N/A	N/A	N/A
Trace Metals-Total						
Copper (µg/L)	55.3	41.6		0.01	1.02	1.02
Zinc (µg/L)	146.2	86.0		0.52	0.29	0.60
Lead (µg/L)	BDL	BDL		N/A	N/A	N/A
Nickel (µg/L)	8.5	7.7		0.53	0.23	0.58
Cadmium (µg/L)	BDL	BDL		N/A	N/A	N/A

8.6   HYDROGRAPHS OF FLOW THROUGH THE FILTER
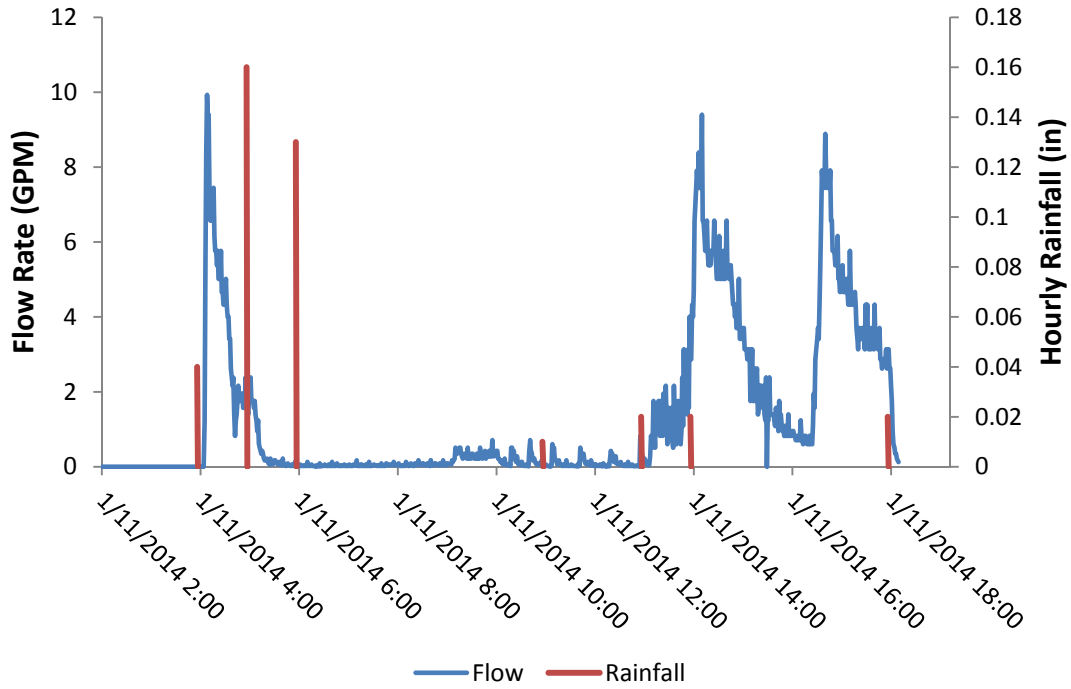
Figure 8.9: Storm 1A hydrograph and rainfall
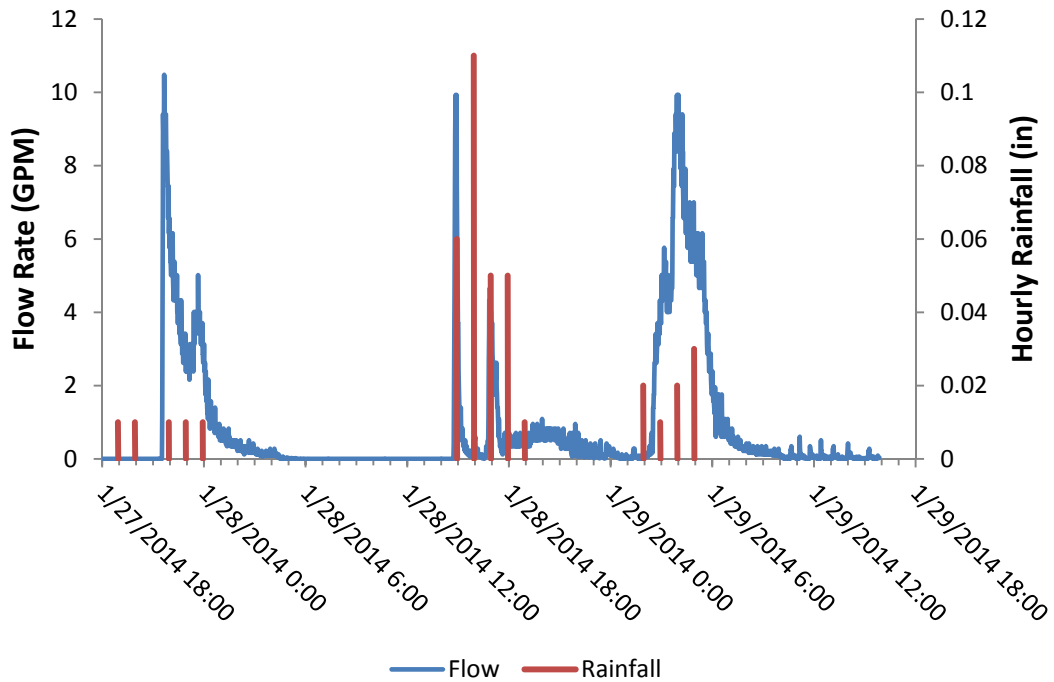
Figure 8.10: Storm 2A hydrograph and rainfall
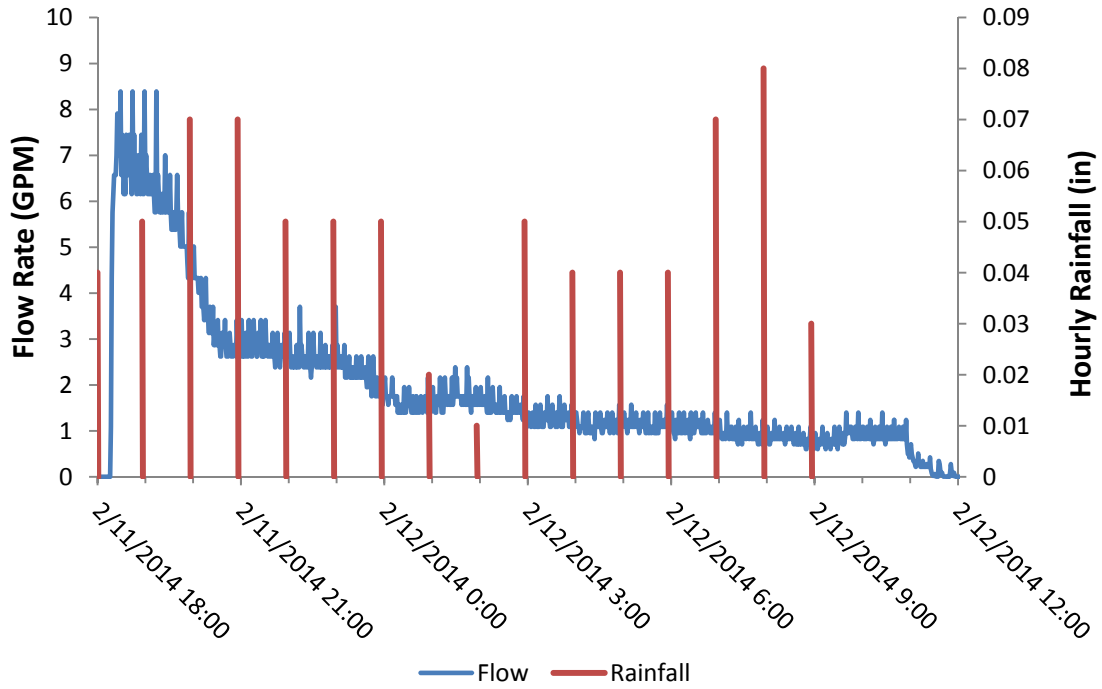
Figure 8.11: Storm 3A hydrograph and rainfall
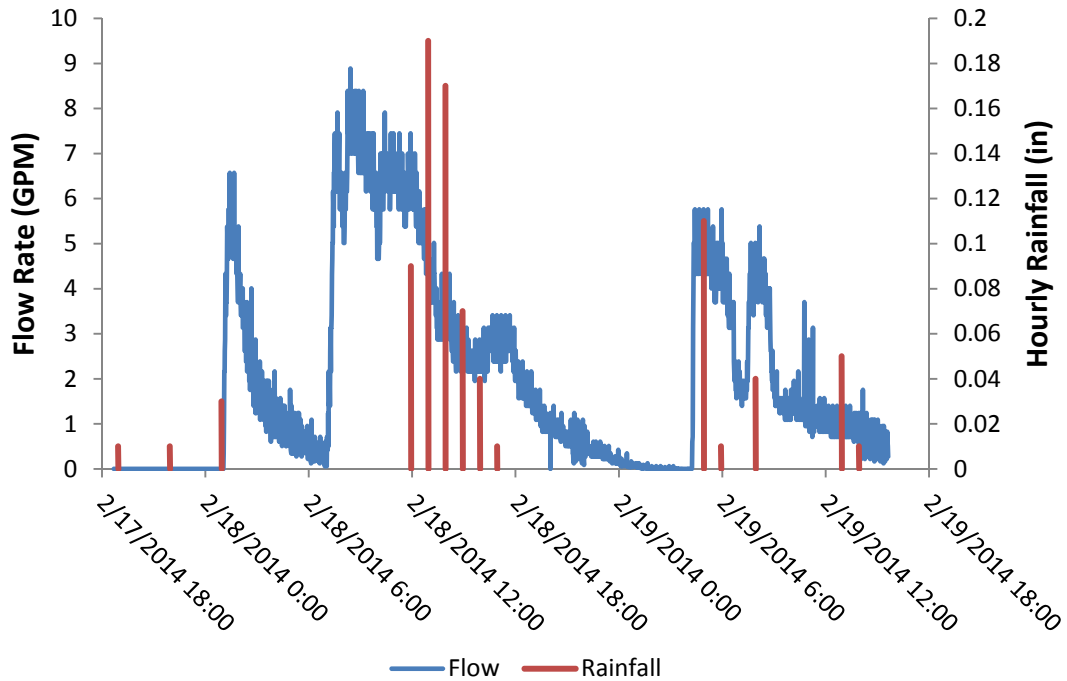
Figure 8.12: Storm 4A hydrograph and rainfall

A-21
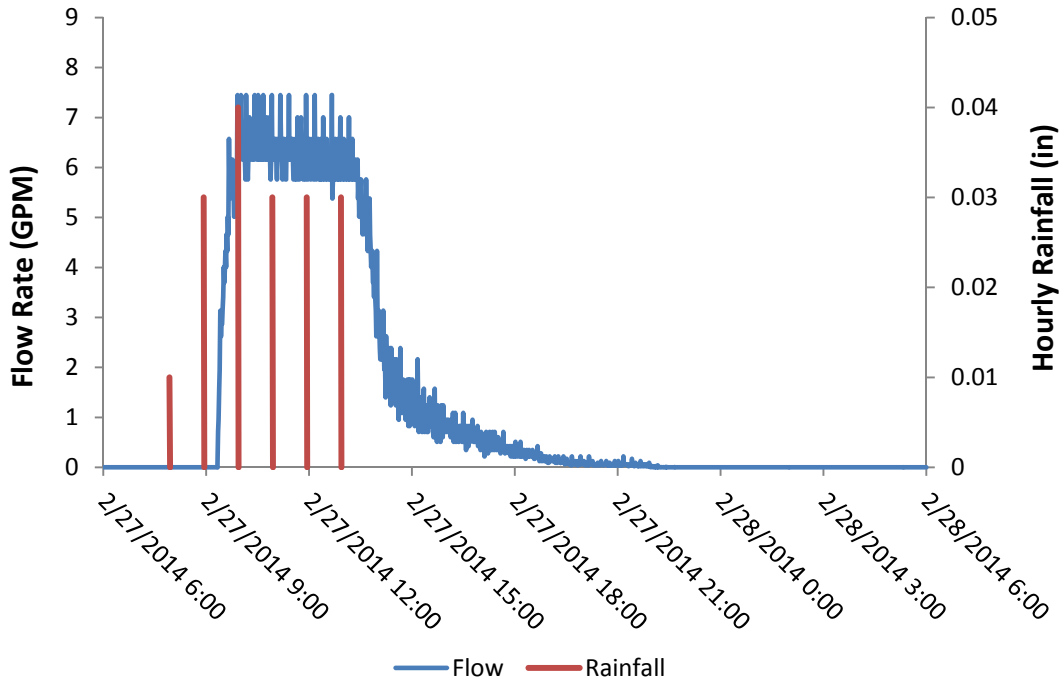
Figure 8.13: Storm 5A hydrograph and rainfall
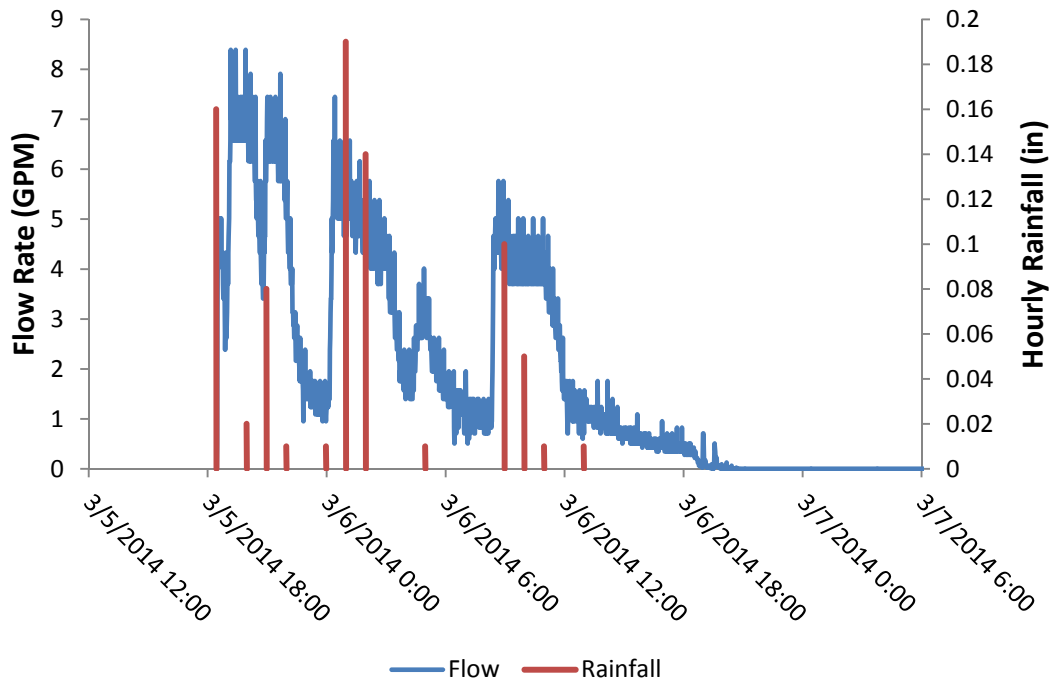
Figure 8.14: Storm 6A hydrograph and rainfall
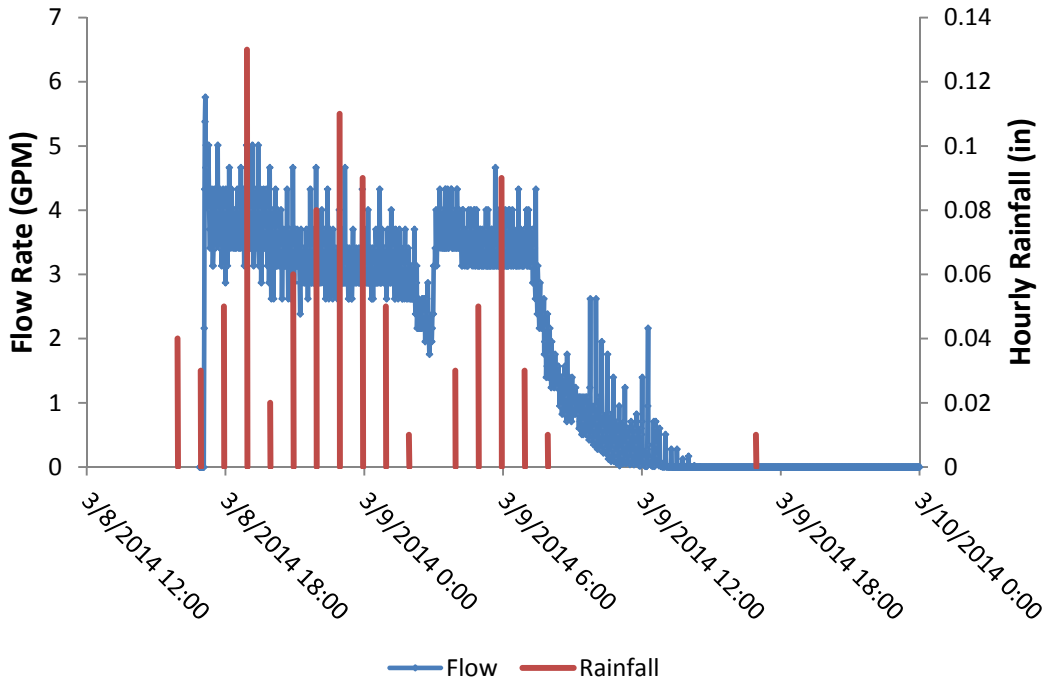
Figure 8.15: Storm 7A hydrograph and rainfall
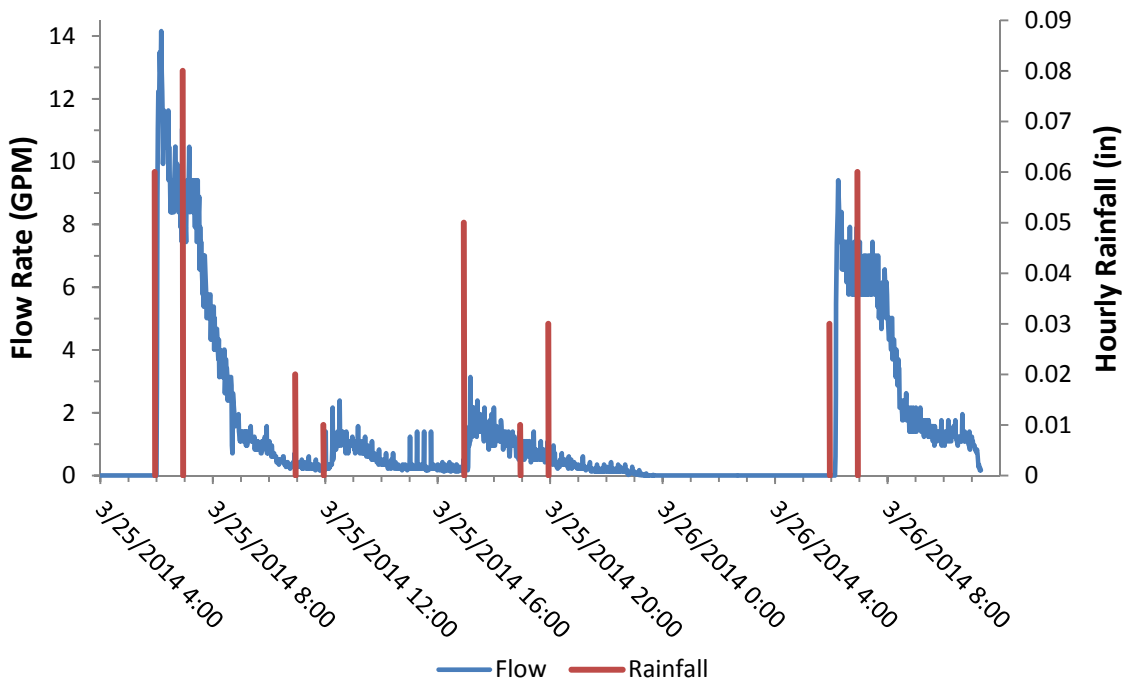
Figure 8.16: Storm 1C hydrograph and rainfall
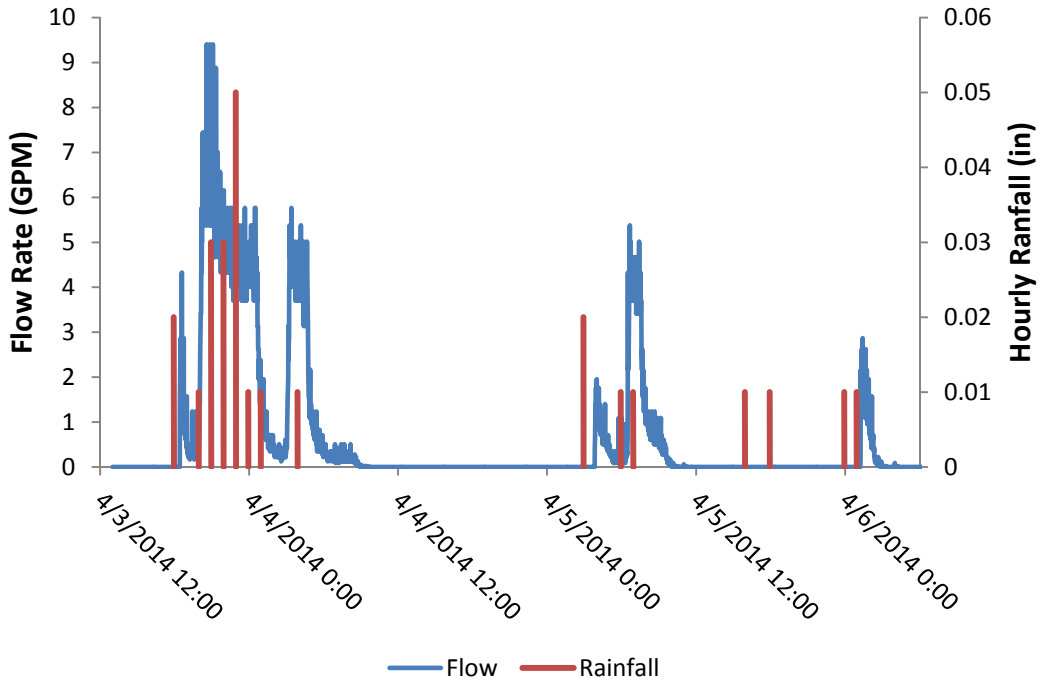
Figure 8.17: Storm 2C hydrograph and rainfall
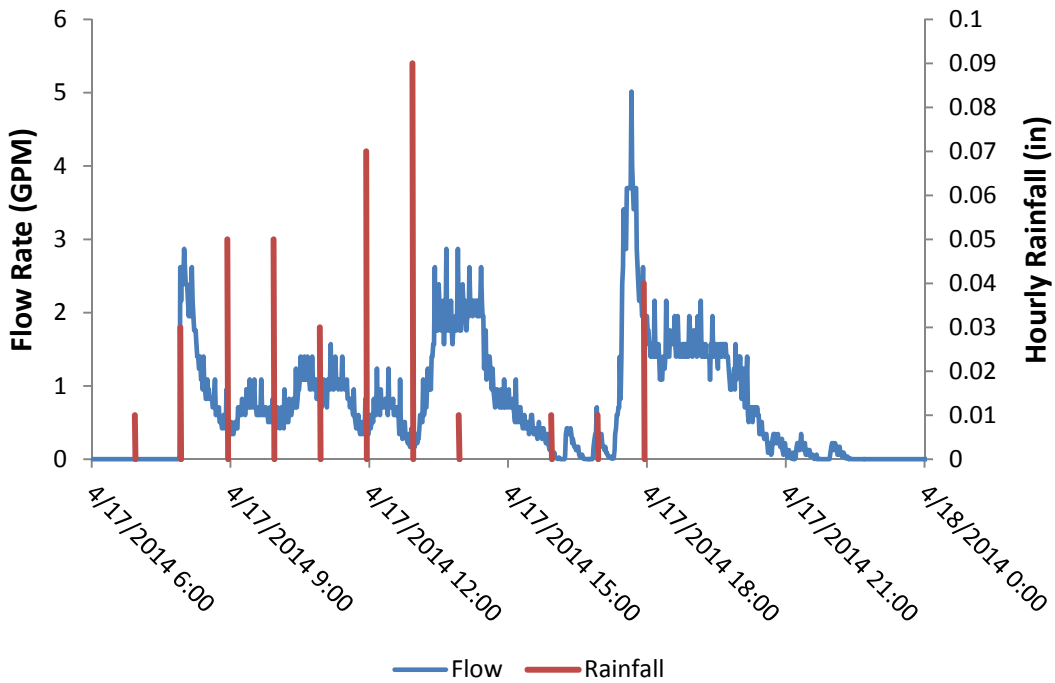
Figure 8.18: Storm 3C hydrograph and rainfall
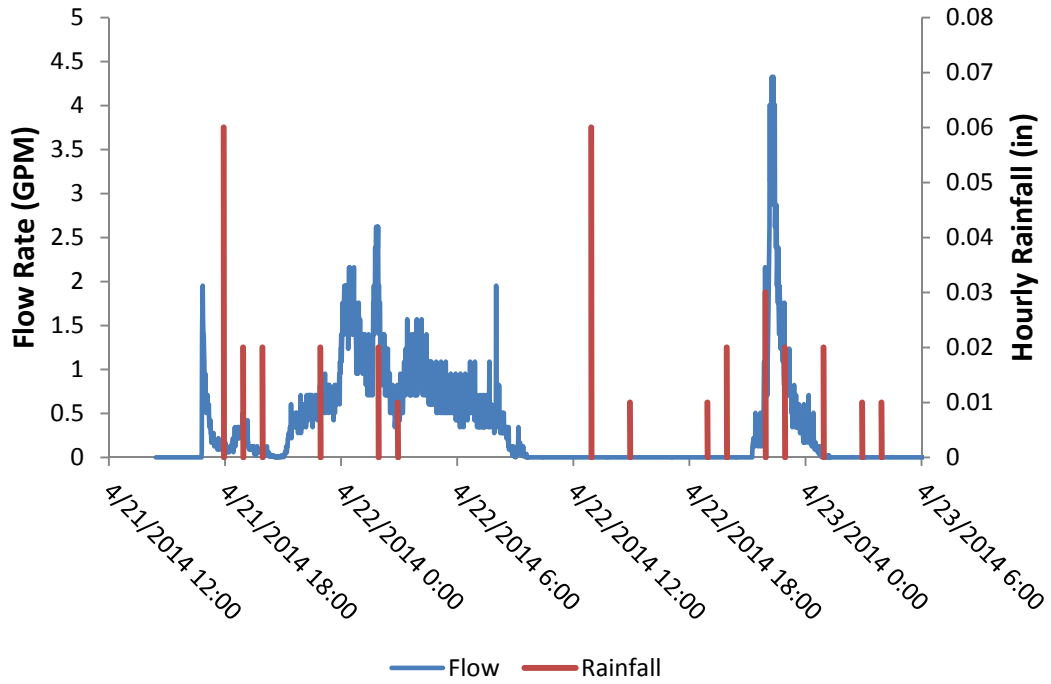
Figure 8.19: Storm 4C hydrograph and rainfall
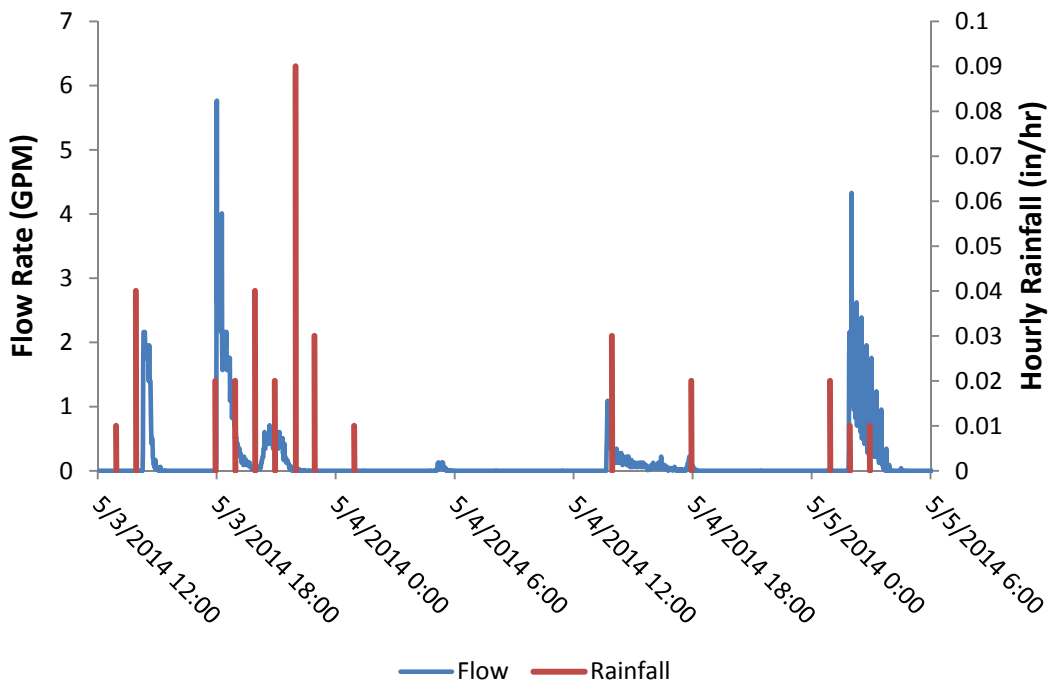
Figure 8.20: Storm 5C hydrograph and rainfall

Mapa, R.B., R.E. Green, and L. Santo. Temporal Variability of Soil Hydraulic Properties with Wetting and Drying Subsequent to Tillage. *Soil Science Society of America Journal*, Vol. 50, No. 5, 1986, pp. 1133-8.

Summers, R.S., S.M. Kim, K. Shimabuku, S.-H Chae, and C.J. Corwin. Granular Activated Carbon Adsorption of MIB in the Presence of Dissolved Organic Matter. *Water Research*, Vol. 47, No. 10, 2013, pp. 3507-13.